



Università di Foggia

FACULTY OF MEDICINE AND SURGERY

PhD Course in Experimental and Regenerative Medicine

XXX Cicle

*Multi-integrated approach based on HPT-JT
families for the identification of a set
of biomarkers of Parathyroid Carcinoma*

Tutor

Prof. V.M. Fazio

PhDStudent

Luigia Cinque

Supervisor

Dr. Vito Guarnieri

A.A. 2016/2017

TABLE OF CONTENTS

ABSTRACT	pg.1
CHAPTER 1: PRIMARY HYPERPARATHYROIDISM	pg.6
1.1 PRIMARY HYPERPARATHYROIDISM (PHPT)	pg.6
1.2 MULTIPLE ENDOCRINE NEOPLASIA TYPE 1 (MEN1)	pg.10
1.3 HYPERPARATHYROIDISM-JAW TUMOR SYNDROME (HPT-JT)	pg.13
1.4 PARAFIBROMIN AND WNT	pg.16
1.5 HEDGEHOG PATHWAY (Hh)	pg.18
1.5.1 MENIN AND Hh	pg.19
1.5.2 PARAFIBROMIN AND Hh	pg.21
1.6 INTEGRINS	pg.23
CHAPTER 2: OBJECTIVES	pg.27
2.1 AIM OF THE STUDY	pg.27
2.1.1 FIRST TASK: IDENTIFICATION OF GENES/PROTEINS/ MOLECULAR PATHWAYS ASSOCIATED TO KP BY WES AND EXPRESSION PROFILING	pg.28
2.1.2 SECOND TASK: DRUG TEST ON HEK293 CELL LINES	pg.28
2.1.3 THIRD TASK: VALIDATION OF THE VARIANTS IDENTIFIED, IMMUNOHISTOCHEMISTRY (ON GOING)	pg.29
2.2 PATIENTS	pg.30
2.2.1 PHENOTYPIC/GENETIC DESCRIPTION OF THE 5 HPT-JT FAMILIES UNDER STUDY	pg.30
2.2.2 SPECIAL CLINICAL CASE: FAMILI VI-MEN+KP	pg.43
2.2.3 INTRAFAMILIAL ANALYSIS	pg.46
CHAPTER 3: RESULTS	pg.49

3.1	FIRST TASK: IDENTIFICATION OF GENES/PROTEINS/ MOLECULAR PATHWAYS ASSOCIATED TO KP BY WES AND EXPRESSION PROFILING	pg.49
3.1.1	WES ANALYSIS	pg.49
3.1.2	EXPRESSION PROFILING	pg.53
3.1.3	RT-qPCR	pg.59
3.2	SECOND TASK: DRUG TEST ON HEK293 CELL LINES	pg.64
3.2.1	FUNCTIONAL ASSAY ON THE 5 CDC73 GENE MUTATIONS	pg.64
3.2.2	MEN1 WT AND EXPRESSION OF THE MUTANT PROTEINS	pg.68
3.2.3	ESTABLISHMENT OF PRIMARY PARATHYROID TUMOR CELL LINES	pg.69
3.3	THIRD TASK: VALIDATION OF THE VARIANTS IDENTIFIED, IMMUNOHISTOCHEMISTRY (ONGOING)	pg.71
	CHAPTER 4: DISCUSSION	pg.72
4.1	WES ANALYSIS	pg.74
4.2	DISCUSSION ON MEN1 FAMILY	pg.76
4.3	EXPRESSION PROFILING	pg.79
4.4	DRUG TEST	pg.80
4.5	IHC AND SEARCH ON URINE-SERUM	pg.82
	CHAPTER 5: CONCLUSION	pg.83
	APPENDIX	pg.84
	METHODS	pg.84
1.	DNA AND RNA EXTRACTION	pg.84
2.	WHOLE EXOME SEQUENCING (WES)	pg.84
2.1	BIOINFORMATICS NGS ANALYSIS	pg.85

3.	EXPRESSION PROFILING	pg.86
4.	RT-qPCR	pg.87
4.1	cDNA SYNTHESIS	pg.87
4.2	REAL TIME QUANTITATIVE POLYMERASE CHAIN REACTION (RT-qPCR)	pg.87
5.	FUNCTIONAL ASSAYS	pg.89
5.1	cDNA EXPRESSION VECTORS	pg.89
5.2	CELL CULTURE	pg.89
5.3	PROLIFERATION ASSAY	pg.89
5.4	WESTERN BLOT	pg.90
5.5	PROTEIN DEGRADATION ASSESSMENT	pg.90
	REFERENCES	pg.91

ABSTRACT

Introduzione. Nella sindrome da iperparatiroidismo associato a tumore della mandibola (HPT-JT), il carcinoma paratiroideo (PC) è causato da mutazioni del gene oncosoppressore CDC73 codificante per parafibromina, un componente del complesso PAF1 coinvolto nel rimodellamento della cromatina e nella regolazione del ciclo cellulare.

Le mutazioni del gene MEN1 causano la sindrome omonima (MEN1), le cui lesioni paratiroidee sono benigne nel 99% dei casi ma, negli ultimi 40 anni, sono stati riportati 15 casi di associazione insolita fra PC e la sindrome MEN1 nel mondo.

Il PC è un tumore raro e aggressivo per il quale le attuali terapie sono risultate inefficaci e l'asportazione chirurgica della lesione rimane l'unico approccio curativo. Tuttavia, la distinzione in prima diagnosi fra una lesione paratiroidea maligna e un'iperplasia indolente o un'adenoma benigno rappresenta ancora oggi una sfida, in assenza di segni patognomici, come metastasi a distanza o recidive locali. Finora, sono stati compiuti sforzi infruttuosi per la ricerca di biomarcatori molecolari che potessero indirizzare verso il (migliore) trattamento chirurgico (conservativo/demolitivo) al fine di ridurre il rischio di recidiva e di estendere la sopravvivenza libera da malattia.

Scopo del progetto e metodi. Questo progetto mira a identificare le cause genetiche che portano allo sviluppo di un carcinoma paratiroideo (PC) e a individuare una serie di biomarcatori utili per una inequivocabile e precoce diagnosi di PC. A tal fine sono state applicate strategie di Next Generation Sequencing, quali il sequenziamento dell'intero esoma e studi di espressione genica, a casi familiari (costituiti da uno o più soggetti affetti, portatori non affetti e controlli sani con lo stesso background genetico) piuttosto che a casi sporadici al fine di ridurre, per quanto possibile, la variabilità intrinseca causata dai diversi background genetici. La nostra rara coorte consta di 5 famiglie con HPT-JT e lesione paratiroidea maligna e mutazione costituzionale del gene CDC73 e una famiglia molto rara con mutazione MEN1 associata a PC.

Risultati. Il sequenziamento dell'intero esoma ha mostrato che solo i soggetti affetti di 4 (delle 5) famiglie con HPT-JT reclutate per lo studio, condividono varianti rare (MAF <0,004) in geni codificanti per le integrine (ITGA3, ITGA2B, ITGA11, ITGAB6, ITGA9), recettori di superficie coinvolti nell'adesione cellulare alla matrice extracellulare (ECM) ed essenziali per la proliferazione, la sopravvivenza, l'adesione e la migrazione delle cellule. Inoltre sono state identificate ulteriori varianti nei geni che codificano per proteine coinvolte nel riparo del DNA come FANCC e BRIP1; NOTCH4; RET; BRCA1; BLK; MUC12; KMT2C; geni target della pathway di Hedgehog quali SMO, GLI3, mentre una variante del gene GLI2 è stata identificata solamente nei soggetti affetti della famiglia MEN1 associata a PC.

Lo studio dell'espressione genica è stato condotto confrontando i pazienti affetti vs controlli fra le famiglie con HPT-JT e l'unica famiglia MEN1-PC. L'analisi effettuata ha mostrato un'espressione differenziale dei geni del sistema immunitario e inoltre ha evidenziato che i pazienti MEN1 e HPT-JT utilizzano diversi set di geni per controllare la mobilizzazione del calcio.

Saggi funzionali. Cellule HEK293 sono state trasfettate con vettori di espressione codificanti la forma WT o mutata del gene CDC73: sono state testate 5 diverse mutazioni in presenza/assenza di Bortezomib, un farmaco già utilizzato in clinica per la terapia del mieloma multiplo. Questo inibitore del proteasoma sembra essere in grado di recuperare parzialmente l'espressione di proteine CDC73 mutate a causa di mutazioni missenso, in-frame e persino frameshift.

Conclusioni e prospettive. Questo progetto, seppur preliminare, può aiutarci ad identificare biomarker utili per una diagnosi precoce e immediata di PC al fine di indirizzare verso il miglior approccio chirurgico e identificare i portatori asintomatici nelle famiglie affette per un intervento precoce ed efficace.

Ipotizziamo che l'insorgenza/progressione/aggressività del PC possa essere dovuta alla deregolazione di proteine coinvolte nell'adesione cellula-cellula (come le integrine); allo squilibrio nell'attivazione del sistema immunitario; alla deregolazione della pathway di Hedgehog e alla perdita di

fattori scatenanti, come le proteine implicate nel mantenimento dell'integrità del DNA (FANCC, BRIP1, BRCA1).

Infine, considerando che la ricerca di un farmaco efficace come approccio alternativo al trattamento chirurgico è risultata fino ad oggi vana, per la prima volta, riportiamo il possibile utilizzo di un farmaco chemioterapico ben conosciuto, il Bortezomib, per la terapia del PC dovuto a mutazioni del gene CDC73.

ABSTRACT

Background. As part of the Hyperparathyroidism with Jaw Tumor syndrome (HPT-JT), parathyroid carcinoma (KP) is caused by mutations of the CDC73 tumor suppressor gene, encoding the parafibromin, a PAF1 co-transcription factor, involved in chromatin remodelling and cell cycle regulation.

Mutations of MEN1 gene cause the namesake syndrome (MEN1), in whose parathyroid lesions are benign in 99% of cases: instead, in the last 40 ys, only 15 cases worldwide have been reported with the unusual association of KP in MEN1 syndrome.

KP is a rare, aggressive life-threatening tumor for whose at the present current therapies resulted ineffective and the surgical removal of the lesion remains the only curative approach. However, to recognize in first diagnosis a malignant parathyroid lesion from an indolent hyperplasia or benign adenoma still represents a challenge, in absence of pathognomic signs, such as distant metastasis or local recurrences. So far, unsuccessful efforts have been made in search of clinical biomarkers that could address to the (best) surgery option (conservative/demolitive) in order to reduce the risk of recurrence and to extend the disease free survival.

Purpose and methods. The present project aims to identify the genetic causes leading to the development of a parathyroid carcinoma (KP) and to detect a set of biomarkers for a possible unequivocal, early first diagnosis. We decided to apply high throughput strategies such Whole Exome Sequencing (WES) and Expression Profiling (EP) to familial cases (consisting of one or more affected subjects, non-affected carriers and healthy controls with the same genetic background) rather than to sporadic ones in order to, possibly, reduce the intrinsic variability caused by different genetic backgrounds. Our rare cohort consisted of 5 HPT-JT families with malignant parathyroid lesion and constitutional mutation of the CDC73 gene and a very rare family with MEN1 mutation associated with recurrent and familial KP.

Results. WES analysis revealed that in 4 (out of 5) HPT-TJ families, surprisingly, only the affected subjects shared rare variants (MAF < 0.004) in

genes encoding the integrins (ITGA3, ITGA2B, ITGA11, ITGAB6, ITGA9), cell surface receptors involved in cell adhesion to the extracellular matrix (ECM) and essential for proliferation, survival, adhesion and migration of cells. Moreover, other variants in genes encoding proteins involved in DNA repair such as FANCC and BRIP1; NOTCH4; RET; BRCA1; BLK; MUC12; KMT2C; Hedgehog target genes such as SMO, GLI3 were identified. Finally a variant in GLI2 gene was found in unaffected subjects of MEN1- KP family.

The **EP** analysis compared the affecteds vs controls between HPT-JT families and the unique MEN1-KP family. The analysis showed a differential expression of genes of immune system. The EP also evidenced that MEN1 and HPT-JT patients use different set of genes to control the calcium mobilization.

Functional assay. Human embryonic kidney (HEK293) cell lines were transfected with eukaryotic expression vectors carrying WT or mutated CDC73 gene: 5 different mutations were tested in presence/absence of Bortezomib, a drug already used in clinic for the therapy of multiple myeloma. We proved that this proteasome inhibitor was able to partially rescue the expression of missense, in-frame and even frameshift CDC73 gene deletions.

Conclusions and perspectives. This preliminary project may help to find a biomarkers set for a prompt early diagnosis of KP, in order to suggest the best surgical approach and identify asymptomatic carriers in affected families for an efficient early intervention.

We suppose that the onset/progression/aggressivity of KP may be due to the deregulation of proteins involved in cell-cell adhesion (such integrins); the derangement of immune system; the deregulation of the Hedgehog pathway and the lack of trigger factors, such as the proteins assigned to DNA integrity (FANCC, BRIP1, BRCA1).

Finally we reported, for the first time, the possible use of a well known chemotherapy drug, the Bortezomib, for the therapy of KP CDC73 induced, taking into account that, so far, all the attempts to find an efficient drug as alternative approach to the surgery, resulted ineffective.

CHAPTER 1: PRIMARY HYPERPARATHYROIDISM (PHPT)

1.1 PHPT

Primary hyperparathyroidism (PHPT) is the third more frequent endocrine disorder, after diabetes and thyroid disease. Although mostly sporadic, familial forms of HPT exist among 2-5% of total cases. The most common genetic disorders associated with HPT are Multiple Endocrine Neoplasia (MEN) type 1 and HPT-Jaw Tumor (HPT-JT) syndrome caused by germline mutations of MEN1 and CDC73 gene respectively (1, 2).

PHPT is characterized by hypercalcemia accompanied by an inappropriate secretion of parathyroid hormone (PTH) from one or more neoplastic parathyroid glands (3).

Usually, serum calcium level is maintained within a physiologic narrow range by the action of PTH secreted from parathyroid glands. Parathyroid chief cells express the G protein-coupled calcium-sensing receptor (CaSR) on their surface membrane, which, in response to small changes in the ionized calcium level, negatively regulates PTH secretion. Instead the CaSR is able to inhibit the secretion of pre-formed PTH that, in turn, reduces the proliferation of parathyroid cells and the transcription of the pre-pro PTH gene (by a loop negative feedback). If normocalcemia is not restored, parathyroid glands enhance their secretory capacity: PTH acts on bone, kidney and gut to regulate blood calcium concentration, modulating movement of ions in/out of the bone and the renal tubular reabsorption in order to keep the serum calcium concentration within a narrow range.

When a benign or malignant parathyroid lesion develops, an over secretion of PTH causing hypercalcemia can be observed (4, 1). Parathyroid lesions are benign in up of 99% of cases consisting of parathyroid adenomas (85%) and hyperplasia in the remaining (15%) of cases. Parathyroid carcinomas (KP) is a rare aggressive life-threatening tumor, accounting for less than 1% of all PHPT cases, for whom at the present, current therapies resulted ineffective since the surgical removal of the lesion remains the only curative approach (5).

Distinguishing between a parathyroid benign adenoma from a malignant lesion is challenging and it is based only upon histopathological criteria. Indeed this rare malignant carcinoma is not recognized before surgery and often is not conclusively identified during the operation or at histological examination (6).

In absence of invasion of surrounding structures and/ or metastasis, histopathologic features including fibrous bands and mitotic figures are common and could be suggestive but not pathognomic of malignancy. Instead some of these features are not specific but shared among parathyroid adenomas. So an unequivocal diagnosis of KP is based on the findings of regional or distant metastases, invasion of adjacent soft tissues, thyroid gland and vascular invasion of perineural spaces. These features should alert the surgeon of the possibility of malignancy and should lead to consideration of an *en bloc* resection still being the only chance of cure (6, 7).

In addition to parathyroid adenoma and the rare KP, subsets of tumors with an uncertain malignant potential are referred as to “atypical adenomas” which include those lesions that share some of the histopathological features of KP such as fibrosis, mitoses, capsular invasion but lacking evidences of invasive growth (8, 9).

To recognize in first diagnosis a parathyroid malignant tumor from its benign counterparts still represents a challenge. The immunohistochemistry seems to be a useful but not definitive tool.

Parafibromin protein is encoded by the CDC73 gene (1q32), identified as the master TSG of KP, in 2002 (*see chapter 1.3, for a detailed description*). Parafibromin immunohistochemistry was first reported as a molecular marker for parathyroid tumor classification with parafibromin-positive cases having a low risk of malignancy while cases with reduced protein expression representing either carcinomas or adenomas with CDC73 genemutations (8, 10). Nevertheless, it was found that some parathyroid carcinomas have had positive staining. This result would suggest the need of an additional standardized protocol, to test the validity of this approach and to determine the roles of other genes in the development of these tumors.

Recently Adenomatous Polyposis Coli (APC) has become an additional screening marker for atypical adenoma and KP (9). APC immunoreactivity was shown to be completely lost in the majority of malignant parathyroid tumors while APC expression was retained in all the adenomas under study. The authors concluded that loss of APC and partial loss of parafibromin might co-occur in KP and atypical adenoma allowing to distinguish parathyroid malignant tumors from benign ones.

Fernandez-Ranvier et al, asked whether parathyroid tumors could have a distinctive molecular profile for differentiating benign tumors from malignant ones. They indicated that no single diagnostic marker currently determines whether a parathyroid tumor is an actual carcinoma, but loss of parafibromin and Rb expression and overexpression of galectin-3, a member of the lectin family, generally is able to distinguish KP from other parathyroid tumors (11).

Taking into account the difficulties linked to the histological interpretation of various forms of parathyroid cancer, genetic screening of CDC73 and MEN1 genes along with the immunohistochemistry (IHC) of the corresponding proteins, parafibromin and menin, represents important clinical tools for improving diagnostic accuracy. However these strategies are not always pursued or follow the surgery, thus not fulfilling the need of an unequivocal/prompt diagnosis for the choice of surgery.

So far, many efforts have been made in search of clinical biomarkers that could address to the best surgery option (conservative/demolitive) that, however, resulted unsuccessful. Our preliminary study, based on a metanalysis of all published and personal (*Muscarella...Cinque et al, accepted on Oncotarget*) available biochemical, clinical, histology, molecular data, seems to indicate that early onset of the disease (<40 ys) and high serum calcium levels (>14 mg/dL) may predict the presence of a CDC73 gene mutation. However, novel prognostic biomarkers would be desirable, since prevention and early diagnosis make the difference in this rare cancer disease.

CDC73 and MEN1 genes are the major players involved in the development of parathyroid carcinoma, encoding for parafibromin and menin proteins, respectively, both transcription factors implicated in the regulation of

cell cycle genes and/or chromatin remodelling. On the other hand, both represent two oncosuppressor genes whose the biallelic inactivating mutation is frequent in DNA derived from parathyroid tumors, according to the so-called Knudson "Two hit hypothesis". Two "hits" (i.e. mutations, germline/somatic or somatic/somatic, or germline-somatic/LOH) are required for a tumor to develop a selective growth advantage in an affected cell and resulting in its clonal expansion. While for sporadic tumors both the mutations mostly occur somatically, in hereditary tumors at least one mutation is germline, while the second hit might present as somatic or as loss of heterozygosity (LOH) (12).

1.2 MULTIPLE ENDOCRINE NEOPLASIA TYPE 1 (MEN1)

Multiple Endocrine Neoplasia 1 Syndrome (MEN1) is an autosomal dominant endocrine disorder, primarily characterized by familial hyperparathyroidism (PHPT) and by the occurrence of parathyroid, gastro-entero-pancreatic (in approximately 40% of patients) and pituitary tumors (in approximately 30% of patients). Less frequently MEN1 patients may develop adrenocortical, thyroid, carcinoid tumors, lipomas and leiomyomas (13, 14).

Clinical association of familial PHPT associated with lesions in at least 2 of the 3 “ P ” glands (pancreatic, pituitary, parathyroid) is paradigmatic for a MEN1 clinical diagnosis: “ Familial MEN1 ” refers to a family in which one individual and one or more first-degree relatives have at least 2 of the 3 MEN1 – related tumors (15).

Parathyroid tumors are the most common feature of MEN1 and occur in about 95% of patients. Pancreatic islet cell tumors, which consist of gastrinomas, insulinomas and glucagonomas, occur in about 40% of patients and anterior pituitary tumors, which consist of prolactinomas, somatotrophinomas, corticotrophinomas, or nonfunctioning adenomas, occur in about 30% of patients (14, 16-18). The clinical manifestations of MEN1 are generally related to their products of secretion and less frequently to their primary sites or metastasis. In the absence of treatment, MEN1 tumors result in an earlier mortality (19). Unlike HPT-JT, many MEN1 patients with parathyroid tumors have multiglandular disease (12).

Although MEN1 is inherited as an autosomal dominant disorder, sporadic forms may develop in 8-14% of patients due to *de novo* germline mutations of the gene in approximately the 10% of patients (14, 17).

Moreover, KP is a rare occurrence in MEN1 patients, being the parathyroid lesions almost exclusively benign (adenoma or hyperplasia) up to the 99% of cases. So far, only 15 well-documented cases of KP and 1 atypical adenoma (AA) are known to be associated with MEN1 mutation and of these only in 7, an inactivating mutation of the MEN1 gene was identified (20-22).

The MEN1 gene was primarily identified in 1997 and localized to chromosome 11q13. MEN1 gene consists of 10 exons with a 1.83 Kb coding region. The region ranging from exon 2 to exon 10 is translated while exon 1, the 5' part of exon 2 and the 3' part of exon 10 are untranslated. The main transcript of MEN1 gene is a 2.8 kb mRNA (23, 15) of whose 1821 bp encode for the corresponding protein.

Menin is a 610 amino-acid intracellular protein, ubiquitously expressed but primarily localized in the nucleus in non-dividing cells. Menin has three nuclear localization signals (NLSs) at codons 479-497 (NLS1), 546-572 (NLSa) and 588-608 (NLS2) and, being a nuclear protein, menin acts as a co-transcription factor involved in transcriptional regulation, genome stability, cell cycle regulation and proliferation interacting with a plethora of transcription factors (13, 15).

As transcriptional regulator, menin seems to be a component of histone methyltransferase complexes containing members from the mixed-lineage leukemia (MLL) and trithorax protein family (24). These complexes are responsible of the activation of transcription by methylating the lysine 4 residue of histone H3 (H3K4) of Hox Homeobox genes and the genes for cyclin-dependent Kinase inhibitors, p27 and p18 (25, 26).

Moreover, it was found that menin interacts with: 1) members of the nuclear factor-KappaB (NF-Kb) family (p50, p52, p65) repressing NF-kb-mediated transcriptional activation; 2) Smad3 and the Smad1/5 complex, to inhibit the transforming growth factor-b (TGF-b); 3) bone morphogenetic protein 2 (BMP-2) signaling pathways; 4) transcription factor checkpoint suppressor 1 (CHES1) in response to DNA damage (27).

Menin also interacts with the activating protein-1 (AP1), transcription factors JunD and C-Jun to suppress Jun-mediated transcriptional activation: Kim et al, reported that menin interacts with JunD via recruitment of a mSin3A-histone deacetylase (HDAC) complex to repress JunD transcriptional activity (28).

Independently of the histone methyltransferase complex, menin seems to be able to bind a broad range of gene promoters, functioning as a general transcription regulator that helps to maintain stable gene expression (15).

As far as the role in controlling genome stability, menin has also been shown to interact with a subunit of replication protein (RPA2) and Fanconi anemia complementation group D2 protein (FANCD2) necessary for DNA recombination and replication and for DNA repair respectively (29, 30). Through the interaction with nonmuscle myosin II-A heavy chain (NMHCII-A), fibrillary acidic protein (GFAP) and vimentin, menin plays the role as a regulator of cell division (13). Menin also participates in cell cycle control interacting with the tumor metastases suppressor (NM23H1) and the activator of S-phase Kinase (ASK), a component of Cdc7/ASK Kinase complex involved in cell proliferation. It seems that menin completely represses ASK-induced cell proliferation (31). Furthermore, it has been reported that menin regulates itself by a feedback mechanism (13, 32, 33).

To date, more than 1800 mutations have been reported and the majority (>70%) of these are frameshift and nonsense mutations leading to truncated form with a reduced ability of tumor suppressor thus leading to a derangement of the cell cycle and proliferation.

Indeed, 20% of these MEN1 mutations are missense resulting in inactivated menin that may impair the interactions with other proteins or may reduce menin stability by enhancing proteolytic degradation (13). The mutations are scattered throughout the coding region and the splice-sites of gene, without evidence for clustering. However, no phenotype-genotype correlation between MEN1 gene mutations and clinical manifestation of the disease has so far been reported.

MEN1 germline mutations have been reported in patients with hereditary and sporadic MEN1 syndrome while somatic mutations are detected in approximately 20% of sporadic parathyroid tumors (15). However, 5-10% of MEN1 cases do not harbour mutations in the MEN1 gene (13). More than 90% of MEN1 tumors consist of loss of heterozygosity (LOH) at the MEN1 locus, which is consistent with a tumor suppressor role of MEN1, according to Knudson's two-hit hypothesis. The remaining 10% of the MEN1 tumors, showed other mechanisms for the inactivation of the second allele, for example: intragenic deletions and point mutations by which the second "hit" may occur (13, 34).

1.3 HYPERPATHYROIDISM-JAW TUMOR SYNDROME (HPT-JT)

The HPT-JT syndrome is an autosomal dominant disorder characterized by the co-presence of parathyroid tumors in association with ossifying fibromas of the maxilla and mandible. Parathyroid neoplasm is the first manifestation of the disease and occurs in > 95 % of patients; in particular the frequency of parathyroid carcinoma is high in patients with HPT-JT, up to the 15%.

Patients may develop other related disease manifestations such as renal abnormalities, which affect about 15% of patients and uterine tumors, up to 75% (35).

The Cell Division Cycle 73 (CDC73) gene, firstly identified in 2002 as gene responsible for HPT-JT, consists of 17 exons encoding an ubiquitously expressed and evolutionary conserved 531 amino-acid protein known as parafibromin. CDC73 inactivating mutations identified in HPT-JT patients are scattered throughout the coding region and splice sites of the gene. To date, a total of 118 different coding mutations were identified and the majority of these reported CDC73 mutations are frameshift and nonsense (36), large or whole-gene deletions have also been described (37, 38). Missense mutations are rare and generally affect residues located in the N-terminus of parafibromin (39). Germline coding mutations of CDC73 gene have been identified in 75% of the reported HPT-JT families while 25% of these families, who do not harbour CDC73 mutations or deletions, may have defects involving the promoter or untranslated regions, uncharacterized alternative transcripts or epigenetic modifications (40-42). Moreover, the occurrence of the same germline CDC73 mutation in patients with different diseases such as HPT-JT, sporadic KP or Familial Isolated Hyperparathyroidism (FIHP), demonstrates the lack of a genotype-phenotype correlation while biallelic inactivation of CDC73 gene may be seen in sporadic KP (43).

Parafibromin is identified as a component of the PAF1 complex, a key transcriptional regulatory complex that directly interacts with RNA polymerase II subunit A. As part of the human PAF1 complex that binds at the residues 223-415, parafibromin is required for expression of several cellular genes involved in

cell cycle regulation, cell growth, protein synthesis, lipid and nucleic acid metabolism. Functions attributed to parafibromin are so many: behind the regulation of genetic transcription, parafibromin interacts with the histone methyltransferase complex for histone modifications and chromatin remodeling (44, 45); it regulates cell growth via the downregulation of cyclin D1 expression and Wnt signaling (46, 47) and inhibition of the c-myc proto-oncogene (12, 48).

Parafibromin is also implicated in embryonic development directly regulating genes involving in cell growth and survival like H19, insulin-like growth factor 1 and 2 (IGF1 and IGF2), insulin-like growth factor binding protein 4 (IGFBP4), high mobility AT-hook 1 and 2 (HMGA1 and HMGA2), 3-hydroxy-3-methylglutaryl-coenzyme A synthase 2 (HMGCS2) (49). Parafibromin was shown to have a dual role as a tumor suppressor and oncoprotein depending on the cellular environment. As a tumor suppressor, parafibromin over expression seems to result in inhibition of NIH3T3 and HEK293 cells proliferation; increase in G1 arrest and apoptosis in Hela cells; and in downregulation of the cell cycle regulator cyclin D1.

As oncogene, over expression of parafibromin was proved to enhance growth in cells expressing the SV40 large T-antigen, as the vice-versa: it inhibits growth in cells that do not express the SV40 large T-antigen (50).

The functional role of parafibromin in the nucleus is consistent with the identification of highly conserved nuclear localization signal (NLS) at residues 125-139. Parafibromin localizes into the nucleolar compartment, thereby three nucleolar localization signals (NoLSs) at residues 76-92, 192-194, 393-409 has been reported (51, 52). Absence of parafibromin nucleolar expression was found in sporadic KP with CDC73 mutations even showing a nuclear expression. So the disruption of nucleolar localization might cause parathyroid tumorigenesis independent of nuclear parafibromin expression (53).

Although parafibromin is predominantly a nuclear protein, a lot of evidence suggest the interaction of parafibromin with the actin-binding proteins, actinin-2 and actinin-3 in the cytoplasm, that are involved in organization of the cytoskeletal structure (54).

Parafibromin shares no homologies to known protein domains. However, the 200 aminoacids of the parafibromin C-terminal domain share 27% sequence identity with the yeast Cdc73 protein, a component of the yeast polymerase-associated factor 1 (PAF1) (40). The PAF1 complex interacts with RNA Polymerase II at both the promoter and the coding regions of transcriptionally active genes regulating key transcriptional events of histone modification, chromatin remodeling, initiation and elongation. The yeast Paf1 complex is composed by 5 subunits: Paf1, Ctr9, Leo1, Cdc73 and Rtf1. Deletion of Rtf1 or Cdc73 results in the loss of association of the remaining Paf1 complex members with chromatin and a significant reduction in binding of the complex to RNA pol II (55, 44).

The human PAF1 complex consists of 5 subunits (hPaf1, hCtr9, hLeo1, hCdc73, shared with yeast Paf1 complex, and hSki8, a higher eukaryotic-specific subunit) and it has been reported to have several functions (35):

- The PAF1 complex plays role in both initiation and elongation of the transcription, associating with nonphosphorylated-Ser2 and phosphorylated-Ser5 on the major subunit of RNA polymerase II.
- In the process of transcriptional initiation, the PAF1 complex is required for histone H2B monoubiquitination mediated by Rad6/Bre1, a prerequisite for both H3K4 and H3K79 methylation mediated by Set1 and Dot1 respectively.
- At initiation, the PAF1 complex associates with the Set1-like HMTase complex required for H3K4 methylation.
- The PAF1 complex controls RNA polymerase II C-terminal domain (CTD) serine 2 phosphorylation.
- During elongation, the PAF1 complex has been shown to associate with elongation factors in conjunction with the histone chaperon FACT.

Furthermore, a recent work revealed parafibromin as a transcriptional scaffold whose distinct morphogen intracellular signals converge on, coordinating the expression of specific target genes and generating appropriate cellular responses to each morphogens. Parafibromin competitively interacts with the Wnt and Hedgehog signal effectors, β -catenin and GLI1 respectively,

and also binds Notch intracellular domain (NICD), promoting downstream target genes activation.

The platform function of parafibromin is regulated by its phosphorylation and dephosphorylation status on Y290/293/315, mediated by PTK6 and SHP2 respectively.

The tyrosine-dephosphorylated form of parafibromin at Y290/293/315 is required to bind β -catenin, GLI1 and NICD and seems to enhance the Wnt, Hh and Notch signaling activation. Because of β -catenin and GLI1 binding sites overlap in the N-terminal domain of parafibromin, these two effectors compete, intracellularly, for the same parafibromin region and interact with the PAF1 complex to increase the expression of their target genes, while the interaction between NICD and parafibromin requires the C-terminal region (56). It has been observed a reciprocal inhibition of the Wnt and Hh signals, also reported in human gastric cancer cells (57).

1.4 PARAFIBROMIN AND WNT

Among the most relevant parafibromin functions, there is the activation of the Wnt signaling pathway (46, 47, 58, 59). The Wnt signaling pathway is involved in the development of multicellular organism, in cell proliferation, differentiation, survival, cell motility and apoptosis via its central component β -catenin (60).

In absence of the Wnt ligand, most of endogenous β -catenin is located at the cell membrane, where it is associated with α -catenin and E-cadherin in epithelial cell adherent junctions. The cytoplasmic counterpart is marked for proteasomal degradation by a multisubunit destruction complex, consisting of Axin, APC, protein phosphatase 2 A (PP2A) and GSK3b.

When the Wnt ligand binds the receptor complex, composed by Frizzled and LRP5/6, the inhibitory complex is dissociated and active unphosphorylated β -catenin enters the nucleus and interacts with TCF/LEF DNA binding proteins to initiate transcription of Wnt target genes (60, 61).

Studies in *Drosophila* show that Hyrax, a component of the Wnt/Wg signaling, is a homolog of parafibromin. Parafibromin/Hyrax have been proved to

be a positive regulator in the Wnt pathway and it is required for nuclear transduction of the WNT/Wg signaling in HEK293 cells. Parafibromin binds directly to the C-terminal region of nuclear β -catenin/Armadillo via its conserved N-terminal domain and recruits the other components of the PAF1 complex, in order to regulate the transcription of Wnt target genes encoding for example the c-myc oncoprotein and the cell cycle protein cyclin D1 (47, 62).

Disregulation of the Wnt signaling pathway causes many different human tumor types, including colon, hepatocellular carcinoma, leukemia and melanoma (63) and aberrant activation of Wnt/ β -catenin signaling pathway was observed in a subset of parathyroid carcinomas due to epigenetic APC loss of expression (64). Furthermore, it has also been identified in primary hyperparathyroidism and in parathyroid tumors associated with chronic renal failure (65).

1.5 HEDGEHOG PATHWAY

The Hedgehog pathway (Hh) is an evolutionary conserved regulator of tissue homeostasis and development in both vertebrate and invertebrate embryos, and it is involved in proliferation and self-renewal in adult stem cells. Hh signaling converges to the activation of DNA-binding GLI transcription factors that regulates the expression of Hh target genes (66).

In vertebrates, the canonical Hh pathway is activated by three ligands: Indian (IHH), Desert (DHH) and the most abundant Sonic Hh (SHH).

Secreted Hh ligands induce signalling transduction by binding the transmembrane Patched 1 (PTCH1) receptor. Consequently, attenuating its inhibitory effect, PTCH1 promotes the release of repressed Smoothed (Smo) (67). It has been suggested that activated Smo inhibits Suppressor of Fused (Sufu), Fused and Cos2 complex that sequesters the GLI proteins in the cytoplasm and represses transcription by recruiting the histone deacetylase complex SAP18-MSin3 (68). Once activated and translocated into the nucleus, GLI proteins promote the transcription of genes involved in cell cycle processes, survival and metabolism.

In absence of Hh ligands, GLI1 is transcriptionally repressed while GLI2 and GLI3, once phosphorylated by Dyrk2, are recognized by the F-box protein β -TrCP for proteasome-dependent degradation to generate the truncated repressor forms (69, 70). In presence of Hh ligands, the transcription of GLI1 is activated and the GLI2-GLI3 proteolytic processing is inhibiting, leading to the activation of specific GLI target genes (66, 67).

The members of the GLI family are zinc finger transcription factors that possess different domains: an N-terminal domain of transcriptional repression, lacking in GLI1; central five zinc-finger DNA binding domains and a C-terminal domain of trans activation. These proteins can act as activators or transcriptional repressors of target genes of Hh: GLI1 acts as a transcriptional activator while GLI2 and GLI3 act both by activators and by transcriptional repressors even if evidences supported the hypothesis that GLI3 primarily plays the role of SHH pathway repressor (71, 72).

An aberrant function of Hh pathway occurs in many human tumors such as basal cell carcinoma and medulloblastoma (73).

Among the various candidate genes emerging from the arbitrary filtering of WES data, we focused our attention on the GLI2 gene as there are evidences showing strong implications of menin and parafibromin with the Hh pathway.

Human GLI2 gene consists of 13 exons located on chromosome 2q14. This gene encodes a 1586 amino acid protein belonged to the C2H2-type zinc finger protein subclass of the GLI family that bind DNA through zinc finger motifs.

The functional domains of the human GLI2 protein are not yet well understood. The murine Gli2 ortholog is characterized by a central DNA-binding domain consisting of 5 zinc fingers, a N-terminally repressor domain and a C-terminally transactivation domain (74). Accordingly, a human variant lacking the N-terminal repressor domain (ΔN) in vitro shows a transcriptional activity 30 times higher compared with the full-length protein (75).

1.5.1 MENIN AND HH

Data reported in literature show that:

1) The Hedgehog pathway plays a key role in pituitary development and seem to be involved in pituitary alterations typical of MEN1 syndrome (76). In chicken, zebrafish and rodents the morphogen Sonic Hedgehog (Shh) signals is required during the development of the pituitary gland in early stages (77).

In humans, defects of Shh secretion and signaling during early stages of development are responsible for holoprosencephaly (HPE) with pituitary defects. Several GLI2 genetic variants were reported in patients with pituitary and extra pituitary malformations, craniofacial anomalies, hypopituitarism and Multiple Pituitary Hormone Deficiency (MPHD) and are associated with anterior pituitary hypoplasia. Mutations in GLI2 gene are mainly nonsense or frameshift introducing a premature codon stop, thus resulting in a protein truncated of the functional C-terminal transactivation domain (76).

2) It was demonstrated that a link between menin and Hh signaling exists in menin-mediated tumors. Menin is able to epigenetically repress the Hedgehog pathway in dependent MEN1 tumors and mutations in the MEN1 gene induce an

over activation of the Hh pathway (78). As a component of histone methyltransferase complex, menin can positively or negatively affect gene expression. So mutations in MEN1 gene cause a dysregulation of signaling pathway related to menin transcription function.

As previously described, the Hedgehog signaling pathway is activated by the binding of ligands to the cell surface receptor Patched (PTCH1), thanks to accessory proteins, such as GAS1, BOC or CDO. Upon activated, SMO triggers a signal transduction cascade leading to the activation of GLI transcription factors (GLI1, 2, 3) that allow the transcription of target genes including regulating a variety of processes such as embryonic development, cell cycle and tumorigenesis (67, 79, 80).

Gurung et al, reported that menin normally prevents the over-activation of the canonical Hh signaling pathway in pancreatic islets, repressing expression of GAS 1, a crucial co-factor for Hh ligands binding to PTCH1 receptor (78).

Menin potently suppresses Hh signaling binding the GAS 1 promoter and recruiting protein arginine methyltransferase 5 (PRMT5), a negative transcriptional regulator which dimethylates protein arginine residues, such as histone H4 arginine 3 and histone H3 arginine 8 at this target gene.

MEN1 mutations reduce the interaction between menin and PRMT5 and the repressive dimethylation at GAS 1 promoter both in vitro and in beta cells in vivo. Gurung et al showed that loss of menin enhances Hedgehog (Hh) signaling in murine pancreatic islets and may contribute to increasing beta cell proliferation (78).

Recently Gurung et al. showed that menin can directly repress expression of GLI1 epigenetically via the histone H4 arginine 3 methyltransferase protein PRMT5, independently of the canonical Hedgehog Signaling pathway. Menin binds to the GLI1 promoter and recruits PRMT5 and its histone methylation negatively affects binding of the active GLI1-HDAC complex to the GLI1 promoter with a consequent transcriptional repression (81). Loss of menin lead to increase GLI1 transcriptional activity: upon MEN1 mutations, GLI1 and its target genes, including PTCH1 and c-Myc, resulted elevated in absence of a Hedgehog pathway activating ligand.

The direct non canonical GLI1 activation, independent of mutations in Hh pathway components, may play a role in tumorigenesis of endocrine organs (82).

To date, target-based therapy against MEN1 syndrome is currently lacking, but considering the crosstalk between menin and the Hh effectors, Hh antagonists may provide an effective therapy for treating neuroendocrine tumors with MEN1 mutation.

1.5.2 PARAFIBROMIN AND HH

Parafibromin appears to be involved in the activation of Hedgehog pathway and it is required for the expression of specific Hh target genes.

The detailed way of how nuclear GLIs co-factors are recruited and functionally cooperate to regulate transcription and mediate direct chromatin remodeling of all the Hh target genes remain doubtful: the C-terminal activation domain of GLI3 and Ci, the single *Drosophila* Gli, has been reported to interact with CREB binding protein (CBP) which has HAT activities involved in transcription control (82, 83). Moreover, the C-terminal GLI/Ci domain contains a motif comparable to a consensus binding element for the TATA-box recognition component TAFII31 (84).

Mosimann et al. provided evidences for the involvement of parafibromin/Hyrax as a novel GLI/Ci binding partner and as a positive component in Hh signaling. Impairment of Hyrax function decreases Hh signaling activity in *Drosophila* cell culture and lead to a decrease of Hh target gene expression in vivo, while RNAi-mediated knockdown of parafibromin decreased the transcriptional activity of GLI1 and GLI2 in human cell culture (85).

Like β -catenin, GLIs/Ci directly bind the N-terminus of parafibromin/Hyrax via the domain of interaction with Su (fu) known as Region 1, a highly conserved recruitment site in the N-terminal portion of all the GLIs/Ci factors. The parafibromin region involved in GLI proteins interaction includes amino acids 200-343.

These evidences suggests the role of parafibromin as a GLI/Ci auxiliary factor and the involvement of the PAF1 complex to control Hh target gene expression in human cells.

The N-terminal parafibromin domain also contains residues for binding to β -catenin: GLI and β -catenin proteins seem to use a common site for parafibromin binding, perhaps interacting with the PAF1 complex to increase the expression of their target genes (85).

1.6 INTEGRINS

Integrins are heterodimeric cell surface receptors that mediate cell adhesion to the extracellular matrix (ECM) and are essential for embryonic development, proliferation, survival, adhesion, differentiation, migration of cells. The integrins family comprises 18 α and 8 β subunits that, if combined each other, may formed at least 24 distinct $\alpha\beta$ -heterodimers (86, 87). Specific integrin heterodimers recognize own ECM proteins like collagen, fibronectin and laminin. For instance, integrins αv and $\alpha 5\beta 1$ preferentially bind the RGD sequence on their respective ligand (88).

Integrin receptor is composed by a large extracellular ligand-binding domain, a short transmembrane domain and a small intracellular domain that lacks kinase activity. Upon ligand binding, integrins undergo a conformational changes and by clustering, they recruit and activate kinases and scaffolding molecules to focal adhesions (FA) in order to initiate a trasduction signaling pathway (89). FA are a distinct areas at the cytoplasmic face of the cell membrane and include a variety of intracellular kinases and adaptor molecules regulating cellular motility, survival, proliferation and differentiation such as: Focal adhesion kinase (FAKs), Src family kinases (SFKs), Integrin- linked kinase (ILK), Particularly interesting new cysteine-histidine rich protein (PINCH), Non-catalytic tyrosine kinase adaptor protein 2 (Nck2) and p130 CRK-associated substrate (p130, CAS or BCAR1). Moreover, FA mediate the connection of integrins to the cellular actin cytoskeleton by recruiting proteins such as talin, paxillin, parvins, α -actinin and vinculin (90-92).

The integrin family is crucial for the initiation, progression and metastasis of solid tumors. In several tumor cells, the expression of particular integrins can influence the malignant potential and the progression of neoplasia (89).

Integrins seem to have a dual role in enhancing cell survival or inducing apoptosis.

ECM ligated integrins trasduce positive survival signals thourght increasing expression of BCL-2 or FLIP and activation of PI3K-AKT pathway or nuclear factor κ B (NF- κ B) signalling (93-95). Unligated integrins can promote

pro-apoptotic cascade in a process termed integrin-mediated death (IMD) by recruiting and activating caspase 8. However, some tumors resistant to IMD, can survive in an anchorage-independent manner, resulting in the ability to metastasize (96).

Recent studies reported that some growth factors receptors and oncogenes require specific integrins to enhance tumorigenesis and metastasis. The cooperation between integrin $\alpha 6\beta 4$ and EGF receptors family member ERBB2, induces tumor formation and invasion in patients with breast cancers (97).

Moreover, integrins are also expressed on the surface of tumor-associated host cells such as endothelial cells, fibroblasts, pericytes, bone marrow-derived cells, platelets where are involved in cancer progression by mediating angiogenesis and inflammation. The integrins $\alpha 11\beta 3$ on platelets and $\alpha v\beta 3$ on tumors cells interact through the binding of the same ECM protein fibronectin. This interaction induces tumor cells arrest in tumor-associated blood vessels that show structurally and biologically compromised characteristics, facilitating tumor cells intravasation and metastasis in various sites (98, 99).

ITGA2B, also known as platelet glycoprotein $\alpha 11\beta 3$, is the most abundant receptor on circulating platelets surface where it is usually inactive. If $\alpha 11\beta 3$ were in an active state, platelets would aggregate leading to thrombosis. So ITGA2B takes a very important role in homeostasis (100): in fact, mice lacking $\alpha 11\beta$ or $\beta 3$ subunit shows a bleeding disorder that mimic the human genetic disease Glanzmann thrombasthenia (GT) (101). ITGA2B plays an important role in the hematopoietic stem cell and megakaryocyte/platelet functions (102).

$\alpha 11\beta 3$ is dependent on its membrane-proximal cytoplasmic domain to maintain an inactive state. Deletion of the $\alpha 11\beta$ or $\beta 3$ cytoplasmic domains renders the $\alpha 11\beta 3$ integrin constitutively active. Partial truncations of the $\beta 3$ cytoplasmic domain maintain $\alpha 11\beta 3$ in a low affinity state (103).

Following platelets activation, $\alpha 11\beta 3$ is activated within the cell, so it can bind fibrinogen, von Willebrand factor and fibronectin to form a bridge for the aggregation with other platelets (104).

Studies have revealed a tight link between integrins expressed on tumor cells and tumor microenvironment platelets in the cancer progression. Both elevated number and activated platelets have been found in cancer patients (105). Moreover, several data proved that platelets may contribute to the spread of cancer from a primary site to a different secondary site: recent findings revealed how ITGA2B is crucial for hematogenous metastasis of human breast carcinoma MDA-MB-231 cells (106).

Xiaolin Lu et al. reported that prognosis of cancers like glioblastoma, gastric cancer, ovarian and melanoma may be correlated with integrin expression. They identified ITGA2B as independent prognostic factor of overall survival in patient affected by clear cell renal cell carcinoma (ccRCC). Expression profiling analysis was performed among the 525 patients with ccRCC collected for the study. It emerged a high expression level of ITGA2B correlated with a poor prognosis (107).

ITGA3 or $\alpha3\beta1$ integrin is a receptor for the extracellular matrix (ECM) and belongs to $\beta1$ family of integrins. It is encoded as a preproprotein and proteolytically processed to generate light and heavy chains that comprise the $\alpha3$ subunit. This subunit joins with a $\beta1$ subunit to form an integrin that interacts with extracellular matrix proteins including members of the laminin family. It has been reported that $\alpha3\beta1$ preferentially binds laminins 5, 10, and 11 (108-110). Moreover, expression of gene encoding $\alpha3\beta1$ may be correlated with breast cancer metastasis.

Integrins have been reported to have more complex functions than the traditional ability to bind the ECM components.

Studies on $\alpha3\beta1$ integrin in keratinocytes suggested a role as a transdominant inhibitor of other integrins. In this case, it was observed an increased adhesion to fibronectin and type IV collagen mediated by other integrins, if cells are deficient for $\alpha3\beta1$ (111).

Recently it was found a novel role for $\alpha3\beta1$ integrin as a component of a cell-cell adhesion complex in epithelial cells. $\alpha3\beta1$ integrin interacts with the tetraspanin CD151, a cell surface molecule with four transmembrane domains, to directly stimulate cadherin-mediated adhesion in epithelial cells.

In vivo, $\alpha3\beta1$ integrin and CD151 are coexpressed in a variety of epithelial cells, including basal keratinocytes of the skin and glomerular epithelial cells of the kidney (112). So in addition to $\alpha3\beta1$ binding laminin integrins involved in cell–matrix adhesion, another pool of $\alpha3\beta1$ integrins exists in epithelial cells that are located along baso-lateral membranes and associated with the cadherin-catenin complex (113).

Integrins inhibitors have been approved and are currently used in cardiovascular disease, Crohn's disease, multiple sclerosis. Several integrins inhibitors have also been tested in clinical trials for cancer therapy including monoclonal antibodies and RGD peptide mimetics (111). Preclinical studies showed that integrins antagonists inhibit tumor growth by affecting both tumor cells and tumor-associated host cells (114).

CHAPTER 2: OBJECTIVES

2.1 AIM OF THE STUDY

The project aims to identify the genetic causes leading to the development of a KP and to detect a set of biomarkers useful for a possible unequivocal, early first diagnosis of KP.

NextGen strategy was applied to different HPT-JT families consisting of one or more affected (and carriers of a CDC73 mutation) subjects, non-affected carriers and healthy controls (not carriers). We decided to apply the NGS analysis to familial cases rather than sporadic ones in order to, possibly, reduce the intrinsic variability caused by different genetic backgrounds.

Comparing the data obtained from Whole Exome Sequencing and Expression Profiling of recruited families, it could be possible to infer data about possible biomarkers detectable within the blood (serum/ urine) to:

- better understand the molecular events leading to tumor development;
- to address the best surgical choice in order to reduce the risk of recurrence and to extend the disease free survival.

This approach has been applied to 5 families (out of the less 90) families worldwide identified (<https://cdc73.css-mendel.it/>) with malignant parathyroid lesion and constitutional mutation of the CDC73 gene and a very rare family with MEN1 mutation associated to KP (rather than to benign lesion).

At least one carrier, a proband and a control were selected for each family. Clinically, probands had hyperparathyroidism due to malignant parathyroid lesion. From a histologic point of view, in all the 5 cases, the parathyroid lesion showed clear and unequivocal indications of malignancy, such as: i) invasion of the capsule; ii) a high number of mitotic figures; iii) adherence to peripheral tissues and vascular or perineural invasion. For each family, it was also possible to characterize several relatives with pHPT and/or maxillary or parathyroid lesions.

In MEN1 family, the proband, the brother and the daughter were affected by hyperparathyroidism with pancreatic lesion, lipoma and melanoma. The proband and the brother were also operated for malignant parathyroid

lesion, histologically diagnosed as KP. Screening of the MEN1 coding sequence identified a mutation in exon 9, c.1252G> A /p.D418N, shared by all the affecteds and also by a clinically health nephew.

The multi-faceted research approach based on 5 HPT-JT families, basically consists of three major tasks to be developed sequentially.

2.1.1 FIRST TASK: IDENTIFICATION OF GENES/PROTEINS/ MOLECULAR PATHWAYS ASSOCIATED TO KP BY WES AND EXPRESSION PROFILING

1) Whole Exome Sequencing (WES) to be applied on: germline DNA extracted from blood of the proband, and on germline DNA of an unaffected (carrier) and of a not carrier (control) relative;

2) the Expression Profiling (EP) assay to be performed on: RNA extracted from the same specimens.

2.1.2 SECOND TASK: DRUG TEST ON HEK293 CELL LINES

Human embryonic kidney (HEK293) cell lines were transfected with eukaryotic expression vectors carrying WT or mutated CDC73 gene: 5 different mutations were tested (1 out of the 5 previously identified in one of the HPT-JT families under study).

Transfected cell lines were treated with the Bortezomib (10 μ M), a well-known proteasome inhibitor, yet used in clinics for the treatment of tumor diseases such as multiple myeloma (115).

The following assays were performed:

- cell vitality, in order to investigate whether the Bortezomib is able to influence the tumor growth;

- Western Blot, in order to verify whether the Bortezomib is able to restore the expression levels of mutated parafibromin.

- Colony agar formation assay, in order to verify whether the drug is able to reduce the cellular proliferation (this latter assay is still ongoing).

2.1.3 THIRD TASK: VALIDATION OF THE VARIANTS IDENTIFIED, IMMUNOHISTOCHEMISTRY (ONGOING)

1) After prioritization, some of the variants resulted from the WES will be searched by Sanger sequencing on a selected validation cohort consisting of sporadic parathyroid, atypical and classic, adenoma tissues.

2) proteins resulted as more suggestive from WES will be assayed by IHC on FFPE tissues of the validation cohort. As other possible option, proteins yet reported in literature as differentially expressed in KP or atypical or classic adenoma (116) will be assayed by IHC as well on the validation cohort.

2.2 PATIENTS

2.2.1 PHENOTYPIC/GENETIC DESCRIPTION OF THE 5 HPT-JT FAMILIES UNDER STUDY

Family I (Figure 1a)

The index case first came to our attention at 29 yr, for a hypertensive crisis and acute heart failure. He had nephrocalcinosis with chronic renal failure and a serum calcium of 10.2 mg/dl (reference interval, 8.2–10.4 mg/dl). The family history was negative for parathyroid disease, but renal stones were reported in siblings and more distant paternal relatives. After 6 months, serum calcium was 11.5 mg/dl, creatinine = 2.1 mg/dl, phosphate = 2.45 mg/dl, intact PTH = 160 pg/ml (reference interval, < 72 pg/ml). Ultrasonography of the neck showed a 15-mm nodule behind the left lobe of the thyroid and parathyroid scintigraphy with ^{99m}Tc-SestaMIBI showed uptake at the base of the left thyroid lobe. The patient underwent left hemithyroidectomy and excision of a 1.5-cm hard parathyroid nodule.

Microscopy revealed oxyphil cells arranged in a trabecular or nesting pattern and nonoxyphil cells of the usual type with nondescript diffuse architecture and fibrous banding. Mitotic figures and capsular invasion were observed, without evidence for metastatic spread suggesting a diagnosis of atypical parathyroid adenoma. Moreover, another normal parathyroid gland was identified and biopsied. Two weeks postoperatively, serum calcium decreased to 8.32 mg/dl while PTH decreased to 42 pg/ml.

The 69-year old mother of index case was apparently clinically unaffected, despite her carrier status while, there was a strong paternal family history for renal stones. With identification of the CDC73 gene mutation, more extensive monitoring was initiated. Jaw pantomograms and renal ultrasonograms were performed in carriers, but were uniformly negative for tumors or cysts, although a number of carriers and noncarriers showed renal stones (Table 1). By transabdominal ultrasonography, uterine leiomyomata were found in 2 out of 5 women. Serum calcium concentrations in first-degree relatives of the index case

were normal, although the serum PTH was modestly elevated in 3 of 6. Ultrasonography of the neck with attention to the thyroid gland and surrounding structures was performed and was positive in 2 of these relatives, initiating a diagnostic work-up. In a sister (II:8), a 10-mm nodule was observed below the left lobe of the thyroid, consistent with a parathyroid gland (Figure 1b). Serum calcium was 10.0 mg/dl, and the ionized fraction, 1.26 mmol/liter, but serum PTH was 101 pg/ml (reference interval, < 72 pg/ml). The patient underwent excision en bloc of the left thyroid lobe, isthmus, and parathyroid nodule and removal of the lymph nodes surrounding the laryngeal recurrent nerve. A hard 1.0-cm parathyroid nodule was found and histopathologic examination revealed chief cells with intratumoral dense fibrous banding, mitotic figures, and full-thickness capsular invasion extending into the surrounding tissues but not the adjacent lymph nodes, warranting a diagnosis of parathyroid carcinoma. Three normal parathyroids were identified, and the ipsilateral gland was excised with the left lobe of the thyroid. The two contralateral glands were biopsied and found to be histologically normal. Postoperatively, serum PTH and calcium decreased to 66 pg/ml and 8.88 mg/dl, respectively. In a brother (II:1), an extrathyroidal nodule below the right lobe was observed on ultrasonography and SestaMIBI scan, but serum calcium (9.92 mg/dl), blood ionized calcium (1.25 mmol/liter), and PTH (56 pg/ml) were normal. The patient elected to undergo excision en bloc of the right thyroid lobe, isthmus, and suspected parathyroid nodule. Histologically, the nodule was a 1-cm extrathyroidal goiter nodule, not a parathyroid tumor. Among the more distant relatives of the index case, a 27-yr-old carrier niece (III:3) was found to have an increased serum calcium (11.8 mg/dl), ionized calcium (1.54 mmol/liter), and serum PTH (106 pg/ml). Neck ultrasonography showed a spindle nodule in the posterior aspect of right thyroid lobe, which was also positive on SestaMIBI scan. Aspirate fluid contained high PTH (1000 pg/ml) and low thyroglobulin (0.5 ng/ml) concentrations. Excision en bloc of the thyroid lobe with nodule, isthmus, and lymph nodes surrounding the laryngeal recurrent nerve revealed a 2-cm atypical parathyroid adenoma with capsular invasion. Two months postoperatively, serum calcium and PTH were 8.72 mg/dl and 55 pg/ml, respectively. As part of a second annual screening of all

affected individuals and asymptomatic carriers, the index case (now age 41) underwent repeat neck ultrasonography, and an extrathyroidal nodule below the remaining right lobe was noted. Serum calcium (9 mg/dl), blood ionized calcium (1.25 mmol/liter), and PTH (61 pg/ml) were in the normal range. Aspirate fluid from ultrasonographically guided fine-needle aspiration showed a high PTH (1000 pg/ml) and low thyroglobulin (0.2 ng/ml) and consistent with a parathyroid origin. The patient underwent excision en bloc of the thyroid lobe with the nodule and the lymph nodes surrounding the laryngeal recurrent nerve. Histologically, neoplastic parathyroid tissue was found throughout the 1.2-cm encapsulated nodule. Capsular invasion was apparent, but without invasion of surrounding tissues, suggesting the diagnosis of a second primary atypical parathyroid adenoma. Another parathyroid gland was also identified at surgery and excised, but was histopathologically normal.

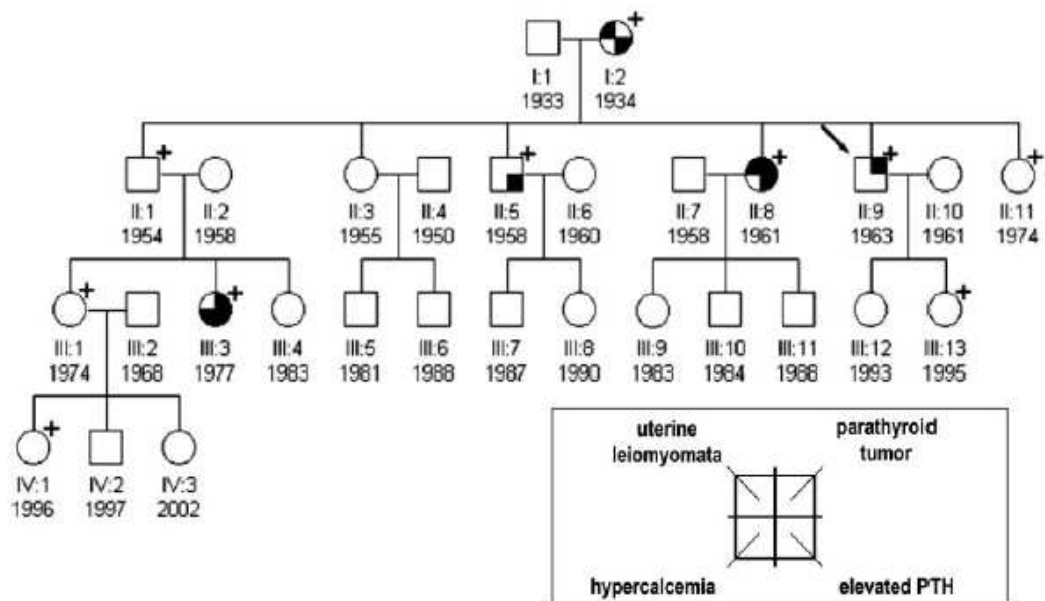


Figure 1a. Family pedigree of Family I. Clinical status is indicated by open symbols (unaffected or unknown) and filled symbols (affected). Filled quadrants indicate a diagnosis as indicated in the inset legend. Proband is indicated by the arrow. The presence (+) or absence (-) of a mutation in tested family members is shown.

Clinical findings in carriers from the HRPT2-positive kindred

	Age	Sex	Ca _t	Ca _i	PTH	Vit D	Parathyroid pathology	Jaw	Ultrasonography			
									Neck	Kidney	Pelvis	
Affected carriers												
II-9 (1) ^a	29	M	11.5	ND	160 ^b	ND	Atypical adenoma	ND	+	NC		
II-9 (2) ^a	41	M	9.0	1.25	61	109.0	Atypical adenoma	-	+	NC		
II-8	42	F	10.0	1.26	101	28.0	Carcinoma	-	+	S		M
III-3	27	F	11.8	1.54	106	35.5	Atypical adenoma	-	+	S		-
Asymptomatic carriers												
I-2	69	F	9.65	1.20	84	38.0 ^c		-	-	-		M
II-1	49	M	9.92	1.25	56	18.3		-	+ ^d	S		
II-5 ^e	45	M	10.0	1.28	82	33.0		-	-	S		
II-11	29	F	9.65	1.20	55	19.0		-	-	-		-
III-1	29	F	9.33	1.12	47	61.0		-	-	-		-
III-13	8	F	10.1	1.29	42	25.5		ND	-	-		-
IV-1	7	F	10.5	1.27	14	39.3		ND	-	-		-

Ca_t, Total serum calcium (reference range, 8.2–10.4 mg/dl in adults and 8.8–10.8 mg/dl in children); Ca_i, ionized serum calcium (reference range, 1.12–1.31 mmol/liter); PTH, reference range, 11–72 pg/ml; Vit D, 25OH vitamin D (reference range, >50 nmol/liter). Jaw, Jaw pantomogram results: -, negative; ND, not determined. Neck ultrasonography, presence (+) or absence (-) of extra thyroidal nodule. NC, Nephrocalcinosis; S, stones; M, leiomyomata.

^a II-9 (1), Index case at age of 29; II-9 (2), index case at age of 41.

^b Reference range, 12–55 pg/ml.

^c Correction of vitamin D insufficiency over 1 yr was followed by normalization of the 25OHD level (to 64 nmol/liter) and serum PTH (to 58 pg/ml), while ionized calcium is essentially unchanged (1.21 mmol/liter).

^d II-1, At surgery, an extrathyroidal goiter nodule was excised (see text).

^e Patient lost to follow-up.

Table1. Clinical and biochemical data of proband and relatives.

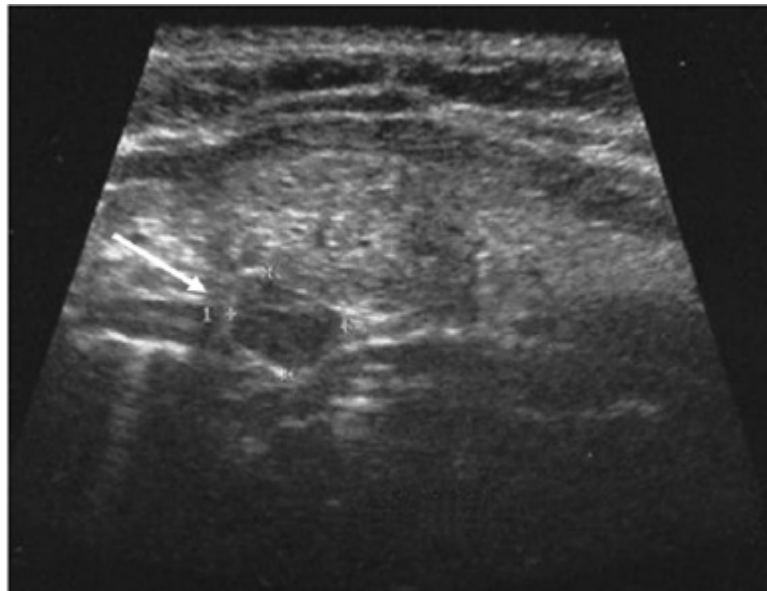


Figure 1b. Ultrasonography of the neck in patient II-8 shows an extrathyroidal 10-mm diameter nodule below the left thyroid lobe (white arrow) consistent with a parathyroid mass.

Further considerations on this family.

In this family, we report a phenotype restricted to parathyroid neoplasms. Although the penetrance is clearly reduced, as evidenced by the unaffected status of the carrier mother of the proband, the predisposition to carcinoma or atypical adenoma, the latter potentially malignant, rather than

adenoma, is high. Such a variable penetrance underscores the importance of appropriate surveillance.

Moreover, in our index case, the appearance of a second parathyroid neoplasm 12 yr after the first had been completely resected indicates that more aggressive surgical intervention with ipsilateral hemithyroidectomy and total parathyroidectomy may be warranted in some. On the other hand, the ability to detect the tumor at an early stage may mean that close surveillance is sufficient, given the clinical burden and costs that lifelong replacement therapy with calcium and vitamin (or, in the future, recombinant human PTH) can represent. Experience with a single family cannot define which surgical approach is indicated in others, but our observations can contribute to the development of better guidelines.

Family II (Figure 2)

A 28-yr-old female presented with a slowly growing mass for two years in her left mandible. Laboratory data revealed severe hypercalcemia (total serum calcium 16 mg/dl) and elevated levels of parathyroid hormone (660 pg/ml). Phosphorus and alkaline phosphatase levels were 1.9 mg/dL and 948 IU/L, respectively, and renal functions were normal. The patient also suffered from severe osteoporosis, renal colics and a lytic lesion in the right tibia. Ultrasound of the neck suggested a right inferior parathyroid tumor (20 mm) that was confirmed by a ^{99m}Tc sestamibi scan. The parathyroid tumor was excised under general anaesthesia and histologically diagnosed as a parathyroid carcinoma. The removal of the parathyroid tumor resulted in a severe hungry bone syndrome, which required administration of calcium and vitamin D. Two months after surgery the serum calcium and parathyroid hormone levels reversed to the normal range. Six months later the left mandible tumor was removed and histological examination confirmed the diagnosis of ossifying fibroma. The total bone mineral density increased 6 months after parathyroidectomy. Two years after treatment the patient is well with no evidence of tumor recurrence and a complete recovery of facial deformity. Anamnestic analysis of all available relatives from the paternal side revealed that subject II:1 was operated in the

past for a parathyroid adenoma, while subject II:2 was found to be operated for uterine leiomyomata. No other clinical data were available from the other relatives at the time of this report.

Molecular screening of germline DNA of the proband revealed a novel germline mutation of the exon 15 of the CDC73 gene, c.1379delT, that is predicted to introduce a premature stop codon at position 478 (p.L460Lfs*18). Subsequent screening of available relatives revealed that also the proband's father (II:4), uncle (II:6) and aunt (II:1) (both from the paternal side) are carriers of the same deletion (Figure2). Since subject II:2 was found to be negative upon the screening, the uterine leiomyomata in this subject are not considered to be part of the classical hyperparathyroidism-jaw tumors (HPT-JT) syndrome. The c.1379delT deletion is novel, since it has not been reported either in the Mutation Discovery Database (http://www.mutationdiscovery.com/md/MD.com/home_page.jsp, last access: June 2014), nor in the 1,000 genomes database (<http://www.ncbi.nlm.nih.gov/variation/tools/1000genomes>, last access: June 2014).

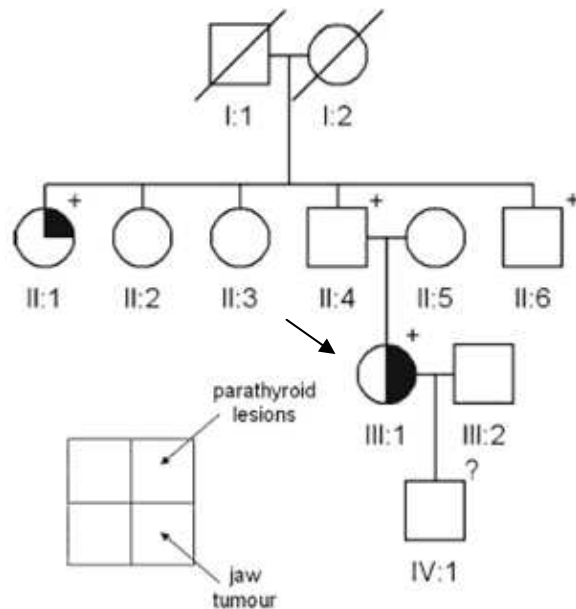


Figure2. Family pedigree of Family II. Clinical status is indicated by open symbols (unaffected or unknown) and filled symbols (affected). Filled quadrants indicate a diagnosis as indicated in the inset legend. Diagonal slash mark through a symbol indicates deceased. Proband is indicated by the arrow. The presence (+) or absence (-) of a mutation in tested family members is shown.

Further consideration on this clinical case.

While the N-terminal moiety of the parafibromin protein contains NLS and NoLS sequences, i.e., nuclear and nucleolar localization signals, respectively (117, 51), the central core (227-413 aa) encompasses several binding domains for β -catenin (47), the GLI protein (47), the PAF1 complex (44) and SV40 large antigens (50). However, no functional domain has so far been attributed to the C-terminal moiety. More recently, a study of a putative yeast orthologue (118) and a crystallographic analysis of human parafibromin have raised the possibility that the C-terminal domain may contain a GTPase-like fold, whose enzymatic activity has been lost during evolution (119).

It has been hypothesized that the initial binding to GTP diverged towards other proteins and that, in vertebrates, the C-terminal moiety of parafibromin may play an important role in other, yet unidentified, protein-protein interactions (120).

In this family a novel CDC73 gene deletion, namely c.1379delA, affecting the C-terminal moiety of the encoded protein was identified. Western blot and immunohistochemistry proved that the deletion, resulting in loss of the last 70 residues, makes the corresponding mutant protein subjected to proteasome degradation leading to the loss of up to 2/3 of its expression. Moreover, the mutant induced a significant overgrowth of transfected cells. This result was obtained in the presence of endogenous parafibromin, in line with a previous report showing an interfering effect of mutant parafibromin on the endogenous wild-type form (121).

For two carriers (II:4 and II:6) of the CDC73 deletion in the proband's family, anamnestic data were not available at the time of the report. However, it is anticipated that they will also manifest at least some of the symptoms, taking into account that the overall penetrance of CDC73 mutations is ~70% (122).

The in silico modelling analysis indicates that the CDC73 deletion may cause a conformational change similar to that reported for a few other mutations, with a predicted stronger affinity of GTP for the mutant form. Taking into account that the protein does not have any GTPase activity (118, 119), it is anticipated that the mutation may affect the affinity for one or more other (not

yet identified) protein interactor(s). As yet, however, it remains to be established whether the observed pathogenicity is due to the degradation of mutant protein, the concurrent loss of binding to other protein partners, or both. The identification of such putative C-terminal binding partners may help to elucidate this issue and, ultimately, contribute to our understanding of the CDC73-associated phenotype.

Family III (Figure 3)

The index case was diagnosed with PHPT in 2000 when she was 29. In 2006 she was operated for hemithyroidectomy (sx) and parathyroidectomy (sx) and a KP along with papillifer micro thyroid carcinoma where excised and histologically diagnosed. After the first operation, the proband was further re-operated other three times (the last one in Apr 2013) for local recurrent malignant parathyroid lesions or located into the trachea epithelium. She was also affected by uterine leiomiomas and by a 8 mm lesion located in the adipose tissue under the right jaw. At the last follow up, 6 months ago, iCa was elevated (= 1.52; vn 1.12-1.31) due to the presence of an additional lesion of 2x1 cm located into the paratracheal region, suggestive of a reoccurrence of the disease. Her older brother, carrying for the same mutation, was admitted for the first follow up in 2007 and he has been found always in healthy status, up to the last control, 6 months ago.

CDC73 gene molecular screening identified a novel frameshift mutation of the exon 7, namely c.518_521delTGTC, that was predicted to cause a premature stop codon at the residue 201 (p.S174Lfs*27). The mutation was confirmed in the unaffected brother, while it was impossible to analyze the third brother.

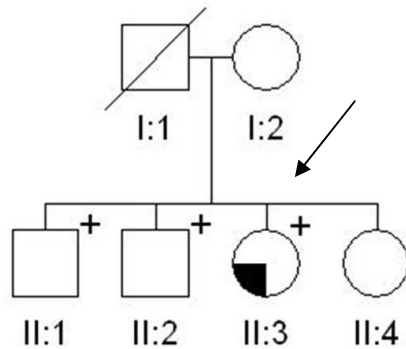


Figure3. Family pedigree of Family III. Clinical status is indicated by open symbols (unaffected or unknown) and filled symbols (affected). Filled quadrant indicates a diagnosis of carcinoma. Diagonal slash through a symbol indicates deceased. Proband is indicated by the arrow. The presence (+) or absence (-) of a mutation in tested family members is shown.

Family IV (Figure 4)

The proband was operated for the first time in 2013 when he was 22 years old, for the excision of a histologically diagnosed bone tumor with giant cells. After one he was re-operated for the same tumor at the same localization and then biochemical and instrumental screening revealed hypercalcemia (Ca = 15.6 mg/dL; vn 8.1 – 10.4, PTH = 1469 pg/mL; vn 10-65) due to a parathyroid lesion that was excised and a histological diagnosis as KP. Other analysis revealed concurrent hypogammaglobulinemia confirmed in the 53-year-old mother, who carries the same mutation and was operated for breast cancer and hysterectomy due to multiple uterine leiomyomata. Other anamnestic data reported renal lithiasis in the proband, mother and grandmother (on the maternal side). Genetic screening led to the identification of a novel CDC73 frameshift mutation of the exon 3, namely c.251delC, that was predicted to cause a premature stop codon at the residue 109 (p.P84Lfs*25). The familial screening identified the mutation in the mother and in the unaffected brother.

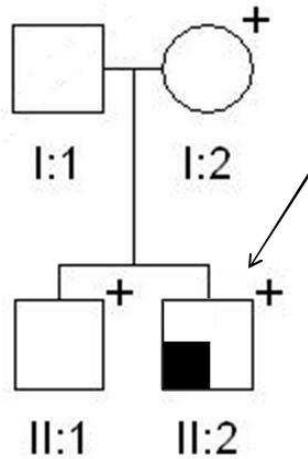


Figure 4. Family pedigree of Family IV. Clinical status is indicated by open symbols (unaffected or unknown) and filled symbols (affected). Filled quadrant indicates a diagnosis of carcinoma. Proband is indicated by the arrow. The presence/absence (+/-) of a mutation in tested family members is shown.

Family V (Figure 5a)

The index case (Figure 5a, II:6, 37 ys male) was referred by the Unit of Endocrinology to the Medical Genetics Unit of Sant'Orsola Malpighi Hospital for a previous familial history of KP and adenoma. The older brother (II:3), affected by hypercalcemia and nephrocalcinosis, underwent resection of a fibroma of the maxilla in 1986 at 22 ys, then to a parathyroid adenoma and hyperplasia at 33 ys and finally to an ossifying KP with infiltration of the capsula and vascular invasion when he was 42. He deceased at 46 ys for the consequences of a pathologic femur fracture and presented diffuse metastases at the liver, pelvi and vertebrae. The mother (I:2) had undergone hysterectomy due to uterine leiomyomata at 38 ys and for a parathyroid adenoma at 62 ys. Biochemical assessment of the index case confirmed the diagnosis of hyperparathyroidism with severe hypercalcemia (serum Ca_{adj} = 14.9 mg/dL, nr = 8.4 – 10.2 mg/dL; PTH = 703 pg/mL, nr = 15-65 pg/mL). Imaging investigation (i.e. ultrasonography and Nuclear Magnetic Resonance of the neck) showed an extrathyroidal lesion (max diameter 2 cm) close to the left lobe that, after the surgery, histologically consisted of an ossifying KP with capsular infiltration and invasion of the vessels and of the surrounding tissues. Familial anamnesis also reported the niece (III:2)

operated on for uterine fibromas in 2012, at 23 ys. Other relatives did not present any symptoms correlated to the HPT-JT syndrome, while unrelated thyroid disease (multinodular goitre or autoimmune thyroiditis) was shared by almost all the subjects (Table 2).

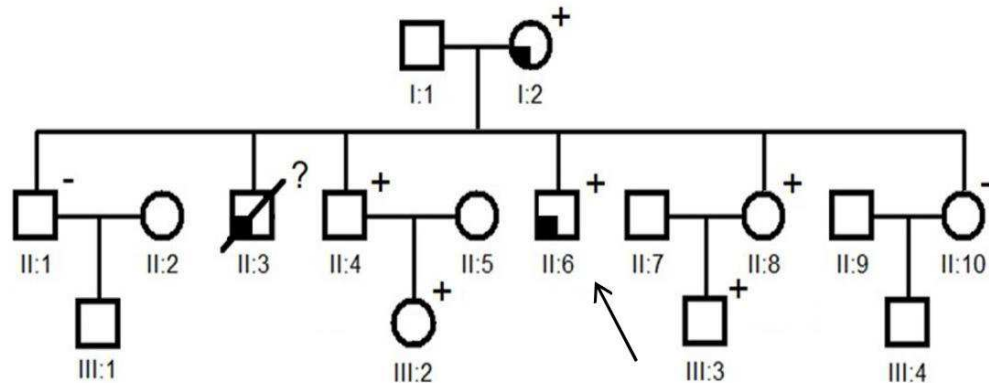


Figure 5a. Family pedigree of Family V. Clinical status is indicated by open symbols (unaffected or unknown) and filled symbols (affected). Filled quadrants indicate a diagnosis of adenoma (I:2) and carcinoma (II:3 and II:6). Diagonal slash mark through a symbol indicates deceased. Proband is indicated by the arrow, while the presence/absence (+/-) of the mutations or not yet tested (?) status is shown.

Subjects	Sex	Age at gene testing	HPT-JT Tumour (AaO)	serum Ca (age)	PTH (age)	Other manifestations (age)
I:2	F	68	- PA (62)	9.3 mg/dL (62) 8.8 mg/dL (70)	102 pg/mL (62) 23 pg/mL (70)	- uterine fibroids with hysterectomy (38) - multinodular goitre with left emithyroidectomy (45), non AT - multinodular goitre with right emithyroidectomy (62), non AT - rheumatic polyarthritis (64) - no osteoporosis, no renal lithiasis
II:3	M	NP	- fibroma of the maxilla (22) - PA + hyperplasia (33) - ossifying PC (42) - rib metastases from PC (46)	16.8 mg/dL (42)	1358 pg/mL	- hypercalcemia associated with nephrocalcinosis: parathyroidectomy left superior and inferior (33) - hospitalization for renal failure, nephrocalcinosis, hypercalcemia (42) - deceased at age 46 (diffuse metastases)
II:4	M	46	- parathyroid hyperplasia (48) - ossifying adenoma (48)	11.4 mg/dL (47)	90 pg/mL (47)	- mi cronophrilithiasis (47); - multinodular goitre (47) - AT (47) - no osteoporosis - total thyroidectomy and parathyroidectomy
II:6	M	44	- PC (37)	14.9 mg/dL (37)	703 pg/mL (37)	- chronic diarrhea (since pediatric age) nephrolithiasis (33) - multinodular goitre with follicular lesion at left lobe, total thyroidectomy (37)
II:8	F	42	/	9.3 mg/dL (42)	20 pg/mL (42)	- multinodular goitre (21) - right thyroidectomy (27) - no hypercalcemia, no parathyroid lesion
III:2	F	25	/	9.4 mg/dL (25)	33 pg/mL (25)	- uterine fibroids (23)
III:3	M	12	/	9.7 mg/dL (14)	26 pg/mL (14)	/

PA = Parathyroid Adenoma; PC = Parathyroid Carcinoma; AT = Autoimmune Thyroiditis; NA = Not Available; serum Ca normal range = 8.4 – 10.2 mg/dL; PTH normal range 15-65 pg/mL; NP = Not Performed

Table 2. Clinical and biochemical data of the subjects of the HPT-JT family carrying the large deletion.

The search of coding mutation of *CDC73* gene resulted unsuccessful. Then we applied an array CGH approach with specific DNA chip (Figure 5b) on the DNA belonging to the proband's mother. Partial deletion of the *CDC73* gene and the hemizygous status was detected.

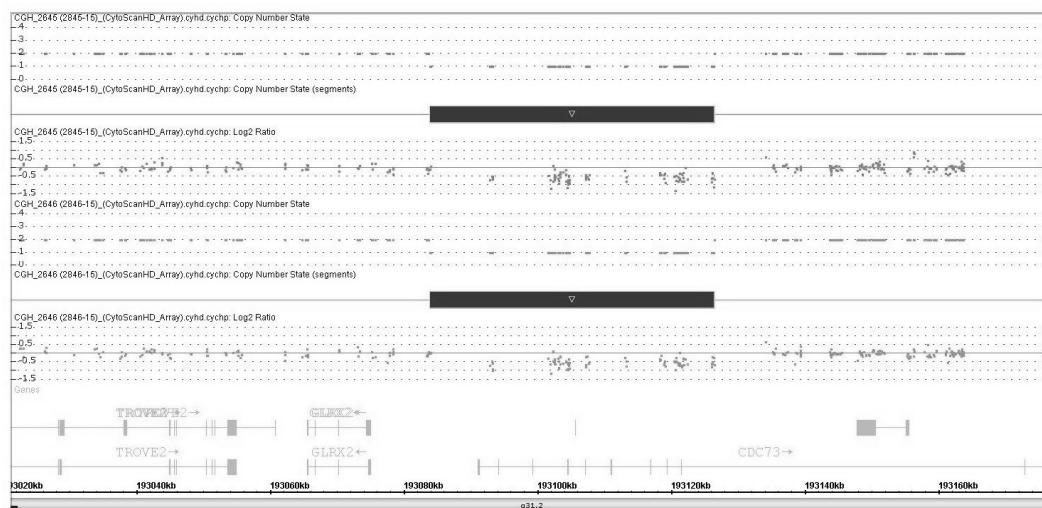


Figure 5b. CytoScan HD Array analysis results of the patients (proband and mother). Intensity data (log₂ ratio value) of each probe is drawn along chromosome 1 from 193.084 to 193.126 Mb (USCS Genome Browser build February 2009, hg19). The grey bar represents the 1q31.2 deletion identified, encompassing exons 1 to 10 of the *CDC73* gene.

The deletion involved the first 10 exons of the *CDC73* gene and was confirmed by MLPA (with the following breakpoints: left breakpoint 193, 083, 733-193, 083, 949 and the right breakpoint 193, 126, 404-193, 126, 441) (Figure 5c) and by RT-qPCR (Figure 5d). The analysis was then extended to the whole family and the deletion confirmed on all the living affected members and in some unaffected carriers.

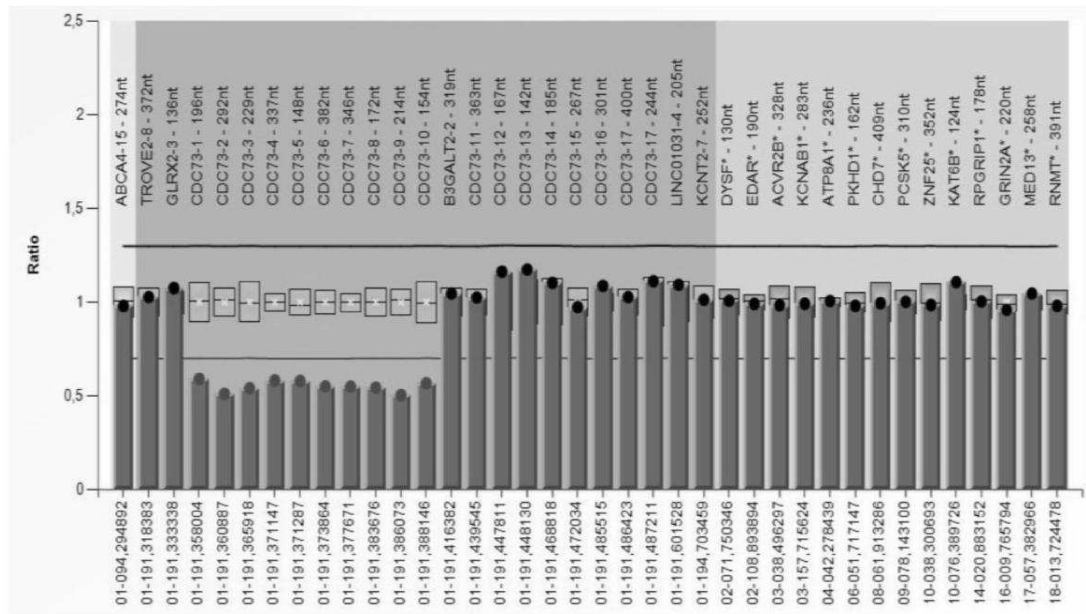


Figure 5c. Results of MLPA analysis show a large deletion of 1–10 exons of CDC73 gene in the proband.

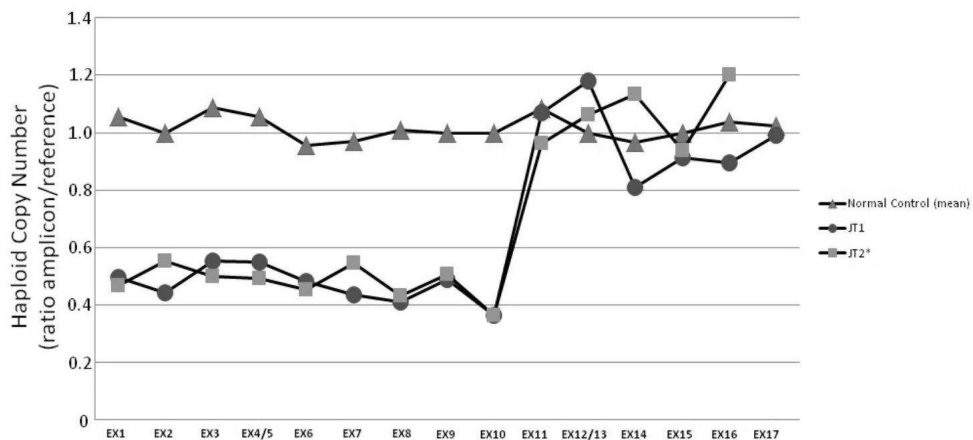


Figure 5d. Gene copy number of the seventeen CDC73 exons $\Delta\Delta$ of the proband and mother of Family V. The relative copy number was determined using the Ct method and was normalized to the human (GAPDH) gene and normal control sample. The figure shows that the patients carried hemizygous deletion in exons 1–10 of the CDC73 gene. Other exons have two normal copies. (Muscarella et al, manuscript in preparation).

2.2.2 SPECIAL CLINICAL CASE: FAMILY VI - MEN+KP

Family VI (Figure 6a)

We report a 61-year-old man (Figure 6a, II:4) admitted in the April 2013 at our Health Care Centre for follow-up of a pathologically diagnosed parathyroid carcinoma (size 7.3 cm) showing capsular invasion histologically and infiltration into the esophagus clinically.

During surgery another parathyroid gland was removed, histologically consistent with hyperplasia. The patient acknowledged a history of nephrolithiasis with repeated renal colic and the presence of bilateral adrenal lesions (each of 3 cm in diameter) were observed at abdominal ultrasonography and confirmed at computed tomography (CT). At admission, laboratory values were unremarkable. Initial assessment of available first-degree relatives (Figure 6a) revealed the presence of hypercalcemia and hypercalciuria with high levels of PTH in a brother (II:6; serum calcium albumin adjusted, (Caalb adj) = 11.84 mg/dL, nr: 8.4-10.2 mg/dL; PTH = 286 pg/mL, nr: 10-65 pg/mL) and a daughter (III:1; Caalb adj = 10,72 mg/dL, PTH = 77 pg/mL). In the brother, subsequent imaging investigation showed an extrathyroidal lesion in the upper left lobe of 4.6 cm that was removed, and a pathological diagnosis of parathyroid carcinoma was made (see below). In the daughter, two extrathyroidal nodules (1.4 cm and 1 cm in diameter) were detected at neck ultrasonography and confirmed by 99mTc-Sestamibi scan. However, they have not been biopsied or excised at the time of this report. Biochemical evaluation of the other relatives, the paternal nephew, one proband's brother and sister (Figure 6a: III:1, II:1 and II:3, respectively) was negative. The brother (II:6) had suffered from renal stones and had been operated on for an in situ melanoma and lipoma and during the follow up for such diseases, bilateral adrenal lesions had been discovered (see Table 3).

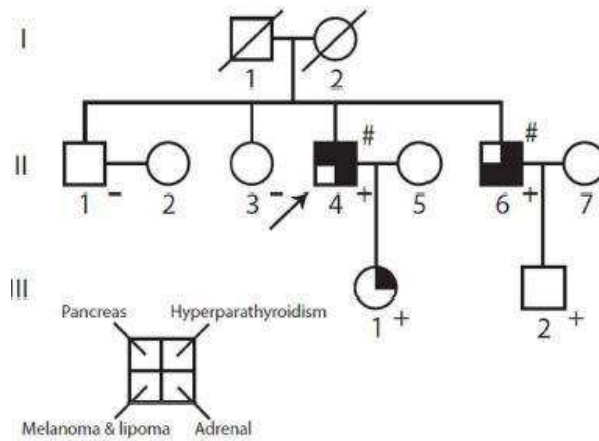


Figure 6a. Clinical status is indicated by open symbols (unaffected or unknown) and filled symbols (affected). Filled quadrants indicate a diagnosis as indicated in the inset legend. Histological diagnosis of carcinoma is indicated (#). A diagonal slash mark through a symbol indicates deceased. Proband is indicated by the arrow. The presence (+) or absence (-) of a mutation in tested family members is shown.

	Sex	Age	Ca ²⁺ _i ^a	PTH ^c	PHPT	Kidney Stones	Pituitary	Pancreas	Parathyroid	Size (cm)	Adrenal	Other	MEN1	CDC73	IHC	
															menin	parafibrin
II:4 ^a	M	62	NA	NA	yes	yes	no	multiple PNET	carcinoma, hyperplasia	7.3	yes	prostate	p.D418N	neg	NP	NP
II:6	M	55	1.48	286	yes	yes	no	no	carcinoma	4.6	yes	melanoma lipoma schwannoma	p.D418N	neg	pos	pos
III:1	F	26	1.34	77	yes	yes	NA	NA	NA	1.4/1	no	no	p.D418N	NP	/	/
III:2	M	21	1.30	43	no	no	no	no	no	/	no	no	p.D418N	NP	/	/

^a: proband; ^b: normal range: 1.12-1.32mmol/L; ^c: normal range: 10-65 pg/mL; NA = Not Available; NP = Not Performed; / = Not Applicable; PNET = pancreatic neuroendocrine tumour; PTH = parathyroid hormone; PHPT = primary hyperparathyroidism; IHC = immunohistochemistry; neg = negative; pos = positive

Table 3. Clinical and molecular features of proband and relatives.

No coding gene mutation or genomic deletion at the CDC73 genetic locus (1q31.2) was detected; no large genomic deletion was found at the MEN1 genetic locus (11q13.1). Screening of the MEN1 coding sequence identified a previously reported mutation in exon 9, namely c.1252G>A, encoding p.D418N (Figure 6b). Screening of the available relatives confirmed carrier status in the two hypercalcemic first degree relatives (II:6 and III:1), but also in a currently normocalcemic nephew (III:2). An unaffected sister and brother (II:1 and II:3) were both negative. No loss of heterozygosity (LOH) was detected in the DNA extracted from the carcinomatous tissue of the proband's brother.

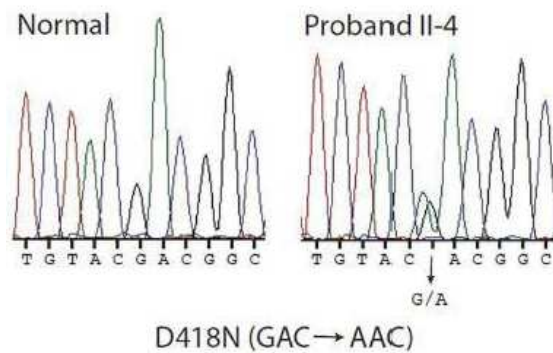


Figure 6b. Detection of a mutation in the MEN1 gene. Direct sequence analysis of the exon 9 genomic DNA amplicon of proband II-4 (right) revealed a heterozygous G to A transition encoding the missense D418N mutation compared with an unrelated normal individual (left).

Pathologic findings and IHC of tumors excised from MEN1 subjects.

As previously stated, the main concern about parathyroid carcinoma is making an irrefutable diagnosis that is usually only made by the pathologist. More and more in these clinical cases, the pathological diagnosis was made accordingly to according to the 2004 World Health Organization classification criteria of Tumors of Endocrine Organs. And, due to the rarity of these occurrences, the diagnosis was further blindly reviewed by different experienced pathologists.

In the proband and brother of Family VI, microscopic evaluation revealed parathyroid tumors showing obvious, clear-cut capsular penetration with infiltration of the surrounding extraglandular adipose tissue. Necrosis was not observed (Figure 6c). Neoplastic cells demonstrated strong and diffuse menin immunoreactivity on tissues from the proband's brother of the Family VI (data not shown).

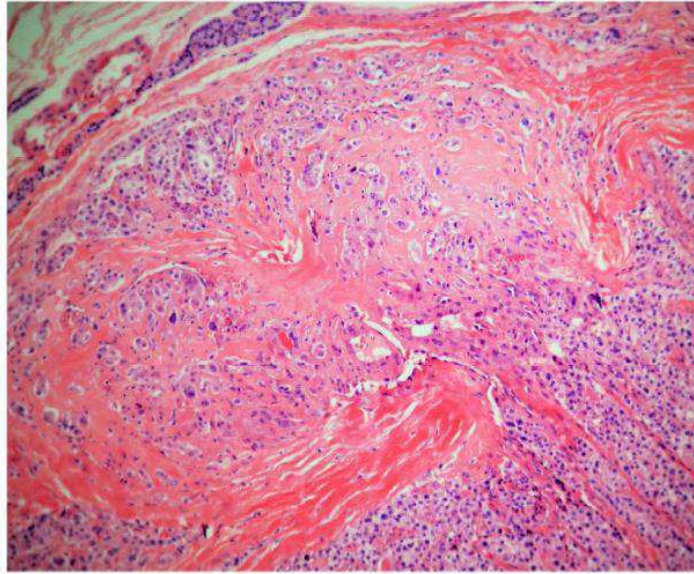


Figure 6c. (H&E X10) Fungus-like capsular infiltration by neoplastic cells of parathyroid carcinoma. 235x208mm (300 x 300 DPI).

Further considerations on this family. The diagnosis of familial parathyroid carcinoma prompted us to search for coding mutations and/ or large genomic deletions of the CDC73 gene, a search that was negative. Our search for an MEN1 mutation was positive, and after its identification, gastrointestinal echoendoscopy of the proband revealed multiple pancreatic lesions (PNETs) < 1 cm in diameter, while pituitary MRI was negative. In the brother (II:6), a right lesion close to the pharynx was identified during follow up, and removed. Histopathological diagnosis was an ancient schwannoma.

2.2.3 INTRAFAMILIAL ANALYSIS (Table 4)

In the **Family I**, the proband was operated for the first time when he was 29 for the removal of an atypical adenoma, and then, 12 ys later, for the removal of a parathyroid carcinoma. His niece was operated at 27 ys for the removal of a parathyroid carcinoma; his sister was operated two times (for the removal of a KP and TA) at 42 and 47 ys. However the proband's mother, although carrier for the same mutation (c.685_689delAGAG) never manifested any symptoms throughout her life and she passed away at 82 ys for natural causes.

In the **Family II**, the proband was operated for the removal of a parathyroid carcinoma when she was 28 ys; her aunt was operated for the removal of a parathyroid adenoma at 35 ys. However, the proband's father, carrying for the same mutation (c.1379delA) is in good health till now at 55 ys.

In the **Family III**, the proband was operated 4 times in less than 10 ys for the removal of parathyroid carcinoma and atypical adenoma lesions. However her brother, although carrying for the same mutation (c.518_521delTGTC) never manifested any symptoms till now that he is 50 ys.

In the **Family IV**, the proband was recovered in urgency because of a severe osteolytic lesions at the jaw at 22 ys and the for the removal of a parathyroid carcinoma 1 y later. His mother carries the same mutation (c.251delC) but she was operated for breast cancer and multiple uterine leiomiomas, these latters reported as associated to the HPT-JT.

In the **Family V**, the proband was operated for an ossifying parathyroid carcinoma (2cm) with capsular infiltration and invasion of vessels and of the surrounding tissue when he was 37. He presented a previous familial history of KP and adenoma: the older brother underwent to resection of a fibroma of the maxilla, parathyroid adenoma and ossifying KP with infiltration of the capsula and vascular invasion and finally he died at 46 ys for diffuse metastases at the liver, pelvi and vertebrae; the mother was operated for a uterine leyomiomata at 38 ys and for a parathyroid adenoma 24 ys later; the niece operated on for uterine fibromas at 23 ys. Array CGH and MLPA analysis showed that the proband, mother, one of brothers, one of sisters, one niece and one nephew, carry the same large deletion of exon1-exon10 of the CDC73 gene.

In the **Family VI**, the proband was admitted at Casa Sollievo della Sofferenza hospital for the follow-up of a pathologically diagnosed parathyroid carcinoma (size 7.3 cm) showing capsular invasion and infiltration into the esophagus and an hyperplastic second gland. The patient suffered from nephrolithiasis with repeated renal colic and he presented bilateral adrenal lesions. In the brother a parathyroid carcinoma (size 4.6 cm) was removed while in the daughter two extrathyroidal nodules (1.4 cm and 1 cm in diameter) were identified. The brother suffered from renal stones and was operated for an in

situ melanoma and lipoma and during the follow up for such diseases, bilateral adrenal lesions were discovered. While no coding gene mutation or genomic deletion at the CDC73 genetic locus (1q31.2) was detected, screening of the MEN1 coding sequence identified a mutation in exon 9, namely c.1252G>A, encoding p.D418N in the proband, his brother, daughter and in normocalcemic nephew.

Family	Age	Age Diag	Ca (mg/dL)	PTH (pg/mL)	Histol	CDC73	MEN1
#1	52	30	11,5	160	K/AA	c.685_689delAGAG	negative
#2	32	29	16	650	K	c.1379delT	negative
#3	44	35	13	660	K	c.518_521delTGTC	negative
#4	24	22	15,5	1469	K	c.251delC	negative
#5	70	22	12,5	1250	K	delEX1-10	negative
#6	55	53	11,84	286	K	negative	c.1252G>A

Table 4. Clinical and genetic features of the probands of each family.

One of the final goal of the project is to identify a possible genetic signature involved in the onset of the disease. Instead looking at the phenotype of the different 5 HPT-JT families, interestingly, some affected subjects manifested the disease with an early onset, while (in the same family) other relatives (mother or son), although carrying for the same mutation never manifested any symptoms.

CHAPTER 3: RESULTS

3.1 FIRST TASK: IDENTIFICATION OF GENES/PROTEINS/ MOLECULAR PATHWAYS ASSOCIATED TO KP BY WES AND EXPRESSION PROFILING

3.1.1 WES ANALYSIS

In order to investigate whether a genetic background could influence the onset of the disease the whole exome data were filtered by comparing "affected vs carriers vs controls".

After classic prioritization approach as explained above, the WES performed on all the subjects (affected, carriers and not carriers) revealed several thousand of genetic variants. Thus, we decided to apply more restrictive criteria as follows:

- 1) we arbitrary we imposed that the affecteds carried a variant, while both the carriers and the controls did not;
- 2) we considered variants present only in the coding/splicing sequence;
- 3) we considered variants leading only to aminoacidic change (non synonymous);
- 4) the variants were not present in SNP database, or they were present with very low frequency ($MAF < 0.05$).

Following these restricted criteria, we carefully examined the variants for all the families and we deduced the table 5, where we show the selection parameters, along with the variants and the type of change and predictive effect as resulted by online software tools analysis.

	DFM	DFPC	DFLMP	Ref	Alt	Func.refGene	Gene.refGene	AAChange.refGene	1000g2015aug_all	avsnp144	SIFT_pred	Polyphen2_pred
F1	1	1	0	C	G	exonic	NOTCH4	exon22:c.G4037C:p.R1346P	0,0111821	.	T	P
	1	1	0	T	C	exonic	ITGA11	exon8:c.A880G:p.R294G	.	.	D	D
	1	1	0	C	T	exonic	ITGA3	exon6:c.C929T:p.A310V	0,00219649	rs61730088	D	D
	FP	FV	FC	Ref	Alt	Func.refGene	Gene.refGene	AAChange.refGene	1000g2015aug_all	avsnp144	SIFT_pred	Polyphen2_pred
F2	1	0	0	A	G	exonic	SLC3A1	exon2:c.A568G:p.M190V	0,000199681	rs574476585	D	D
	1	0	0	C	T	exonic	ITGA2B	exon29:c.G2965A:p.A989T	0,000798722	rs78165611	D	B
	1	0	0	C	A	exonic	RET	exon2:c.C166A:p.L56M	0,00119808	rs145633958	T	P
	1	0	0	C	T	exonic	BRIP1	exon6:c.G577A:p.V193I	0,00139776	rs4988346	.	B
	1	0	0	G	A	exonic	SMO	exon4:c.G808A:p.V270I	0,00239617	rs111694017	T	B
	1	0	0	G	A	exonic	FANCC	exon2:c.C77T:p.S26F	0,00259585	rs1800361	D	D
	1	0	0	C	T	exonic	BRCA1	exon10:c.G3119A:p.S1040N	0,00978435	rs4986852	D	D
	1	0	0	G	A	exonic	GLI3	exon15:c.C4609T:p.R1537C	0,0191693	rs35364414	D	D
	FT	FG	FM	Ref	Alt	Func.refGene	Gene.refGene	AAChange.refGene	1000g2015aug_all	avsnp144	SIFT_pred	Polyphen2_pred
F3	1	0	0	G	A	exonic	BLK	exon4:c.G211A:p.A71T	0,0123802	rs55758736	D	B
	1	0	0	C	T	exonic	ITGA2B	exon29:c.G2965A:p.A989T	0,000798722	rs78165611	D	B
	CG	PF	CR	Ref	Alt	Func.refGene	Gene.refGene	AAChange.refGene	1000g2015aug_all	avsnp144	SIFT_pred	Polyphen2_pred
F4	1	0	0	C	T	exonic	MUC12	exon2:c.C2012T:p.T671I	.	rs200428302	T	.
	1	0	0	del12	-	exonic	NOTCH4	exon1:c.36_47del:p.12_16del
	RM	RD	RG	Ref	Alt	Func.refGene	Gene.refGene	AAChange.refGene	1000g2015aug_all	avsnp144	SIFT_pred	Polyphen2_pred
F5	1	0	0	T	C	exonic	ITGB6	exon8:c.A998G:p.E333G	0,000199681	rs142185271	T	B
	1	0	0	A	G	exonic	RNF217	exon1:c.A257G:p.Q86R
	1	0	0	C	T	exonic	KMT2C	exon16:c.G2726A:p.R909K	.	rs199504848	T	D
	1	0	0	G	A	exonic	KMT2C	exon7:c.C925T:p.P309S	.	rs138627563	T	D
	1	0	0	G	T	exonic	MUC4	exon2:c.C1980A:p.D660E	.	.	T	B
	1	0	0	G	T	exonic	TRIM62	exon1:c.C112A:p.H38N	.	.	T	D
1	0	0	G	T	exonic	ITGA9	exon3:c.G413T:p.R138L	.	.	D	B	

	RM	RC	RF	RG	RL	Chr	Start	End	Ref	Alt	Func.refGene	Gene.refGene	ExonicFunc.refGene	AAChange.refGene	1000g2015aug_all	avsnp144	SIFT score	SIFT_pred	Polyphen2_score	Polyphen2_pred
F6	1	1	1	1	0	chr7	100638828	100638828	C	T	exonic	MUC12	nonsyn SNV	exon2:c.C4984T:p.P1662S	7q22.1	rs56914801	0,88	T	.	.
	1	1	1	1	0	chr2	121744002	121744002	C	A	exonic	GLI2	nonsyn SNV	exon12:c.C2105A:p.P702G	2q34.2	rs764830136	0,31	T	1	D
	1	1	1	1	0	chr11	64572604	64572604	C	T	exonic	MEN1	nonsyn SNV	exon10:c.G1252A:p.D418N	11q13.1	rs104894264	0	D	1	D

Table 5. WES data for all the families under study.

Looking separately at the different families we were able to notice what follows:

Family I. We considered 2 affecteds vs 1 control. The analysis identified 3 possible variants in the **NOTCH4**, **ITGA11** and **ITGA3** genes. The NOTCH4 protein belongs to a superfamily of transmembrane protein and structured with an extracellular domain consisting of multiple repeats of the epidermal growth factor-like (EGF), and an intracellular portion with many multiple different domains. Notch signaling is an overall conserved intercellular signaling pathway regulated through binding to their cognate ligands. Recent findings confirmed the role of NOTCH4 in carcinogenesis and tumour progression in glioblastoma (123), melanoma (124), NSLC (125), nasopharyngeal carcinoma (126) (*For more specific details about the ITGA genes, please refer to the chapter 1, paragraph 1.6*).

Family II. In this family we considered 1 affected vs 1 control and 1 carrier. We were able to detect many interesting variants falling in different proteins variably involved in the tumour progression. The **RET** gene encodes a

transmembrane receptor, member of the tyrosine protein kinase family. It takes part to several cellular differentiation and growth processes and mutations of this gene cause the Multiple Endocrine Neoplasia type II and the Hirschprung disease, to whom the variant p.L56M, was previously associated (127). **FANCC** and **BRIP1** are proteins belonging to the Fanconi anemia complementation group (including other many proteins). The corresponding namesake disease is characterized by cytogenetic instability, hypersensitivity to DNA crosslinking agents, increased chromosomal breakage and defective DNA repair (128, 129). Interestingly, we also identified 2 rare variants in the **SMO** and **GLI3** genes, encoding for 2 proteins involved in the Hedgehog pathway (*for more detail please refer to chapter 1, paragraphs 1.4 and thereafter*). Finally we identified a rare variant in the **BRCA1** gene, known as involved in the onset of the breast tumor (130) and a rare variant in the **ITGA2B** gene (*for more detail on the Integrins, please refer to the chapter 1, paragraph 1.6*)

Family III. We compared 1 affected vs 1 control and 1 carrier. Very interestingly, we found the same rare variant in the **ITGA2B** already found in Family II. Moreover, a rare variant was also identified in the **BLK** gene, encoding a nonreceptor tyrosine-kinase of the src family of proto-oncogenes involved in cell proliferation and differentiation (131). The protein has a role in B-cell receptor signaling and B-cell development and it could be important for the general derangement of lymphocytes organization and activation resulted from the Expression Profiling (*please see next paragraph*).

Family IV. Also in this family, we compared 1 affected vs 1 control and 1 carrier. Unexpectedly, we identified an “*in-frame*” deletion of the **NOTCH4** gene (please see above) and a rare variant in the **MUC12** genes. The MUC12 gene encodes an integral membrane glycoprotein member of the mucin family, implicated in epithelial renewal, differentiation and intracellular signaling. This protein is expressed on the apical membrane surface of epithelial cells of many different tissues and it is downregulated in colorectal cancer tissue (132).

Family V. Also in this family, we compared 1 affected with 1 carrier and 1 control. We were able to detect 2 rare variants in 2 different genes encoding the integrins, **ITGAB6** and **ITGA9** (*see chapter 1, paragraph 1.6*). Moreover, among

the other genes, we highlighted 2 variants in **KMT2C** gene encoding a protein of the MLL (Mixed-Lineage Leukemia) complex, having a histone methylation activity and involved in transcriptional coactivation. Mutations of this gene have been reported associated to a gastric cancer (133).

Among the different variants, we surprisingly noticed that 4 out of the 5 families (Family I, II, III and V) shared rare genetic changes in the integrins ITGA3, ITGA11, ITGA2b, ITGAB6 and ITGA9, belonging to a group of proteins recently proved to be involved in tumorigenesis processes.

Integrins are a family of proteins involved in cell adhesion and interaction and recently they arose great interest as possible markers of cancer initiation, progression, invasion in head-neck squamous cell (134), and nasopharyngeal carcinoma (135), bladder (136) and prostate cancer (137). It has also been reported that these proteins are regulated epigenetically, by through specific miRNAs, suggesting novel possible therapeutic ways to modulate the tumor invasiveness (135-137) (please also see: chapter 1, paragraph 1.6).

As far as the **Family VI** with MEN1 and KP, the so rare concurrent presence of 2 parathyroid carcinomas in the same MEN1 family prompted us to search by our approach (WES and EP) for other possible constitutional genetic players that could have driven a (putative) benign parathyroid lesion towards a malignant one. The hypothesis is that a further mutation in a specific gene may lead to transformation of a benign lesion in malignant one. Data emerged from the analysis of the 3 affected subjects, 1 asymptomatic MEN1 mutation carriers and the 2 healthy not carrier controls.

With regards the WES filtering methods, we arbitrarily imposed that all the carriers for the MEN1 mutation would have also a second mutation, while the control subjects did not. By this way, the analysis shown several variants, the most interesting were in the **MUC12** (please see above) and in the **GLI2** gene. The identified variant of the GLI2 gene, p.P702Q, was highly conserved and recorded in the publicly databases (ExAc and gnomAD, <http://exac.broadinstitute.org/gene>; <http://gnomad.broadinstitute.org/gene>) with very low frequency (8×10^{-6}) thus ruling out the possibility to be even a rare polymorphism (*For more details about the GLI2 protein and its possible*

interaction with parafibromin and menin, please refer to chapter 1, paragraph 1.4).

3.1.2 EXPRESSION PROFILING (EP)

Data analysis was performed using the Partek Genomic Suite 6.6 and Transcriptome Analysis Console software. From comparison between "affected vs control" belonging to the same family, we found that families with parathyroid cancer and CDC73 gene mutation show a different activation of the pathway that regulates calcium metabolism. Probands of the 6 recruited families have hyperparathyroidism, i.e. hypercalcemia associated with an inappropriately high PTH value, but CDC73 mutated families seem to show a different control of calcium mobilization rather than the MEN 1 family.

A number of differences arise between MEN1 and CDC73 peculiar PTs. MEN1 tumors were characterized by increased/ decreased proliferation of tumor cells (Cyclins and Cell Cycle Regulation, $-\log(p\text{-value})= 1,52$; Cdc42 Signaling, $-\log(p\text{-value})= 3.55$; Calcium-induced T Lymphocyte Apoptosis, $-\log(p\text{-value})= 2.85$). These pathways were not deregulated in CDC73 tumors.

Immune system appeared to be differently perturbed by the two kinds of tumors. MEN1 tumors showed an important deregulation of the Antigen Presentation Pathway, $-\log(p\text{-value})= 6.77$; OX40 Signaling Pathway, $-\log(p\text{-value})= 6.19$; T Helper Cell Differentiation, $-\log(p\text{-value})= 2.71$). On the contrary, CDC73 tumors were characterized by a highly significant enrichment of Natural Killer Cell Signaling pathway, $-\log(p\text{-value})= 9.67$.

The activation state of these pathways were assessed on the composing biological functions. Interestingly, it resulted that the *mobilization of Ca^{2+}* were reduced, more importantly in MEN1 (z-score= -1.941) than in CDC73 (z-score= -1.073) tumors. The interesting point is that they fulfil this process by means of two completely different sets of genes.

- It seems that MEN1 tumors tend to control better the mobilization of calcium, in respect to CDC73 tumors, and it uses a completely different team of genes than that used by CDC73.

Gene Symbol	p-value MEN1	Fold-Change MEN1	p-value CDC73	Fold-Change CDC73
SOX6	2.58E-08	1.70002	0.00103898	1.22738
DMTN	2.93E-08	1.62802	3.45E-08	1.43586
ARHGEF12	2.59E-07	2.03985	0.00799309	1.27407
BCL2L1	6.52E-07	1.56661	0.00204994	1.20758
DEFA1B	0.20104	-1.38062	0.0320566	1.50942
FCGR1A	0.102643	-1.31552	0.000242519	1.63733
MS4A2	0.00274648	1.71659	0.998518	1.00024
KIR2DS4	0.383889	-1.17116	0.000807538	-1.62386
FPR1	0.000444987	-1.61308	0.038379	1.22208
KLRC4-KLRK1	0.0459778	-1.34271	5.43E-05	-1.61828
CCR3	0.0591335	-1.39459	0.00161965	-1.54053

Differentially Expression Genes (DEGs) were selected whenever their Fold Change values were significantly (p-value < 0.05) greater than 1.5.

A further issue emerging from the EP analysis concerns the specific genes involved in activation and survival pathways of leukocytes and lymphocytes.

- Parathyroid tumors with CDC73 or MEN1 mutations seem to show a different activation of immune response. In the MEN1 family, leukocytes are less activated and more prone to induce programmed cell death than families with HPT-JT.
- Cell death of cancer cells seem to be more likely in MEN1 than in CDC73 tumors (cell death of cancer cells, z-score= 0.68 vs 0).
- Cell death of MEN1 cancer cells is slightly greater than CDC73 cancer cells.
- Lymphocytes, especially Natural Killer (NK) cells and T-cells, were inhibited in CDC73 tumors (proliferation of lymphocytes, z-score= -1.819; activation of lymphocytes, z-score = -0.834; cytotoxicity of tumor cell lines, z-score= -1.964; killing of cells, z-score= -1.358; cytotoxicity of natural killer cells, z-score= -0.464) and **not** in MEN1 tumors. On the contrary, we found that the function of Leukocytes was slightly more inhibited in MEN1 tumors (activation of leukocytes, z-score= -1.069 vs -0.492 CDC73); being their apoptosis promoted in MEN1 tumors (apoptosis of leukocytes, z-score= 0.516) in respect to CDC73 tumors. Although having a reduced number of granulocytes (z-score= -0.803), in

particular of neutrophils (z-score= -0.762), CDC73, on the other hands, exhibited an increased degranulation activity of phagocytes (z-score= 1.934).

- CDC73 tumors heavily inhibits the activation and the activity of lymphocytes. MEN1 lymphocytes seem not to be affected in this sense. On the other hand, leukocytes are slightly less activated in MEN1 tumors; rather they are pushed to die by apoptosis in MEN1 and not in CDC73 tumors, which, in turn, increased the degranulation activity of phagocytes, although the number of granulocytes are generally lower.

cytotoxicity of tumor cell line				
Gene Symbol	p-value MEN1	Fold-Change MEN1	p-value CDC73	Fold-Change CDC73
PRF1	0.226401	-1.11107	6.00913E-08	-1.52422
KIR2DS4	0.383889	-1.17116	0.000807538	-1.62386
KIR2DL3	0.0708161	-1.3153	3.47682E-06	-1.80523
KIR2DL1	0.338501	-1.1416	0.00100084	-1.43594
KLRC4-KLRK1	0.0459778	-1.34271	5.43237E-05	-1.6182

proliferation of lymphocytes				
Gene Symbol	p-value MEN1	Fold-Change MEN1	p-value CDC73	Fold-Change CDC73
ARG1	0.167359	1.20505	9.52314E-06	1.64831
FOXO3	0.830339	1.02491	1.3178E-06	1.61782
KIR2DS4	0.383889	-1.17116	0.000807538	-1.62386
KLRC4-KLRK1	0.0459778	-1.34271	5.43237E-05	-1.61828
MXI1	0.0024828	1.38152	4.9801E-08	1.64467
MYBL1	0.127144	-1.22209	2.18783E-07	-1.81405
PRF1	0.226401	-1.11107	6.00913E-08	-1.52422
RUNX3	0.0303244	-1.226	1.00882E-07	-1.54642
SLC4A1	0.0315662	1.2927	2.09961E-08	1.81226

killing of cells				
Gene Symbol	p-value MEN1	Fold-Change MEN1	p-value CDC73	Fold-Change CDC73
PRF1	0.226401	-1.11107	6.00913E-08	-1.52422
SH2D1B	0.0816627	-1.26941	2.94365E-05	-1.59751
DEFA1B	0.20104	-1.38062	0.0320566	1.50942
KIR2DL3	0.0708161	-1.3153	3.47682E-06	-1.80523
KIR2DL1	0.338501	-1.1416	0.00100084	-1.43594
KLRC4-KLRK1	0.0459778	-1.34271	5.43237E-05	-1.61828

Differentially Expression Genes (DEGs) were selected whenever their Fold Change values were significantly (p-value < 0.05) greater than 1.5.

activation of lymphocytes				
Gene Symbol	p-value MEN1	Fold-Change MEN1	p-value CDC73	Fold-Change CDC73
FOXO3	0.830339	1.02491	1.3178E-06	1.61782
KIR2DL1	0.338501	-1.1416	0.00100084	-1.43594
KIR2DL3	0.0708161	-1.3153	3.47682E-06	-1.80523
KLRC2	0.00611658	-1.50692	3.76473E-05	-1.63127
KLRC4-KLRK1	0.0459778	-1.34271	5.43237E-05	-1.61828
MGST1	0.846023	1.02465	3.94375E-05	1.53424
PRF1	0.226401	-1.11107	6.00913E-08	-1.52422

quantity of granulocytes				
Gene Symbol	p-value MEN1	Fold-Change MEN1	p-value CDC73	Fold-Change CDC73
CCR3	0.0591335	-1.39459	0.00161965	-1.54053
PRF1	0.226401	-1.11107	6.00913E-08	-1.52422
FCGR1A	0.102643	-1.31552	0.000242519	1.63733
TSTA3	0.126861	-1.2382	9.21377E-05	1.55835
RORA	0.00540136	-1.43821	5.4924E-06	-1.61914

quantity of neutrophils				
Gene Symbol	p-value MEN1	Fold-Change MEN1	p-value CDC73	Fold-Change CDC73
PRF1	0.226401	-1.11107	6.00913E-08	-1.52422
FCGR1A	0.102643	-1.31552	0.000242519	1.63733
TSTA3	0.126861	-1.2382	9.21377E-05	1.55835
RORA	0.00540136	-1.43821	5.4924E-06	-1.61914

degranulation of phagocytes				
Gene Symbol	p-value MEN1	Fold-Change MEN1	p-value CDC73	Fold-Change CDC73
CCR3	0.0591335	-1.39459	0.00161965	-1.54053
ANXA3	0.357961	-1.14578	7.50034E-05	1.61713
FCGR1A	0.102643	-1.31552	0.000242519	1.63733
DEFA1B	0.20104	-1.38062	0.0320566	1.50942

cytotoxicity of natural killer cells				
Gene Symbol	p-value MEN1	Fold-Change MEN1	p-value CDC73	Fold-Change CDC73
CCR3	0.0591335	-1.39459	0.00161965	-1.54053
FCGR1A	0.102643	-1.31552	0.000242519	1.63733
ANXA3	0.357961	-1.14578	7.50034E-05	1.61713
DEFA1B	0.20104	-1.38062	0.0320566	1.50942

Differentially Expression Genes (DEGs) were selected whenever their Fold Change values were significantly (p-value < 0.05) greater than 1.5.

activation of leukocytes				
Gene Symbol	p-value MEN1	Fold-Change MEN1	p-value CDC73	Fold-Change CDC73
BCL2L1	2.2856E-07	1.74378	0.0086679	1.20404
CLC	0.003073	-1.74081	0.133548	-1.22365
FPR1	0.000444987	-1.61308	0.038379	1.22208
HLA-DQA1	7.42066E-10	2.77153	0.653113	-1.04458
HLA-DRB1	1.64568E-05	-1.74799	0.00376162	-1.30129
KLRC2	0.00611658	-1.50692	3.76473E-05	-1.63127
SLPI	0.0329714	-1.53306	0.0553678	1.33048

apoptosis of leukocytes				
Gene Symbol	p-value MEN1	Fold-Change MEN1	p-value CDC73	Fold-Change CDC73
BCL2L1	2.2856E-07	1.74378	0.0086679	1.20404
CAST	1.48477E-08	-1.58478	0.516156	-1.03276
CCNB1	0.000221454	1.87687	0.169696	1.17675
E2F2	8.58501E-08	1.77345	0.154301	1.10095
MS4A2	0.00274648	1.71659	0.998518	1.00024
SLPI	0.0329714	-1.53306	0.0553678	1.33048

Differentially Expression Genes (DEGs) were selected whenever their Fold Change values were significantly (p-value < 0.05) greater than 1.5.

A further comparison "affected vs carriers" was carried out in order to understand whether deregulation of leukocyte and lymphocytic activation pathways affects the penetrance of the disease. It would be important to investigate whether the presence of the CDC73 or MEN1 mutation causes deregulation of these pathways and the consequent tumorigenicity or whether it is independent from the carrier status, thus playing *per se* the role of necessary factor for the onset of the pathology.

Furthermore, from the comparison affected vs healthy CTRL in the family VI, it is interesting to note a concurrent up-regulation of genes involved in the migration of cells and metastasis processes such as **ITGAB3**, **VCAN**, **MMP9**. Among all the genes differentially expressed in this family, two are upstream regulators, **IL1B** and **TGFB1**, able to control other differentially regulated genes identified. Evidences suggest that IL1B controls the expression of ITGAB3, HERC5, F13A1 genes.

Moreover, regarding the rare genetic variants in integrins genes identified in 3 families, we decided to examine *in depth* the possibility that integrins could be involved somehow in the onset and progression of the disease. By comparing the expression levels of integrins resulted from the EP, no macroscopic differences were noted between the different subjects (particularly affecteds vs carriers). However, we decided to verify the expression levels also by a RTqPCR methodology using a specific primer mix for ITGA3 and ITGA2B.

3.1.3 RT-QPCR

A relative quantification with standard curves was developed for each target genes and GAPDH as reference gene. The standard curve is built by plotting the log of the starting quantity of template against the Ct value obtained. mRNA levels in each sample were determined as the ratio of the target genes expression levels to the GAPDH expression. Calibration curves for the target genes and GAPDH gene (used as calculation method) were constructed and sample concentration was calculated using the plasmid standard curve, resulting in plasmid concentrations expressed as copy number of corresponding standard molecules.

ITGA3

In **Family I** the ITGA3 gene expression level has been evaluated with the relative quantification method using GAPDH as a control gene.

The R2 values for all standard curves generated ranged between 0,9972 and 0,9988 (Figure 7a).

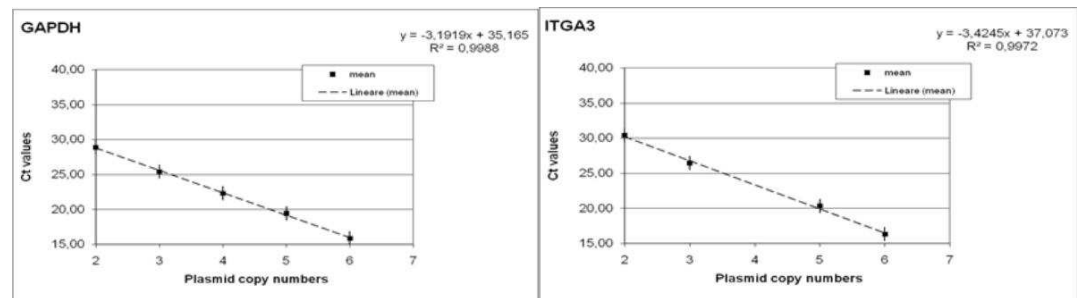


Figure 7a. Standard curves obtained from serial dilutions of GAPDH (as reference gene) and ITGA3 vectors.

Figure 7b shows that in Family I only the proband had ITGA3 mRNA over expression while CTRL and carrier did not.

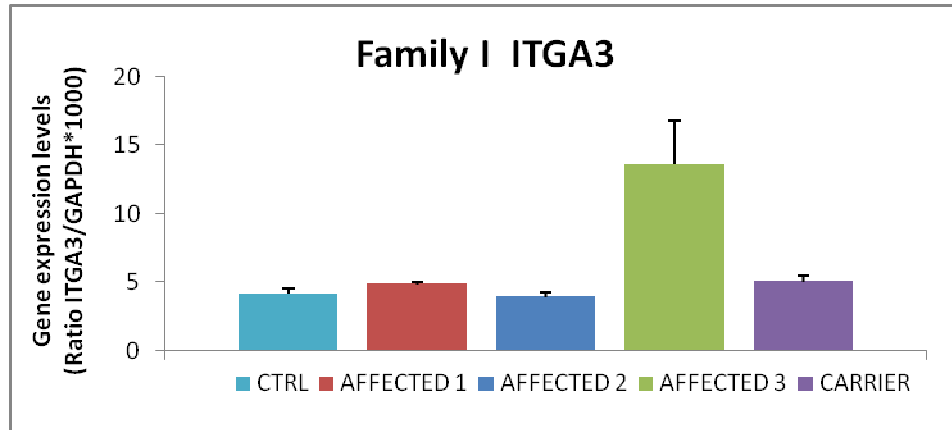


Figure 7b. Values were reported as the ITGA3/GAPDH ratio*1000.

ITGA2B

In **Family II** and **III** the ITGA2B gene expression level was evaluated with the relative quantification method using GAPDH as a control gene. The R2 values for all standard curves ranged between 0,9985 and 0,9988 (Figure 8a).

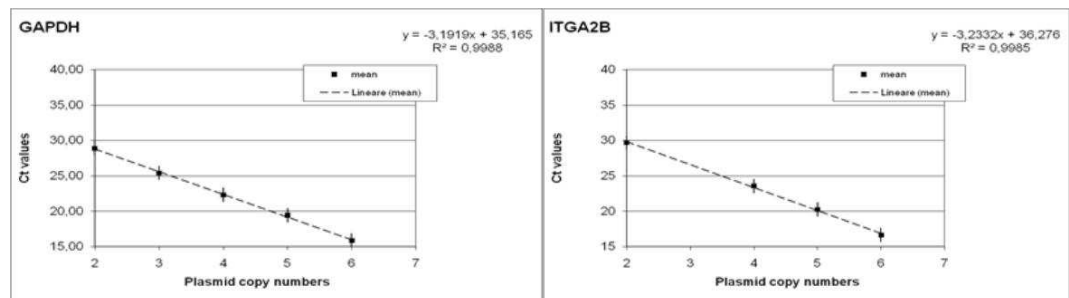


Figure 8a. Standard curves obtained from serial dilutions of GAPDH (as reference gene) and ITGA2b vectors.

In the **Family II** ITGA2B mRNA was differentially expressed with higher level in the carrier and lower level in CTRL subject (Figure 8b).

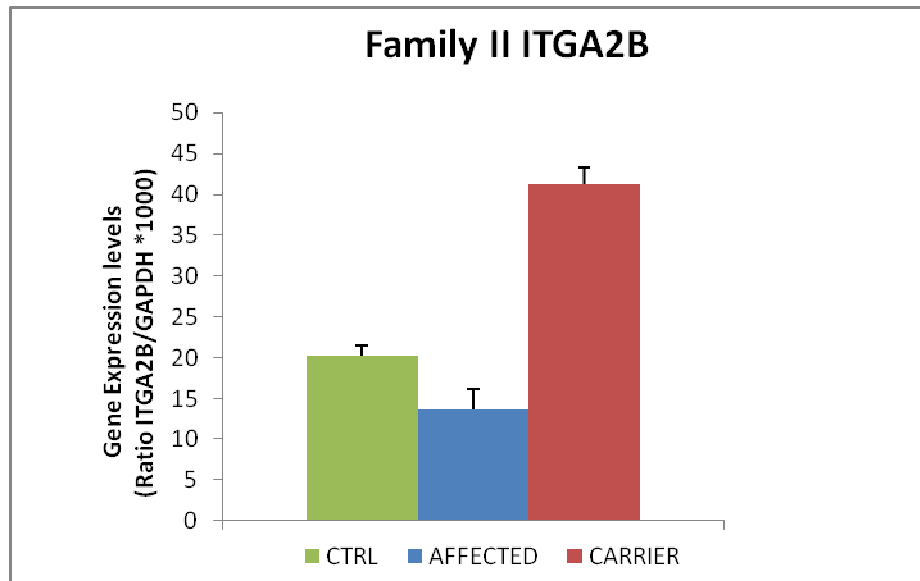


Figure 8b. Values were reported as the ITGA2B/GAPDH ratio*1000.

In **Family III** the carrier shows a higher ITGA2B mRNA expression level compared to CTRL subject and the proband (Figure 8c).

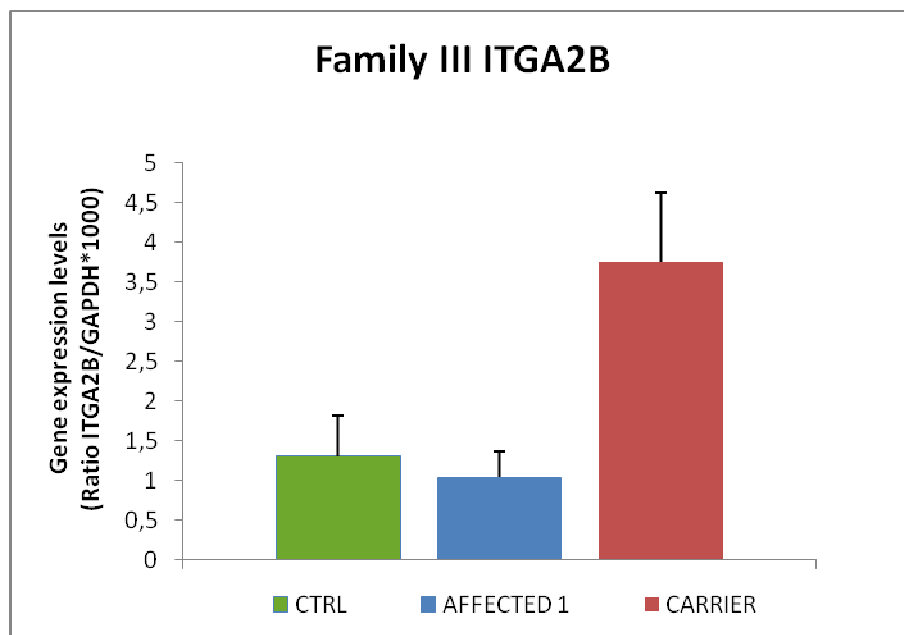


Figure 8c. Values were reported as the ITGA2B/GAPDH ratio*1000.

Hh pathway

In order to investigate the effect of gene variants in the Hh pathway components (GLI2, SMO and GLI3) identified by WES on the onset and progression of KP, we studied the gene expression of SHH, SMO, GLI1, GLI2,

GLI3, the main crucial factors of Hh pathway, in affected/ carrier/ control of **Family VI** and **Family II**. Quantitative RT-PCR assay was optimized as indicated by the equation of the linear regression line, Pearson's correlation coefficient (r) and the coefficient of determination (r^2) ($r > 0.990$ and $r^2 > 0.989$ is desirable). The R^2 values for all standard curves generated ranged between 0,9987 and 1 (Figure 9a).

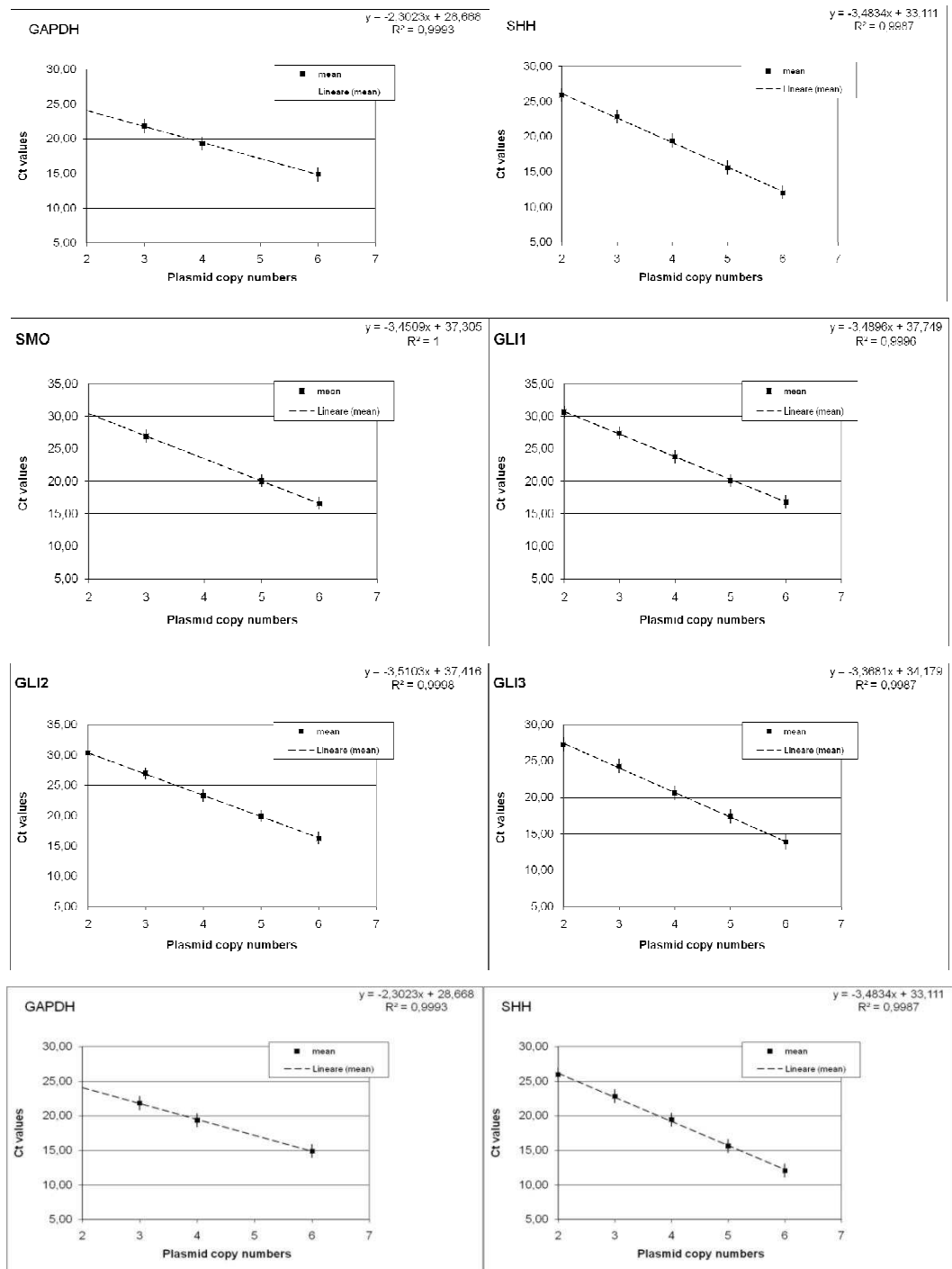


Figure 9a. Standard curves of the reference gene (GAPDH) and the main crucial Hedgehog target genes (SHH, SMO, GLI1, GLI2, GLI3).

Figure 9b shows different expression level of mRNAs in Family VI: mRNA of affected subjects were underexpressed compared to CTRLs and carriers for all the target Hh genes analysed; mRNAs levels of carriers were overexpressed. This might suggest for carriers a higher risk of developing an aggressive parathyroid tumor.

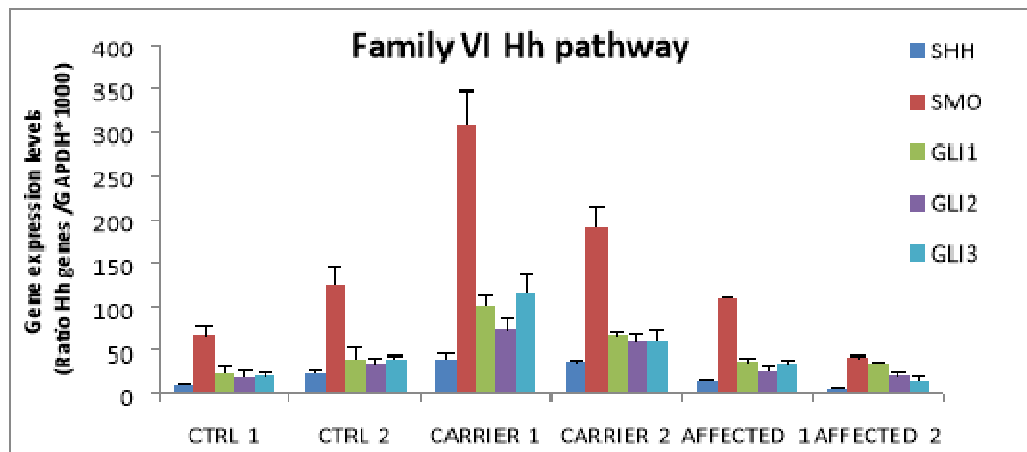


Figure 9b

Figure 9c shows the Hh target genes expression in one control, one carrier and one affected in Family II: as an opposite result compare to Family VI, the mRNA of the affected subject resulted more expressed than the control and the carrier, especially for SMO, GLI1 and GLI3 genes.

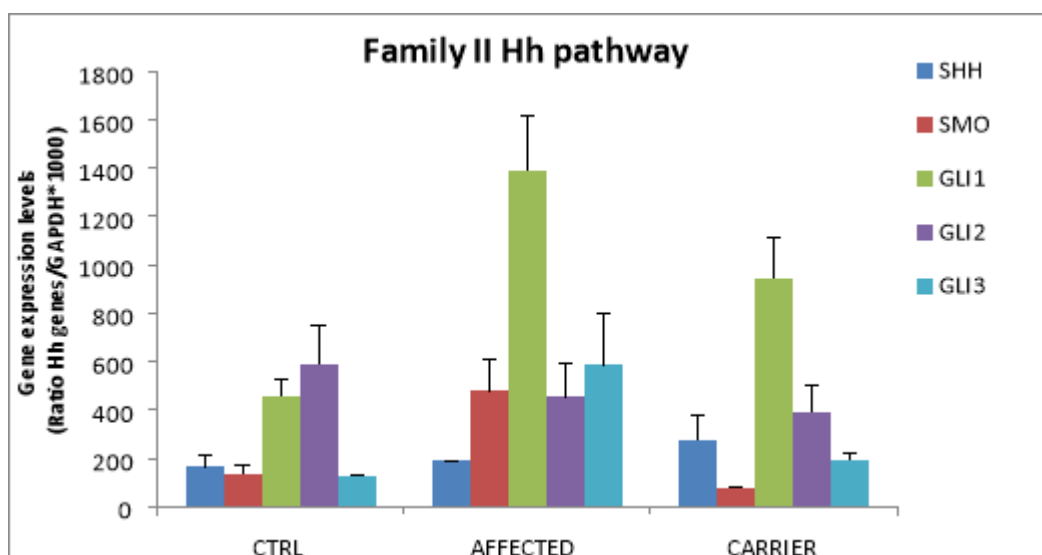


Figure 9c.

3.2 SECOND TASK: DRUG TEST ON HEK293 CELL LINES

3.2.1 FUNCTIONAL ASSAYS ON THE 5 CDC73 GENE MUTATIONS

Rationale. In 2013 we reported the functional assay on 3 CDC73 mutations identified in 3 different HPT-JT families (121). The 3 variants did not cause a premature truncation of the protein, being a missense change (p.R77P) and 2 “in-frame” deletions of 2 and 4 residues, respectively, located into the NoLS (Nucleolar Localizations Signals, p.Val85_Val86del and p.Glu81_Pro84del). Although the mutations were not supposed to lead to a frank loss of (protein) expression, our work demonstrated that the corresponding mutated proteins were subjects to an early proteasome degradation up to 70% of the total amount and to a mislocalization of the residual protein. A similar result was previously reported on some MEN1 mutations identified in sporadic MEN1 cases (138). The Authors demonstrated that some MEN1 missense mutations were subjected to proteasome degradation and that the use of bortezomib restored the expression and function of the protein. Instead, the Authors even suggested the use of the bortezomib, also as possible novel drug for the therapy of MEN1 patients.

Bortezomib is known to be a proteasome inhibitor that induce apoptosis, reverse drug resistance of multiple myeloma cell lines and patientresistant to conventional therapies. It affects the cell microenvironment by blocking cytokine circuits, cell adhesion, and angiogenesis in vivo (115).

Due to the high homologies in terms of functions, cytoplasmic localization and diseases, whose corresponding genetic mutations may cause, we decided to verify what reported for the menin mutations also for the some CDC73 genetic lesions we had identified in our (previous and current) survey.

Methods. We selected 5 CDC73 mutations: the first three were the same already published in 2013 (p.R77P, p.Val85_Val86del and p.Glu81_Pro84del); other two mutations were a missense change identified in a of sporadic KP case (p.L5F, 139) and a frameshift deletion found in the Family II (p.L460Lfs*18, 140). All the mutations were introduced in a pCMV6-CDC73 WT Myc-Flag tagged expressing vector (121). It has to be note that the vector was modified and the Flag sequence

was moved from the 3' to the 5' end, in order to be expressed in frame also with the truncated proteins. Accordingly, we modified all the vectors carrying the non-frameshift deletions and the missense changes. HEK293 cells were seeded in 96 wells in eight replicates for each vector and in triplicates for 3 different Bortezomib concentrations (10, 50 and 100 μ M final). CDC73 WT and mutant vectors were transfected using the Fugene Transfection Reagent, following manufacturer's instructions. After 24 h Bortezomib was added at the indicated different concentrations. After other 24, 48 and 72 h (48, 72 and 96 h from the transfection, respectively), the cellular proliferation was assayed by the PrestoBlue reagent (ThermoFisher).

Results. The result of the cell proliferation assay performed on 3 different Bortezomib concentrations, suggested the best drug concentration along with the best time of administration to get a good response. As shown in the Figure 10a, the drug response was almost the same for all the concentrations tested and times of administration. So we decided to use the minimal amount (10 μ M final) and the shortest time (24 h), to avoid any possible secondary toxic effect that the drug could have (Figure 10b).

However, two other important considerations rise from this assay:

- 1) HEK293 cells do express an endogenous parafibromin, that counteracts the effect of the transfected mutated forms (this is more evident for the L5F). It is likely that the effect of Bortezomib (as previously happened with the MG132) may be somehow enhanced by the presence of the endogenous parafibromin. Studies in specific cell lines not expressing the CDC73 gene would further clarify this issue.

- 2) The presence of an endogenous parafibromin should not be considered a failure of the assay. Instead, it would exactly mimic the usual human heterozygote condition with single haploinsufficiency of one allele.

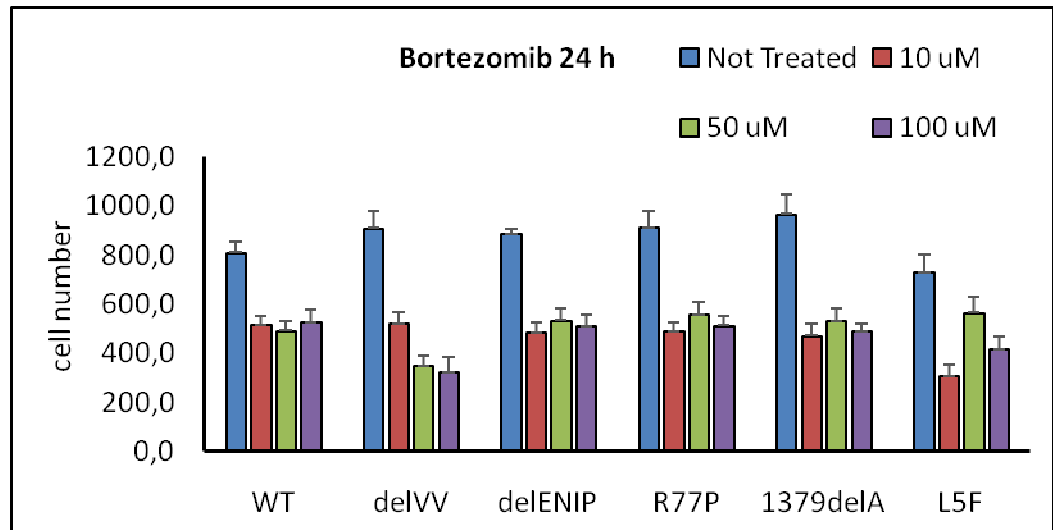


Figure 10a. Cell proliferation assay performed on 3 different Bortezomib concentrations for 24,48,72h. Error bars refer to eight different replicates. p.Val85_Val86del and p.Glu81_Pro84del namely delVV and delENIP from the one-letter code of the deleted residues.

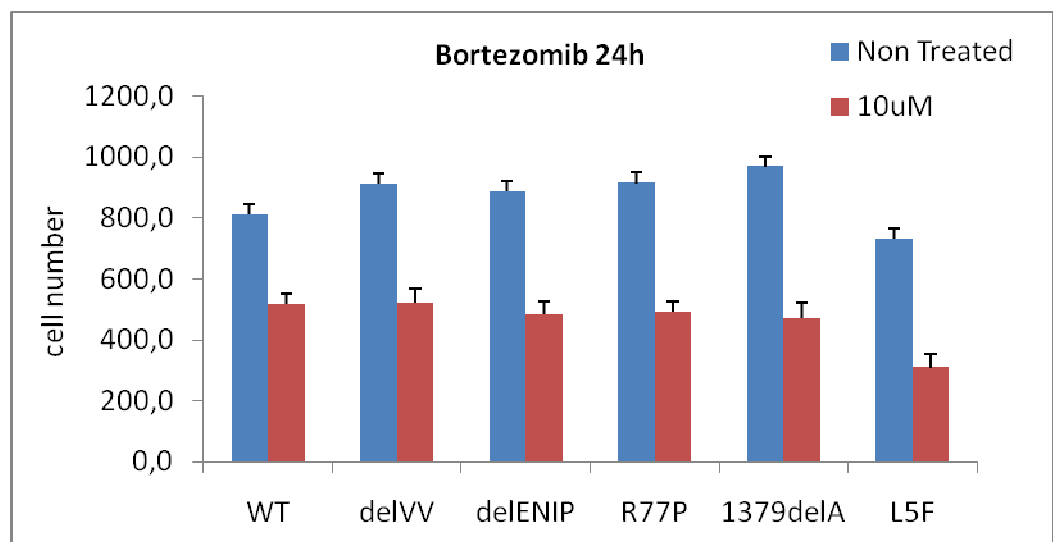


Figure 10b. Cell proliferation assay after treatment with Bortezomib (10uM final concentration) for 24h. Error bars refer to eight different replicates.

These parameters were used in the subsequent Western Blot assay, where we verified the expression of the mutated protein in presence of either the MG132 (25 uM final, used as internal control and yet tested in the previous paper, 121) and Bortezomib 10 μ M. The assay proved that the Bortezomib (10 μ M x 24 h) is able, as the MG132, to block the proteasome degradation of CDC73 mutated proteins. Although the effect is comparable with the one obtained for

the MG132, it has to be note that we assayed the lowest concentration of Bortezomib for the shortest time of administration (Figure 11). Thus, higher concentrations tested for longer time might have a longer effect of the steady state level of the protein. This could be easily verified by a cross assay using the cycloheximide, known as to inhibit the protein synthesis. These assays are ongoing.

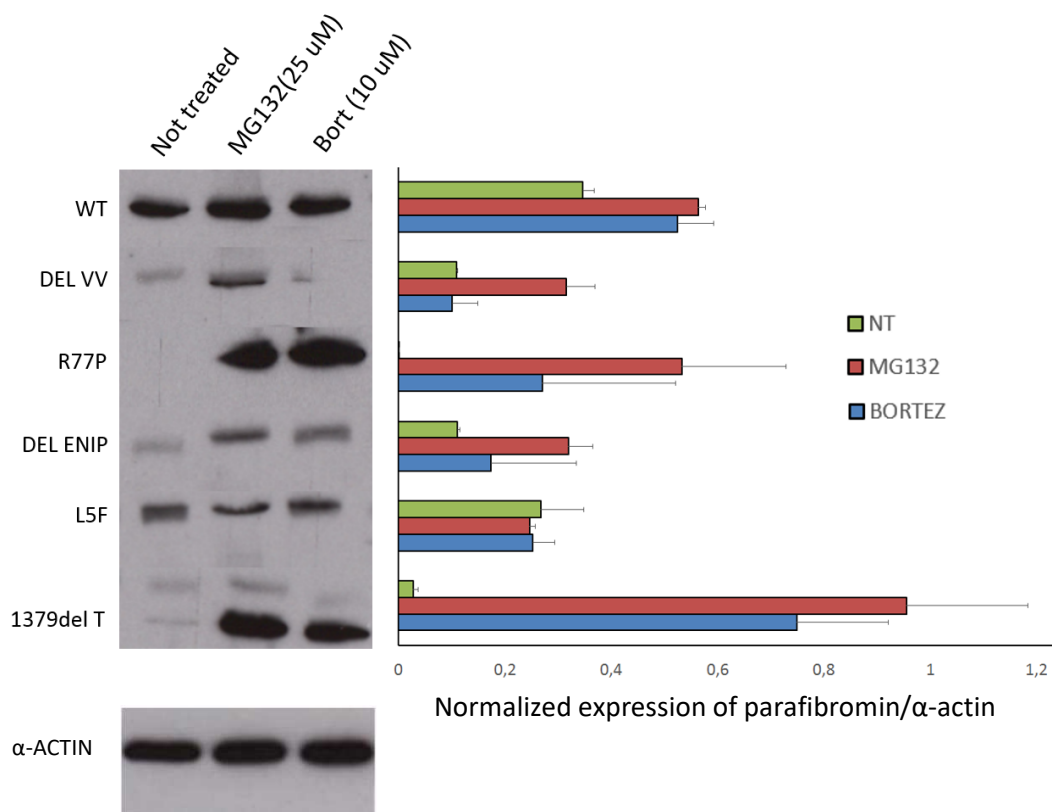


Figure 11. (On the left) Representative western blot of total protein cell lysates from cell transfected with WT and mutant CDC73 vectors detected with Anti-flag antibody. (On the right) Quantification of the western blot data was performed by densitometric analysis. Values were expressed as average of the ratio with respect to control (α - actin). Error bars refer to three different experiments.

3.2.2 MEN1 WT AND EXPRESSION OF THE MUTANT PROTEINS

Family VI: the p.D418N gene mutation was previously identified and characterized by others, and thus the functional effect was clearly elucidated (141, 142). The p.D418N mutation affects menin binding with the suppressor of variegation 3-9 homolog family, SUV39H1, protein, whose complex is involved in the methylation of H3K9 (143); it was never found associated with malignant MEN1 tumors, and specifically KP (13 and references therein).

Starting from WES preliminary results on the identification of GLI2 variant in this family, we performed a Western Blot on HEK293 protein lysate transfected with Wild Type and the mutant P702Q vectors. Immunoblot shows an over-expression of the mutant with respect to the WT (Figure 12).

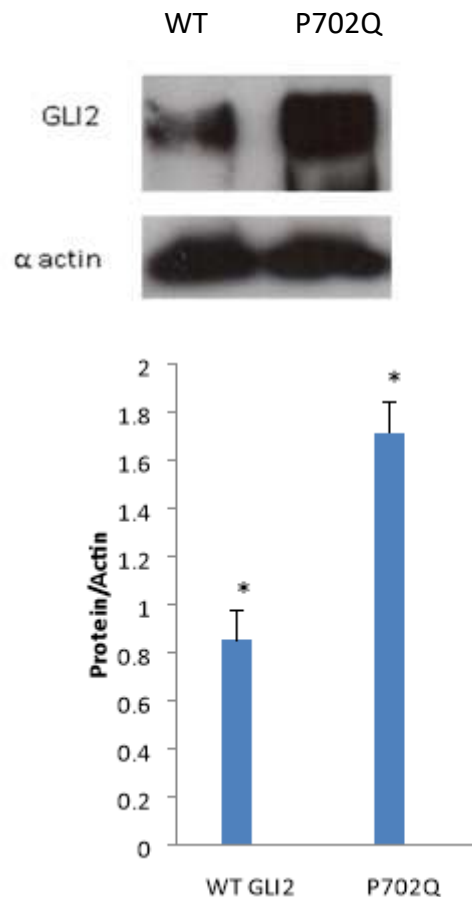


Figure 12. Western Blot analysis of total protein lysates of HEK293 cells transiently transfected with WT or mutant myc-flag tagged GLI2 constructs detected with Anti-flag antibody. The densitometric levels of the vectors were normalized to b actin. Error bars refer to three different experiments. *, P value < 0,05.

Further functional assays will be carried out with the aim to investigate whether a possible synergy between the MEN1 and GLI2 proteins could influence the onset and drive an expected benign towards a malignant parathyroid neoplasm. Thus, we will examine the role of GLI2 variant on HEK293 cells transfected with WT/D418N MEN1 vector alone or in combination with the WT/P702Q GLI2 vector.

3.2.3 ESTABLISHMENT OF PRIMARY PARATHYROID TUMOR CELL LINES

In vitro cell cultures of parathyroid cells have proved to be a challenge, although they would represent a very important issue for several researchers. Instead, to better understand physiology and pathologies of parathyroid gland, the development of an adequate in vitro parathyroid cell model may be highly useful.

It seems to be arduous growing normal in vitro primary cell cultures derived from human parathyroid biopsies because they show a very low proliferative activity (144).

Parathyroid adenomas and hyperplastic glands from patients with secondary hyperparathyroidism due to chronic kidney disease (CKD) have been used more commonly to establish parathyroid cell cultures because they show to have a higher proliferative activity than normal glands (144). Little is known about the development of parathyroid cell systems derived from parathyroid carcinomas in literature, mainly due to the very low frequency of parathyroid cancer (145).

We have unsuccessfully tried to establish a primary culture in vitro isolating parathyroid cells from tissues belonging to patients with parathyroid carcinoma, adenoma or atypical adenoma. The primary culture obtained is a population of cells with a variable morphology and size. Arranged in islets, cells appear polygonal and with an irregular shape with abundant cytoplasm, ovoid nuclei and short cellular extensions (146). In addition to the very slow proliferation rate shown, the main difficulty with human parathyroid primary cell cultures is to limit the expansion of fibroblasts that may invade the whole space

and to inhibit somehow the growth of specific parathyroid cells. The primary culture was subcultured to form a primary cell line but we verified that although the cells seemed viable they lose the ability to proliferate and became senescent after a few number of passages.

3.3 THIRD TASK: VALIDATION OF THE VARIANTS BY IHC (ONGOING)

After prioritization, some of the variants resulted from the WES will be searched by Sanger sequencing on a selected validation cohort consisting of sporadic parathyroid, atypical and classic, adenoma tissues. This task has a several limitation that we tried to overcome:

The validation cohort consists of 15 DNAs extracted from Formalin-Fixed Paraffin Embedded (FFPE) tissues of parathyroid adenomas, atypical adenoma and carcinoma. It is well known that DNA extracted from FFPE tissue is highly degraded and hard to be successfully PCR amplified and sequenced. Likewise, this poor quality DNA can not be processed in a classic WES assay. Finally, the amount of useful DNA extracted from these specimens is not enough to perform the whole validation.

In order to investigate the possible genetic variants of this cohort, we decided to perform the WES on 2 tumor DNAs extracted from fresh frozen carcinoma tissues. Instead, this different DNA is less degraded and suitable for NGS studies. After prioritization, the variants resulted more interesting from the bioinformatic analysis, will be tested on DNA from FFPE tissues by the Digital-PCR, that allows a high detection rate, even using small amount of DNA.

As additional milestone of the project, proteins resulted as more suggestive from WES will be assayed by IHC on FFPE tissues of the validation cohort. As possible option, proteins already reported in literature as differentially expressed in parathyroid carcinoma or atypical or classic adenoma (116) will be assayed by IHC as well on the validation cohort.

This task is ongoing.

CHAPTER 4: DISCUSSION

Parathyroid carcinoma is a rare and life-threatening tumor for whose at the moment therapeutic strategies, rather than the surgical approach, resulted unsuccessful and for whose no specific chemotherapy has been set up. Being the surgery the only curative way, great efforts have been invested in prevention and possible identification in pre-clinical stage of a malignant parathyroid lesion. Instead to discriminate a malignant from a benign neoplasm would greatly help the surgeon in the choice of the approach to pursue, thus resulting in a longer patient survival.

In case of an undoubted malignant lesion, a demolitive *en-bloc* resection of the whole thyroid along with the compromise of the recurrent laryngeal nerve is the best choice, although this operation might have severe implications for the quality of life of the patient. On the other hand, a more conservative surgery is suggested in case of benign lesion or hyperplasia. The main problem lies in the possibility/ability of the surgeon/endocrinologist/radiologist to recognize a parathyroid lesion as malignant or benign. This is not possible in pre-clinical stage unless the patient manifests other pathognomic signs such as metastasis or re-occurrences.

However, in absence of these features, a malignant parathyroid lesion can be ascertained only by the pathologist, thus, after the surgery. This limitation may outcome in a possible relapse of the disease in a patient wrongly firstly diagnosed. And, at the next operation, the patient could be affected by other comorbidities with consequent high risk.

To date, improvements in parathyroid tumors diagnosis have been made by molecular screening of 2 genes, CDC73 and MEN1, and the immunohistochemistry (IHC) of the corresponding proteins parafibromin and menin. However, these strategies can not be always pursued or often follow the surgery, thus they do not fulfill the need of an unequivocal/ prompt diagnosis for the choice of surgery. Genetic/epigenetic (147) factors have been sought by EP/WE (148) studies on sporadic cases but the intrinsic variability of different genetic backgrounds (thousands of data/gene variants were detected, of which

99.9% are confounding polymorphisms) (149) made it hard to identify the real causes of PT.

At present a different design based on familial cases (affected/unaffected with the same genetic background) has not been attempted due to the rarity of surveys of familial malignant PTs forms (KP and AA). Such an approach could filter and eliminate in few step all the harmless and confounding variants, finally pinpointing the ultimate genetic factors of this aggressive tumor.

Moreover, while past studies on genetic factors were performed on sporadic cases belonging to different families, for the 1st time, in this project all these strategies have been centralised in a triple global approach on clinically ascertained families and on subjects having almost the same genetic background. In this way, the causing variants of the disease could be more evident in the background noise of harmless polymorphisms and the identification of asymptomatic carriers in affected families would lead to efficient early intervention. By determining the signature of genetic causes at the base of parathyroid cancer, it would be possible to better understand the molecular pathway leading to tumor development and the identification of a biomarker set for an immediate early parathyroid tumor diagnosis.

Our cohort consisted of 5 families with a germline CDC73 mutation and 1 family with MEN1 mutation associated to a KP. It is important to highlight the rarity of a such cohort.

A metanalysis on all the (up to date) CDC73 gene mutations published, since its first identification in november 2002, reported less than 90 CDC73 occurrences (i.e HPT familial cases), and less than 90 sporadic cases, worldwide (*Muscarella et al, in preparation*). In the same time, it is well known that the association of KP and MEN1 gene mutation is more than rare, accounting for less than the 0.5% (15 KP, in the last 40 ys, 21-23) of all the ascertained MEN1 cases. Here we report not only the 16th case, but the presumed first familial case of MEN1 and KP, suggesting that the classic MEN1 mutation is not enough to give a malignant form, but it needs to be supported from other genetic players (150).

4.1 WES ANALYSIS

More than a study tried to explore and identify the molecular landscape behind the onset and progression of KP, but no definitive results have been obtained. The use of NGS technology helped to detect low frequency mutations in well-characterized cancer genes such as MTOR, KMT2D, in a WES study on a sporadic KP (151), or specific mutations either at germline and somatic levels in PRUNE2 or APOBEC (152) and in kinase family related to cell migration and invasion in a series of 7 sporadic KP (149, 153). However, the genetic-molecular link between the CDC73 mutation and the tumor development remained elusive.

This could be due to the rarity of KP and to the consequent lack of knowledge about etiology and of experimental models. Or maybe it could be due to the different approach used in the different studies. We believe that the analysis of somatic DNA is important to determine the genetic determinants of the invasiveness and aggressivity of a parathyroid lesion. However, the genetic comparison of affecteds vs carriers and vs controls at germline levels may contribute to understand other important factors influencing the onset and the co-morbidities associated to a KP and the penetrance of the CDC73 gene mutation.

Instead we wondered why in some of our families there was a so great difference in the onset of the disease, with subjects developing the disease more than one time and other carriers who never manifest any symptoms.

Looking at the WES data, although if they are preliminar, we noticed that 4 out 5 families carry rare variants in genes encoding the integrins, cell surface receptors involved in cell adhesion to the extracellular matrix (ECM) and essential for proliferation, survival, adhesion and migration of cells. It is interesting to note, that the specific variants have a very low MAF in the general population (< 0.004). This rarity becomes even more significant taking into account that the variants are exclusively shared by the affecteds and not by carriers and controls. Preliminary results of the RT-PCR demonstrated a differential expression levels "presumably" mutated integrin: particularly in two families the ITGA2B resulted highly expressed in the carrier rather than in the affected (Figure 8b, 8c). An opposite result was found for the ITGA3 which

seems to be more expressed at least in one affected rather than in the carrier (Figure 7b). We do not expect in all the families in whose we found these variants, an aberrant expression level of these proteins. However, we strongly believe, that these findings deserve further in-depth studies. Instead it has been proved that integrins are epigenetically regulated by defined miRNA. Thus, should these proteins reveal their potential involvement in KP onset and progression, therapeutic strategies may be developed on this epigenetic base.

Mutations in oncogenes such BRCA1 and RET were found in the Family II, although no other tumors strictly related to these genes (thyroid or breast) were manifested. It is likely that in this specific contest these variants have low penetrance or alternatively, at least for the p.L56M found in the RET gene, the variant may be considered a rare SNP (127). However, in the same family we found other variants in genes encoding proteins involved in DNA repair such as FANCC and BRIP1. Thus, we can not exclude that the onset/ progression/ aggressivity of the disease may be due not just to the presence of one or more trigger factors but maybe to the lack of someone else, such as the proteins assigned to DNA integrity.

We were able to confirm also data previously reported on the involvement of genes encoding the component of the MLL complex, such as KMT2C (154). However, it is important to highlight, that, differently from previous study, the variant was found at germline level, and thus, it could have a magnified effect. MLL complex is strictly correlated with MEN1 gene, being menin a co-transcription factor of the complex. Our finding is in line with the hypothesis that parafibromin and menin seem to be the two faces of the same medal, since they shared common functions, common molecular pathway and molecular partners.

Variants in genes of the Hedgehog pathway, such as SMO and GLI3, in Family II, or in NOTCH4 in Family I and IV, will deserve a specific attention. This because the Hedgehog pathway seems to be recurrently mutated in some of its components as also confirmed by the GLI2 variant in the MEN1 family affected by KP.

It has been reported that parafibromin may bind competitively with β -catenin and GLI1, to amplify the transactivation of Wnt- and Hh-target genes in a mutually exclusive way (56). But, parafibromin binds Notch intracellular domain to activate Wnt and Notch target genes (56). Thus, loss of parafibromin (in mice) would lead to an abnormal intestine epithelial structure, that is normally preserved by Wnt, Hh and/ or Notch signalling. The Authors conclude that parafibromin is crucial to mediate the signals of these morphogens pathways into appropriate transcriptional outputs (56).

Our findings of so many variants (SMO and GLI3, in Family II, NOTCH4 in Family I and IV, GLI2 in the Family with MEN1-KP) could be pure coincidence or it may have a more and important meaning. Instead in the MEN1-KP Family the RT-qPCR confirmed all the carriers have higher expression levels of each component of the Hedgehog complex with respect the affecteds and controls (these latter not carrying any mutation) and particularly of SMO, GLI3 and GLI2 (found also “mutated” in Family II and MEN1-KP). A further approach would be to test these proteins as possible biomarkers (on urine or serum) of the disease progression in wider cohort of patients and possibly at different stage of the disease: preclinical, clinical and post surgery. Nevertheless, should these proteins confirm their potential use as biomarkers and or involvement in the disease, drug therapy would be already clinically available.

4.2 DISCUSSION ON MEN1 FAMILY

Two detailed metanalysis of the last 40 years reported totally 15 cases of KP as associated with MEN1 syndrome, with an overall prevalence of 0.5% (3/590 MEN1 subjects recruited at the Mayo Clinic and at the MD Anderson Cancer Center, 2, 10, 11). Of those 15 cases, only in 7, the MEN1 mutation was identified. For all the 15 index cases, when the familial HPT was proved, there was no any mention about other malignant lesions affecting family members (20-22). These data indicate that the MEN1 gene does not represent a major genetic driver per se of malignancy for the parathyroid lesion. Instead it is likely that the malignant progression of the parathyroid lesion in those cases could be due to additional unknown genetic events, occurring at the somatic level, as

frequently reported in many cancers, with specific signatures of somatic mutations (155).

This has been also confirmed by recent studies on (even small) cohort of 8 DNAs extracted from MEN1 parathyroid tumors. The Authors searched for alternative somatic genetic driver, and they found a rare concurrent mutation in the EZH2 gene, a member of the Polycomb-group (PcG) family involved in H3-K27 methylation (156, 157). Interestingly the mutation identified in 2 (out of 8) parathyroid adenomas was a gain of function mutation affecting the trimethyltransferase activity and causing up to 7% of large follicular lymphomas and 22% of diffuse B-cell lymphomas. However, although this exceedingly rare concurrence was not confirmed on additional 185 specimens and 23 KP (158), we can not exclude that parathyroid neoplasms with MEN1 mutation may benefit from other mutations, especially in gene known as involved in tumor syndromes.

An additional study on 16 tumor DNAs extracted from patients resulted negative at the MEN1 screening on germline DNA, confirmed somatic MEN1 mutations in a small percentage of tumors (35%) while other specimens remained without genetic determinants. This would confirm the atypical nature of parathyroid neoplasms and of the benignity of MEN1-induced lesions and that it is likely that other "extracoding" mutations, such as complex chromosomal rearrangements may play a role (149).

With regard to the Family VI, taking into account the prevalence of MEN1 in general population (0.0033%, 24), given the low frequency of KP in MEN1 syndrome (0.5%, 9 and 10), the co-occurrence of parathyroid carcinoma affecting two siblings of a MEN1 family seems not to be a stochastic event ($0.0033 \times 0.5 \times 0.5 = 0.00082/1000000 = 8.2 \times 10^{-10}$). Given so likewise (and even more) exceedingly rare concurrence we hypothesized a different genetic landscape in our family: the 418N induced a "MEN1 classically benign" parathyroid lesion, while an additional unknown genetic event acted to promote progression towards the malignancy. Here, though, the presence of 2 carcinomas in the same family suggests the genetic event was pre-somatic. Thus, our Family VI may well represent the first reported familial case with KP due to

MEN1 mutation. The WES analysis led to the identification of alternative mutations in many genes, the most promising is GLI2. GLI2 gene is part of the Hedgehog pathway, a evolutionary conserved transcriptional complex involved in a plethora of cellular function and development even from the beginning embrional stages. Hedgehog pathway is deranged in several tumour syndromes. Finally many evidences have been reported about the physical binding of MEN1 and GLI proteins. For these reasons we believe that the GLI2-P702Q mutation can not be considered as "passenger" in this tumoral tissue, but "driver". Further studies will aim to investigate: i) the role (presumably activating) of this mutation in the contest of a MEN1 mutated tumor; ii) the frequency of GLI mutations at somatic level in a validation cohort of somatic DNAs extracted from parathyroid neoplasm; iii) the IHC for GLI proteins on parathyroid tissues (this latter aim is ongoing as part of the third task).

One further point concerns the atypical clinical presentation of the family. The concurrent presence of: i) parathyroid disease in 3 affecteds and gross carcinoma (7.3 and 4.6 cm) in 2 siblings; ii) familial HPT with KP and iii) renal colic, addressed to the HPT-JT. However negative screening of the CDC73 gene prompted us to consider the MEN1 syndrome that was supported by the involvement of adrenal lesions, melanoma, lipoma. This case is instructive in that it highlights the importance of implementing a stepwise complete screening protocol for all the genes showing some association with familial HPT, especially in families with atypical clinical presentation and independently from the age. Instead this would greatly help the identification of carriers unaffected (as the 19 ys old proband's nephew in our family) to address to a more close clinical follow-up.

4.3 EXPRESSION PROFILING

Our analysis of comparison of affecteds vs carriers vs controls showed a differential expression of genes of immune system. The analysis involved HPT-JT families that were compared with the unique MEN1-KP family so far identified worldwide. The results suggest that HPT-JT seems to be characterized by a more pronounced activation of leukocytes rather than what happens in MEN1. In HPT-JT, the “cell death” of cancer cells seems less active than in MEN1, thus reflecting the different grade of severity of the two types of parathyroid lesions: malignant in HPT-JT vs benign in MEN1: instead, to inhibit apoptosis would mean to favor tumor growth and spreading. Particularly, Natural Killer (NK) cells and T-cells were inhibited in CDC73 tumors and not in MEN1 tumors. Moreover, we found that the function of leukocytes was inhibited in MEN1 tumors and their apoptosis enhanced.

A deregulation of the immune system in cancer has recently emerged as dramatic paradigm in several tumor (159, 160). Immune checkpoints are regulated by many signaling processes that are in part controlled by programmed death 1 immunoreceptor (PD-1/CD279) through the interaction with programmed death ligand-1 (PD-L1) and PD-L2. In recent years, it was reported that both in immune cells (ICs) and tumor cells (TCs), the aberrant activation of PD-1/PD-L1 binding represents a crucial self-tolerance pathway that tumor cells have hijacked to escape immune elimination via survival and proliferation pathways (161). However, it became clear that the expression of immune checkpoint molecules on tumor cells has important consequences on the biology of the tumor cells themselves. In particular, a causal relationship between the expression of these molecules and the acquisition of malignant traits has been demonstrated. Thus, immune checkpoint molecules have been shown to promote the epithelial-mesenchymal transition of tumor cells, the acquisition of tumor-initiating potential and resistance to apoptosis and antitumor drugs, and the propensity to disseminate and metastasize. It is conceivable that the deregulation of activation of lymphocytes we found in the HPT-JT may be somehow correlated with the inhibition of response of the

immune system. Unleashing the natural defence against cancer may be thus an option to pursue and to study in-depth.

The EP also evidenced that MEN1 and HPT-JT patients use different set of genes to control the calcium mobilization. Particularly, MEN1 patients seem to have a better control of the calcium variability rather than the HPT-JT patients. Thus seems reflect the variability in terms of calcium values in these diseases, that are, in some cases, very different; just above the upper limit for the MEN1, but higher in HPT-JT.

4.4 DRUG TEST

As clearly stated, KP is a tumor for whose, at the moment, surgical treatment is the unique type of treatment. Specific chemotherapy does not exists and the common protocol resulted, most of the times, unsuccessful. Thus, the identification of novel (or already used in clinic) drugs would be more than desirable.

We started by the evidence that mutations of the CDC73 not supposed to cause a frank loss of parafibromin expression (i.e. missense or in-frame deletions) led, on the contrary, to a almost complete degradation proteasome-induced.

Thus, in keeping with similar results reported on the "twin" protein, menin (138), we decided to verify if the use of Bortezomib could rescue the expression of our parafibromin mutants.

Unexpectedly, we found that, as happened with chemical proteasome inhibitor MG132 (121), also the Bortezomib was able to rescue, the expression of missense, in-frame and even frameshift CDC73 gene deletions. This result is important for the following reasons:

- this is the first time we proved that ascertained causative CDC73 mutations may be rescued, at least, in their expression by the use of a clinical known drug. Should further studies confirm that the Bortezomib is also able to restore along with the expression also the function/interaction of mutated

parafibromin, it would greatly open novel perspectives for the therapy of these patients;

- the preliminary results have been obtained with minimal drug concentrations and for minimal administration time. So we can not exclude that stronger and prolonged restoring effect could be reached with higher dose administrated for longer times;

- the main advantage would lie in the possibility to use a drug already used in clinic, of whose possible side effects are well known. This would save time and money for research in novel drugs and, overall, it would bypass all the phase trials, usually needed for testing a clinical compound.

4.5 IHC AND SEARCH ON URINE-SERUM

Although this task is still ongoing and no data are available, at the moment, encouraging clues come from the literature that are in keeping with some results here reported. Particularly, Erovic et al (116) performed an extensive IHC analysis on 10 KP and 25 AA with several tissue markers known as to be variably involved in tumor proliferation and progression (PDGFR- α and β , VEGFR-2, EGFR, COX-1 and 2, MMP-1, CD9, keratin 7, cdc2p34, cyclin D1, Rb, p27, p21, parafibromin, Bmi-1, 14-3-3 σ , p53, Bcl-2a, Mcl-1, Bcl-xL, Gst- π , Smo, SHH, Gli-1, Gli-2, Gli-3, patched, mTOR, AKT, FoxO-1, Wisp-1, Wisp-2, and β -catenin). They found (obvious) differential expression (between malignant and benign parathyroid lesions) of parafibromin and p27 proteins. However, unexpected results were the different expression of other markers, such as Rb, Bcl-2a, FoxO-1 and, in keeping with what reported above, members of sonic hedgehog pathway (Smo, SHH, GLI 1-2-3).

The main aim of this task is to confirm these findings also in our cohort, In order to widely investigate by IHC and Elisa assays if some of these markers are also detectable within the tumour tissue or patient's serum/urine respectively, possibly reinforcing the assumption that deregulation of Hedgehog pathway may help not only in distinguishing malignant from benign lesions, but also represent a possible biomarkers of first diagnosis to predict the outcome and to suggest the best surgical approach.

CHAPTER 5: CONCLUSION

The approach used in this study took into account: the rarity of the cohort, the atypical clinical presentation, and the most high-throughput technologies. The results here reported, although preliminary, are innovative and open to novel research field.

Though all our findings need to be confirmed on larger cohorts, the clinical scenario depicts a possible "continuum" from classic benign lesions induced by MEN1 mutation towards the malignant forms caused by CDC73 inactivation, passing through the mid (extremely rare) condition of a MEN1 syndrome associated to a KP.

Our results seem to define that the different grade of malignity rising up from the MEN1 to HPT-JT may depend on several factors and among these:

- proteins involved in DNA repair process (FANCC, BRIP1, BRCA1), that may confer a such resistance to cellular mechanisms of self limitation;
- proteins involved in cell-cell adhesion (such integrins) that may contribute to the dissemination of the tumor cells;
- the Hedgehog pathway, whose deregulation has been clearly previously confirmed by literature data and, in this project, it found the experimental confirm in MEN1-KP and HPT-JT patients;
- the derangement of immune system, that seems specifically accompany the CDC73 mutation in the HPT-JT.

However, to confirm this hypothesis of a such clinical and molecular landscape, it needs to investigate the last part of this scenario: the MEN1 syndrome in its "classic" form of benign parathyroid lesions. Unfortunately, so far we were unable to include this part in the project, that will be (hopefully) developed in future.

KP is a rare untreatable cancer, but novel insights either on genetic and clinical field acquired in the last years made this tumor less unknown and maybe more vulnerable. A lot of work needs to reach the goal of a targeted therapy.

APPENDIX

METHODS

1. DNA AND RNA EXTRACTION

From the peripheral blood of the recruited subjects, DNA was extracted using phenol-chloroform extraction technique (162).

Moreover, it has been optimized DNA extraction from formalin-fixed, paraffin-embedded tumor tissue sections with new kits (QIAMP DNA FFPE KIT, Qiagen).

RNA of available subjects has been extracted from peripheral blood using the Paxgene Blood RNA Kit (QIAGEN) following the manufacturer's protocols (163).

2. WHOLE EXOME SEQUENCING (WES)

WES analysis was carried out at the University of Bari with the Illumina TruSeq Exome Enrichment kit (62M). For the WES library preparation, was used the Sure SelectQXT Target Enrichment for Illumina Multiplexing Sequencing System (Agilent Technologies, Santa Clara, CA, USA), using the procedure describe in appendix

[\(<http://www.agilent.com/cs/library/usermanuals/Public/G9681-90000.pdf>\)](http://www.agilent.com/cs/library/usermanuals/Public/G9681-90000.pdf)

Agilent Technologies, Santa Clara, CA, USA).

The SureSelect QXT kit combines a transposase based library preparation method with SureSelect's target capture system. Enrichment probes are 120 nt long baits that allow the capture known coding DNA sequences (CDS) from the NCBI Consensus CDS Database as well as other major RNA coding sequence databases, such as Sanger miRBase (164).

Briefly, 50 ng of genomic DNA is enzymatically fragmented and adaptors are added to the ends of the fragments in a single reaction. The adaptor-tagged DNA libraries are then PCR amplified using an appropriate pair of dual indexing primers, and the PCR product is quantified using Agilent High Sensitivity D1000 DNA Assay kit on the Tape Station 2200 (Agilent Technologies, Santa Clara, CA, USA). For the hybridization, an amount of 750-1500 ng of library is required. The

next step is the capture with streptavidine-coated magnetic beads and the amplification of the capture libraries to add index tags.

Sequencing libraries were then sequenced using the NextSeq500 SequencingSystem (Illumina Inc., San Diego, CA, USA), performing paired-end runs covering at least 2x150 nucleotides, using High Output 300 cycles flow cells (Illumina Inc., San Diego, CA, USA). NextSeq 500 uses a chip-based bridge amplification procedure followed by sequencing by synthesis using reversible terminator dye nucleotides.

2.1 Bioinformatic NGS analysis

The analysis of NGS sequencing data was performed according standard bioinformatics procedures. At first, raw individual sequence files (*.fastq) were checked for their quality through the FastQC tool (165), in order to detect trends in base call quality scores according to read position, adapter content, base compositional bias, etc. Quality-checked reads were mapped against the hg19 version of the human reference genomic sequence through the BWA aligner (166); the produced alignments (*.bam) were also processed through the GATK suite (167). Refined *.bam alignments were used to calculate on-target and off-target sequencing coverage statistics (in particular, average target depth of coverage and proportion of target sites at 20X minimal coverage) by using the TEQC R Package (168). Finally, variants were detected by means of the GATK v3.7 Haplotype Caller and annotated by using ANNOVAR Package with respect to the hg19 RefSeq gene and transcript annotation (169). Functionally annotated variants were also checked for their presence in public variant collections, like dbSNP v149 and its ClinVar specialized database (170) and ExAC v0.3 (171). Furthermore, variants with a missense functional impact were also annotated with pathogenicity predictors, by querying the dbNSFP resource (172). Identification of candidate pathogenic variants was performed by imposing several filtering criteria, excluding: variants with low functional impact (intronic, synonymous, located in UTRs, etc.); variants with high allelic frequency in public

databases (> 1%); variant with inconsistent segregation among related samples; variant mostly predicted as neutral by computational tools.

3. EXPRESSION PROFILING

Analysis of gene expression profiles using microarrays on familial probands/carriers/relatives (affected/unaffected) under studied was carried out at the IRCCS Casa Sollievo della Sofferenza. The quality of the nucleic acid obtained was evaluated by capillary electrophoresis at Bioanalyzer 2100 (Agilent Technologies), considering the RNA (RNA integrity Number) reference value as its reference parameter, whose value should be close to 10. The RNA was subsequently dosed using the Nanodrop 2000 spectrophotometer and diluted, if necessary, at a concentration of 100 ng/ μ L. This RNA was used to perform gene expression profiles by microarrays using the Affymetrix GeneChip[®] Human Transcriptome 2.0 Array containing about 6 million probes representative of both the coding and non-coding part of the human genome. 400,000 full-length transcripts were combined from available public data sources: RefSeq NCBI, UCSC Genes, Vega, GENCODE, Ensembl, Mammalian Gene Collection. Additional long non-coding content was combined from the UCSC genome browser, noncode.org, Broad Human Body Map. Probes are distributed across the full length of the gene including specific probes (>339.000 probe sets) covering splice junction, providing a complete and accurate picture of overall gene expression with the additional ability for transcript isoform analysis. Each sample has been processed and labeled using the Gene Chip WT Plus Reagent Kit (Affymetrix) following the manufacturer's instruction (173). Briefly, on 100 ng of total RNA, a random priming method was used to generate cDNA from all RNA transcripts present in a sample. The cDNA was fragmented and labeled with biotin using terminal deoxynucleotidyl transferase (TdT) before hybridization in a GeneChip Hybridization Oven 645 (Affymetrix). Following hybridization and post-hybridization washes, the arrays were scanned using the Affymetrix GeneChip Scanner 3000 7G to generate the raw data (CEL file). The quality control steps of the experiment were performed using the Expression Console ver.1.3 (Affymetrix). To reduce noise, probe sets that do not map to an Entrez gene

were removed. Batch effects were removed by the Partek's batch effect removal algorithm. Functional and pathway analyses were carried out by Ingenuity Pathway Analysis (IPA). IPA analysis was based on the preliminary calculation of the activation z scores (we considered z-scores < -2 (minimum inhibition threshold) as significant), used to predict the activation or inhibition state of molecules. Inference of activating or inhibiting molecules or biological functions was based on confirmation by the literature of the results of our experiments. An enrichment score (Fisher's exact test, P-value) was calculated to measure the overlap between observed and predicted regulated gene sets (174). Differentially Expression Genes (DEGs) were selected whenever their Fold Change values were significantly (p-value < 0.05) greater than 1.5.

4. RT-QPCR

4.1 cDNA synthesis

Total RNA extracted was subsequently dosed using the Nanodrop 2000 spectrophotometer and 500ng of total RNA was subjected to reverse transcription using SuperScript III first-strand Synthesis Supermix (Invitrogen) according to the manufacturer's instructions (https://tools.thermofisher.com/content/sfs/manuals/superscript_firststrandsupermix_man.pdf) and diluted, if necessary, at a concentration of 100 ng/uL.

4.2 Real-Time quantitative Polymerase Chain Reaction (RT-qPCR)

Fluorescence based real time quantitative PCR (RT-qPCR) was set up in 384-well plates in a total volume of 10 μ l containing 1 μ L cDNA, 0,5 μ L 20x PrimePCR Assay (Biorad) specifically designed on each target genes sequence (ITGA2B, ID:qHsaCID0013206; ITGA3, ID:qHsaCED0056641; GLI1, ID:qHsaCED0043346; GLI2, ID:qHsaCED0003858; GLI3, ID:qHsaCED0001509; SMO, ID:qHsaCED0019995; SHH, ID:qHsaCED0037736) and 5 μ L of 2xSsoAdvanced universal SYBR Green (Biorad) (<http://www.biorad.com/webroot/web/pdf/lsr/global/english/primePCR/LIT10026370.pdf>).

The thermal cycling protocol is programmed as follows:

Step	Temperature	Time	No. of Cycles
Activation	95°C	2 min*	1
Denaturation	95°C	5 sec	40
Annealing/Extension	60°C	30 sec	40
Melt Curve**	65-95°C (0.5°C increments)	5 sec/step	1

Reactions were run on ABI PRISM 7900 Sequence Detection System (Applied Biosystems). Transcription levels of target genes were normalized using the expression level of the Glyceraldehyde phosphate dehydrogenase (GAPDH) as reference gene. To evaluate the specificity of the PCR reaction, a melt curve analysis was performed at the end of the PCR cycles: the final product was subjected to graded temperature-dependent dissociation to verify the amplification of just/only one product. In this case, the melt curve displays a single sharp peak confirming the specificity of primer annealing. No template control (NTC) was included for each PCR Prime Assay to verify the lack of reagent contaminations.

A relative quantification method with standard curve was developed for each of target genes and GAPDH. cDNA of each subjects was amplified and 3uL of PCR fragments for all the target genes and GAPDH were cloned in StrataClone PCR Cloning Vector pSC-A (Stratagene, Agilent Technologies) to construct the standard curves for real-time qPCR. Plasmid DNA from the selected transforming cells was isolated by using the QIAprep Spin Miniprep Kit (Qiagen). Vectors were serially diluted and five plasmids, in the range of 1×10^6 copies to ten copies, were used to construct the standard curves for real-time PCR. To establish quantitative range and main detection limit, 10-fold serial dilutions of plasmid containing inserts were analyzed in triplicate by RTqPCR.

5. FUNCTIONAL ASSAY

5.1 cDNA expression vectors

All the CDC73 variants and the GLI2 variant (p.P702Q) were introduced in a Myc-Flag tagged human CDC73 or GLI2 cDNA expressing pCMV6 vector (Origene). Briefly, mutagenesis reactions were conducted in a total volume of 50 uL containing 100 ng DNA, 5 ul 10X buffer, 8 uMol (final) dNTPs and 1U Pfu Taq polymerase (Promega), 125 pmol (final) of each primer.

PCR conditions were: 95°C x 2 min, and 18 cycles of 95°C x 30 sec, 55°C x 1 min and 72 °C X 12 min. One microlitre of Dpn1 (New England Biolabs) was added to digest parental DNA and 3 uL used to transform DH5a cells (Invitrogen). Colony PCR and sequencing identified the mutated clones. Midipreps were performed with Plasmid Midi Kit (QIAGEN) (175).

5.2 Cell culture

Human embryonic kidney (HEK293) cells (ECACC) were cultured in DMEM/Ham's F12 (BioSpa) supplemented with 10% Fetal Bovine Serum (BioSpa) and 1% penicillin/streptomycin (BioSpa) and incubated at 37°C in a humidified, 5% CO₂ incubator. Wild-type and mutant vectors were transfected in duplicate or in eight replicates (for Western blot and cell proliferation assays, respectively) using Lipofectamine 2000 Transfection reagent (Invitrogen) following the manufacturer's instructions (176). For each experiments HEK293 cells were used with a number of passages < 10.

5.3 Proliferation assay

Twenty thousands cells were seeded in 96 well plates: CDC73 WT and mutants vectors were transfected in eight replicates with Lipofectamine 2000 (Invitrogen) as previously described. After 24h from transfection, 10 µL of 37°C. Then the absorbance at 590 nm was measured with an Elisa reader (177). Presto Blu Reagent (Life Technologies) was added to each well and incubated for 1 h.

5.4 Western blot

Total cell proteins were extracted in RIPA buffer (150 mM NaCl, 50 mM Tris-HCl, 1% Nonidet P-40, 0.1% sodium dodecyl sulfate, 0.5% sodium deoxycholate, pH 8.0) and 50ug of proteins were loaded onto a 10% SDS polyacrylamide gel. Proteins were electrotransferred to PVDF membrane (Millipore, Billerica, MA), blotted overnight at 4°C with rabbit anti Flag monoclonal antibody (Cell Signaling Technology) and for 1h at room temperature with the horseradish peroxidase-conjugated goat anti-rabbit IgG antibody (Santa Cruz) as secondary antibody.

Membranes were stripped with Re-Blot Solution (Millipore) and α -actin mouse monoclonal antibody (Sigma Aldrich) was blotted as loading control. For quantitative measurement, films were scanned by densitometry and the spots corresponding to proteins were analysed by using the ImageJ-National Institutes of Health image-processing program (<http://rsbweb.nih.gov/ij/>).

5.5 Protein degradation assessment

After 48 hours from the transfection, MG132 (Sigma Aldrich, 25 μ M final concentration) was added to one set of cells and protein extraction performed 4 hours later.

After 24 hours from the transfection, treatment with Bortezomib (Selleck Chemicals, 10 μ M final concentration) was made for 24 h and total cell proteins were extracted.

REFERENCES

1. Simonds William F. Genetics of Hyperparathyroidism, including Parathyroid Cancer. *Endocrinol Metab Clin N Am* 46, 2017; 2:405-418. doi: 10.1016/j.ecl.2017.01.006.
2. Pepe J, Cipriani C, Pilotto R, De Lucia F, Castro C, Lenge L, et al. Sporadic and hereditary primary hyperparathyroidism. *J Endocrinol Invest*. 2011; 7 Suppl :40-4.
3. Adami S, Marcocci C, Gatti DJ. Epidemiology of primary hyperparathyroidism in Europe. *Bone Miner Res*, 2002;17 (Suppl 2): N18-23.
4. Bilezikian JP, Cusano NE, Khan AA, Liu JM, Marcocci C, Bandeira F. Primary hyperparathyroidism. *Nat Rev Dis Primers* 2016; 2:16033. doi: 10.1038/nrdp.2016.33.
5. Schulte KM, Talat N. Diagnosis and management of parathyroid cancer. *Nat Rev Endocrinol*. 2012; 10:612-22. doi: 10.1038/nrendo.2012.102.
6. Ricci G, Assenza M, Barreca M, Liotta G, Paganelli L, Serao A. Parathyroid Carcinoma: the importance of high clinical suspicion for a correct management. *Int J Surg Oncol*. 2012;2012:649148. doi: 10.1155/2012/649148.
7. Kebebew E, Arici C, Duh QY, Clark OH. Localization and reoperation results for persistent and recurrent parathyroid carcinoma. *Arch Surg*. 2001; 8:878-85.
8. DeLellis RA. Challenging lesions in the differential diagnosis of endocrine tumors: parathyroid carcinoma. *Endocr Pathol*. 2008; 4:221-5. doi: 10.1007/s12022-008-9050-2.
9. Juhlin CC, Nilsson IL, Johansson K, Haglund F, Villablanca A, Höög A. Parafibromin and APC as screening markers for malignant potential in atypical parathyroid adenomas. *Endocr Pathol*. 2010; 3:166-77. doi: 10.1007/s12022-010-9121-z.
10. Kumari N, Chaudhary N, Pradhan R, Agarwal A, Krishnani N. Role of Histological Criteria and Immunohistochemical Markers in Predicting Risk of Malignancy in Parathyroid Neoplasms. *Endocr Pathol*. 2016; 2:87-96. doi: 10.1007/s12022-016-9426-7.

11. Fernandez-Ranvier GG, Khanafshar E, Tacha D, Wong M, Kebebew E, Duh QY, et al. Defining a molecular phenotype for benign and malignant parathyroid tumors. *Cancer*. 2009; 2:334-44. doi: 10.1002/cncr.24037.
12. Cardoso L, Stevenson M, Thakker RV. Molecular genetics of syndromic and non-syndromic forms of parathyroid carcinoma. *Hum Mutat*. 2017; 12:1621-1648. doi: 10.1002/humu.23337.
13. Lemos MC, Thakker RV. Multiple endocrine neoplasia type 1 (MEN1): analysis of 1336 mutations reported in the first decade following identification of the gene. *Hum Mutat*. 2008; 1:22-32.
14. Trump D, Farren B, Wooding C, Pang JT, Besser GM, Buchanan KD, et al. Clinical studies of multiple endocrine neoplasia type 1 (MEN1). *Quart Jour Med*. 1996; 9:653-69.
15. Thakker RV. Multiple endocrine neoplasia type 1 (MEN1). *Best Pract Res Clin Endocrinol Metab*. 2010; 3:355-70.
16. Brandi ML, Gagel RF, Angeli A, Bilezikian JP, Beck-Peccoz P, Bordi C, et al. Guidelines for diagnosis and therapy of MEN type 1 and type 2. *J Clin Endocrinol Metab*. 2001; 12:5658-71.
17. Scarpelli D, D'Aloiso L, Arturi F, Scillitani A, Presta I, Bisceglia M, et al. Novel somatic MEN1 gene alterations in sporadic primary hyperparathyroidism and correlation with clinical characteristics. *J Endocrinol Invest*. 2004; 11:1015-21.
18. Benson L, Ljunghall S, Akerström G, Oberg K. Hyperparathyroidism presenting as the first lesion in multiple endocrine neoplasia type 1. *Am J Med*. 1987; 4:731-7.
19. Burgess JR, Greenaway TM, Shepherd JJ. Expression of the MEN-1 gene in a large kindred with multiple endocrine neoplasia type 1. *J Intern Med*. 1998; 6:465-70.
20. Singh Ospina N, Sebo TJ, Thompson GB, Clarke BL, Young WF Jr. Prevalence of 6 parathyroid carcinoma in 348 patients with multiple endocrine neoplasia type 1 case report and review of the literature. *Clinical Endocrinology (Oxf)* 2014.
21. Christakis I, Busaidy NL, Cote GJ, Williams MD, Hyde SM, Silva Figueroa AM, et al. Parathyroid carcinoma and atypical parathyroid neoplasms in MEN1 patients; A clinico-pathologic challenge. The MD Anderson case series and review of the

- literature. *International Journal of Surgery* 2016; 31: 10-6.doi: 10.1016/j.ijso.2016.05.035.
22. Cinque L, Sparaneo A, Cetani F, Coco M, Clemente C, Chetta M, et al. Novel association of MEN1 gene mutations with parathyroid carcinoma. *Oncology Letters* 2017; 1: 23-30.doi: 10.3892/ol.2017.6162.
23. Lemmens I, Van de Ven WJ, Kas K, Zhang CX, Giraud S, Wautot V, et al. Identification of the multiple endocrine neoplasia type 1 (MEN1) gene. *The European Consortium on MEN1.Hum Mol Genet.* 1997; 7:1177-83.
24. Hughes CM, Rozenblatt-Rosen O, Milne TA, Copeland TD, Levine SS, Lee JC, et al. Menin associates with a trithorax family histone methyltransferase complex and with the *hoxc8* locus. *Mol Cell.* 2004; 4:587-97.
25. Karnik SK, Hughes CM, Gu X, Rozenblatt-Rosen O, McLean GW, Xiong Y, et al. Menin regulates pancreatic islet growth by promoting histone methylation and expression of genes encoding p27 Kip1 and p18 INK4c. *Proc Natl Acad Sci U S A.* 2005; 41:14659-64.
26. Milne TA, Hughes CM, Lloyd R, Yang Z, Rozenblatt-Rosen O, Dou Y, et al. Menin and MLL cooperatively regulate expression of cyclin-dependent kinase inhibitors. *Proc Natl Acad Sci U S A.* 2005; 3:749-54. Epub 2005 Jan 7.
27. Thakker RV. Multiple endocrine neoplasia type1 (MEN1) and type4 (MEN4). *Molecular and Cellular Endocrinology.* 2014; 1-2: 2–15. doi: 10.1016/j.mce.2013.08.002.
28. Kim H, Lee JE, Cho EJ, Liu JO, Youn HD. Menin, a tumor suppressor, represses JunD-mediated transcriptional activity by association with an mSin3A-histone deacetylase complex. *Cancer Res.* 2003; 19:6135-9.
29. Sukhodolets KE, Hickman AB, Agarwal SK, Sukhodolets MV, Obungu VH, Novotny EA, et al. The 32-kilodalton subunit of replication protein A interacts with menin, the product of the MEN1 tumor suppressor gene. *Mol Cell Biol.* 2003; 2:493-509.
30. Jin S, Mao H, Schnepf RW, Sykes SM, Silva AC, D'Andrea AD, Hua X. Menin associates with FANCD2, a protein involved in repair of DNA damage. *Cancer Res.* 2003; 14:4204-10.

31. Schnepf RW, Hou Z, Wang H, Petersen C, Silva A, Masai H, et al. Functional interaction between tumor suppressor menin and activator of S-phase kinase. *Cancer Res.* 2004; 18:6791-6.
32. Zablewska B, Bylund L, Mandic SA, Fromaget M, Gaudray P, Weber G. Transcription regulation of the multiple endocrine neoplasia type 1 gene in human and mouse. *J Clin Endocrinol Metab.* 2003; 8:3845-51.
33. Fromaget M, Vercherat C, Zhang CX, Zablewska B, Gaudray P, Chayvialle JA, et al. Functional characterization of a promoter region in the human MEN1 tumor suppressor gene. *J Mol Biol.* 2003; 1:87-102.
34. Friedman E, Sakaguchi K, Bale AE, Falchetti A, Streeten E, Zimering MB, et al. Clonality of parathyroid tumors in familial multiple endocrine neoplasia type 1. *N Engl J Med.* 1989; 4:213-8.
35. Newey PJ, Bowl MR, Thakker RV. Parafibromin--functional insights. *J Intern Med.* 2009; 1:84-98. doi: 10.1111/j.1365-2796.2009.02107.x.
36. Newey PJ, Bowl MR, Cranston T, Thakker RV. Cell division cycle protein 73 homolog (CDC73) mutations in the hyperparathyroidism-jaw tumor syndrome (HPT-JT) and parathyroid tumors. *Hum Mutat.* 2010; 3: 295-307. doi: 10.1002/humu.21188.
37. Casco A, Huarte-Mendicoa CV, Javier Leandro-Garcı L, Leto R, Suela J, Santana A, et al. Detection of the first gross CDC73 germline deletion in an HPT-JT syndrome family. *Genes Chromosomes Cancer* 2011; 11: 922-9. doi: 10.1002/gcc.20911.
38. Bricaire L, Odou MF, Cardot-Bauters C, Delemer B, North MO, Salenave S, et al. Frequent large germline HRPT2 deletions in a French National cohort of patients with primary hyperparathyroidism. *J Clin Endocrinol Metab* 2013; 2: E403-8. doi: 10.1210/jc.2012-2789.
39. Masi G, Iacobone M, Sinigaglia A, Mantelli B, Pennelli G, Castagliuolo I, et al. Characterization of a new CDC73 missense mutation that impairs Parafibromin expression and nucleolar localization. *PLoS One.* 2014; 5:e97994. doi: 10.1371.
40. Carpten JD, Robbins CM, Villablanca A, Forsberg L, Presciuttini S, Bailey-Wilson J, et al. HRPT2, encoding parafibromin, is mutated in hyperparathyroidism-jaw tumor syndrome. *Nat Genet.* 2002; 4:676-80.

41. Cetani F, Pardi E, Borsari S, Viacava P, Dipollina G, Cianferotti L, et al. Genetic analyses of the HRPT2 gene in primary hyperparathyroidism: germline and somatic mutations in familial and sporadic parathyroid tumors. *J Clin Endocrinol Metab.* 2004; 11:5583-91.
42. Bradley KJ, Cavaco BM, Bowl MR, Harding B, Cranston T, Fratter C, et al. Parafibromin mutations in hereditary hyperparathyroidism syndromes and parathyroid tumors. *Clin Endocrinol (Oxf).* 2006; 3:299-306.
43. Shattuck TM, Välimäki S, Obara T, Gaz RD, Clark OH, Shoback D, et al. Somatic and germ-line mutations of the HRPT2 gene in sporadic parathyroid carcinoma. *N Engl J Med.* 2003; 18:1722-9.
44. Rozenblatt-Rosen O, Hughes CM, Nannepaga SJ, Shanmugam KS, Copeland TD, Guszczynski T, et al. The parafibromin tumor suppressor protein is part of a human Paf1 complex. *Mol Cell Biol.* 2005; 2:612-20.
45. Yart A, Gstaiger M, Wirbelauer C, Pecnik M, Anastasiou D, Hess D, et al. The HRPT2 tumor suppressor gene product parafibromin associates with human PAF1 and RNA polymerase II. *Mol Cell Biol.* 2005; 12:5052-60.
46. Woodard GE, Lin L, Zhang JH, Agarwal SK, Marx SJ, Simonds WF. Parafibromin, product of the hyperparathyroidism-jaw tumor syndrome gene HRPT2, regulates cyclin D1/PRAD1 expression. *Oncogene.* 2005; 7:1272-6.
47. Mosimann C, Hausmann G, Basler K. Parafibromin/Hyrax activates Wnt/Wg target gene transcription by direct association with beta-catenin/Armadillo. *Cell.* 2006; 2:327-41.
48. Lin L, Zhang JH, Panicker LM, Simonds WF. The parafibromin tumor suppressor protein inhibits cell proliferation by repression of the c-myc protooncogene. *Proc Natl Acad Sci USA* 2008, 105: 17420–17425.
49. Wang P, Bowl MR, Bender S, Peng J, Farber L, Chen J, et al. Parafibromin, a component of the human PAF complex, regulates growth factors and is required for embryonic development and survival in adult mice. *Mol Cell Biol.* 2008; 9:2930-40. doi: 10.1128/MCB.00654-07.
50. Iwata T, Mizusawa N, Taketani Y, Itakura M, Yoshimoto K. Parafibromin tumor suppressor enhances cell growth in the cells expressing SV40 large T antigen. *Oncogene.* 2007; 42:6176-83.

51. Hahn MA, Marsh DJ. Nucleolar localization of parafibromin is mediated by three nucleolar localization signals. *FEBS Lett.* 2007; 26:5070-4.
52. Lin L, Czapiga M, Nini L, Zhang JH, Simonds WF. Nuclear localization of the parafibromin tumor suppressor protein implicated in the hyperparathyroidism-jaw tumor syndrome enhances its proapoptotic function. *Mol Cancer Res.* 2007; 2:183-93.
53. Juhlin CC, Haglund F, Obara T, Arnold A, Larsson C, Höög A. Absence of nucleolar parafibromin immunoreactivity in subsets of parathyroid malignant tumors. *Virchows Arch.* 2011; 1:47-53. doi: 10.1007/s00428-010-1032-3.
54. Agarwal SK, Simonds WF, Marx SJ. The parafibromin tumor suppressor protein interacts with actin-binding proteins actinin-2 and actinin-3. *Mol Cancer.* 2008;7:65. doi: 10.1186/1476-4598-7-65.
55. Mueller CL, Porter SE, Hoffman MG, Jaehning JA. The Paf1 complex has functions independent of actively transcribing RNA polymerase II. *Mol Cell.* 2004; 4:447-56.
56. Kikuchi I, Takahashi-Kanemitsu A, Sakiyama N, Tang C, Tang PJ, Noda S, et al. Dephosphorylated parafibromin is a transcriptional coactivator of the Wnt/Hedgehog/ Notch pathways. *Nat Commun.* 2016;7:12887. doi: 10.1038/ncomms12887.
57. Yanai K, Nakamura M, Akiyoshi T, Nagai S, Wada J, Koga K, et al. Crosstalk of hedgehog and Wnt pathways in gastric cancer. *Cancer Lett.* 2008; 1:145-56. doi: 10.1016/j.canlet.2007.12.030.
58. Bradley KJ, Bowl MR, Williams SE, Ahmad BN, Partridge CJ, Patmanidi AL, et al. Parafibromin is a nuclear protein with a functional monopartite nuclear localization signal. *Oncogene* 2007; 8,1213–1221.
59. Zhang C, Kong D, Tan MH, Pappas DL, Jr Wang PF, Chen J, et al. Parafibromin inhibits cancer cell growth and causes G1 phase arrest. *Biochemical and Biophysical Research Communications* 2006,350(1),17–24.
60. Willert K, Jones KA. Wnt signaling: is the party in the nucleus? *Genes Dev.* 2006; 11:1394-404.
61. Gordon MD, Nusse R. Wnt signaling: multiple pathways, multiple receptors, and multiple transcription factors. *J Biol Chem.* 2006; 32:22429-33.

62. Juhlin CC, Haglund F, Villablanca A, Forsberg L, Sandelin K, Bränström R, et al. Loss of expression for the Wnt pathway components adenomatous polyposis coli and glycogen synthase kinase 3-beta in parathyroid carcinomas. *Int J Oncol.* 2009; 2:481-92.
63. Polakis P. Wnt signaling in cancer. *Cold Spring Harb Perspect Biol.* 2012; 5. pii: a008052. doi: 10.1101/cshperspect.a008052.
64. Svedlund J, Aurén M, Sundström M, Dralle H, Akerström G, Björklund P, et al. Aberrant WNT/ β -catenin signaling in parathyroid carcinoma. *Mol Cancer.* 2010;9:294. doi: 10.1186/1476-4598-9-294.
65. Björklund P, Akerström G, Westin G. Accumulation of nonphosphorylated beta-catenin and c-myc in primary and uremic secondary hyperparathyroid tumors. *J Clin Endocrinol Metab.* 2007; 1:338-44.
66. Stecca B, Ruiz I, Altaba A. Context-dependent regulation of the Gli code in cancer by HEDGEHOG and non-HEDGEHOG signals. *J Mol Cell Biol.* 2010; 2:84-95. doi: 10.1093/jmcb/mjp052.
67. D'Amico D, Canettieri G. Translating Hedgehog in Cancer: Controlling Protein Synthesis. *Trends Mol Med.* 2016; 10:851-862. doi: 10.1016/j.molmed.2016.08.003.
68. Cheng SY, Bishop JM. Suppressor of Fused represses Gli-mediated transcription by recruiting the SAP18-mSin3 corepressor complex. *Proc Natl Acad Sci U S A.* 2002; 8:5442-7.
69. Pan Y, Bai CB, Joyner AL, Wang B. Sonic hedgehog signaling regulates Gli2 transcriptional activity by suppressing its processing and degradation. *Mol Cell Biol.* 2006; 9:3365-77.
70. Wang B, Fallon JF, Beachy PA. Hedgehog-regulated processing of Gli3 produces an anterior/posterior repressor gradient in the developing vertebrate limb. *Cell.* 2000; 4:423-34.
71. Hooper JE, Scott MP. Communicating with Hedgehogs. *Nat Rev Mol Cell Biol.* 2005; 4:306-17.
72. Riobo NA, Manning DR. Pathways of signal transduction employed by vertebrate Hedgehogs. *Biochem J.* 2007; 3:369-79.
73. Wicking C, Smyth I, Bale A. The hedgehog signalling pathway in tumorigenesis and development. *Oncogene.* 1999; 55:7844-51.

74. Sasaki H, Nishizaki Y, Hui C, Nakafuku M, Kondoh H. Regulation of Gli2 and Gli3 activities by an amino-terminal repression domain: implication of Gli2 and Gli3 as primary mediators of Shh signaling. *Development*. 1999; 17:3915-24.
75. Roessler E, Ermilov AN, Grange DK, Wang A, Grachtchouk M, Dlugosz AA, et al. A previously unidentified amino-terminal domain regulates transcriptional activity of wild-type and disease-associated human GLI2. *Hum Mol Genet*. 2005; 15:2181-8.
76. Flemming GM, Klammt J, Ambler G, Bao Y, Blum WF, Cowell C, et al. Functional characterization of heterozygous GLI2 missense mutation in patients with multiple pituitary hormone deficiency. *Endocrinol Metab* 2013; 3:E567-E575. doi: 10.1210/jc.2012-3224.
77. Treier M, O'Connell S, Gleiberman A, Price J, Szeto DP, Burgess R, et al. Hedgehog signaling is required for pituitary gland development. *Development*. 2001; 3:377-86.
78. Gurung B, Feng Z, Iwamoto DV, Thiel A, Jin G, Fan CM, et al. Menin epigenetically represses Hedgehog signaling in MEN1 tumor syndrome. *Cancer Res*. 2013; 8:2650-8. doi: 10.1158/0008-5472.CAN-12-3158.
79. Allen BL, Song JY, Izzi L, Althaus IW, Kang JS, Charron F, et al. Overlapping roles and collective requirement for the coreceptors GAS1, CDO, and BOC in SHH pathway function. *Dev Cell*. 2011; 6:775-87. doi: 10.1016/j.devcel.2011.04.018.
80. Izzi L, Lévesque M, Morin S, Laniel D, Wilkes BC, Mille F, et al. Boc and Gas1 each form distinct Shh receptor complexes with Ptch1 and are required for Shh-mediated cell proliferation. *Dev Cell*. 2011; 6:788-801. doi: 10.1016/j.devcel.2011.04.017.
81. Gurung B, Feng Z, Hua X. Menin directly represses Gli1 expression independent of canonical Hedgehog signaling. *Mol Cancer Res*. 2013; 10:1215-22. doi: 10.1158/1541-7786.MCR-13-0170.
82. Akimaru H, Chen Y, Dai P, Hou DX, Nonaka M, Smolik SM, et al. Drosophila CBP is a co-activator of cubitus interruptus in hedgehog signalling. *Nature*. 1997; 6626:735-8.

83. Dai P, Akimaru H, Tanaka Y, Maekawa T, Nakafuku M, Ishii S. Sonic Hedgehog-induced activation of the Gli1 promoter is mediated by GLI3. *J Biol Chem.* 1999; 12:8143-52.
84. Yoon JW, Liu CZ, Yang JT, Swart R, Iannaccone P, Walterhouse D. GLI activates transcription through a herpes simplex viral protein 16-like activation domain. *J Biol Chem.* 1998; 6:3496-501.
85. Mosimann C, Hausmann G, Basler K. The role of Parafibromin/Hyrax as a nuclear Gli/Ci-interacting protein in Hedgehog target gene control. *Mech Dev.* 2009; 5-6:394-405. doi: 10.1016/j.mod.2009.02.002.
86. Schwartz MA, Ginsberg MH. Networks and crosstalk: integrin signalling spreads. *Nat Cell Biol.* 2002; 4:E65-8.
87. Watt FM. Role of integrins in regulating epidermal adhesion, growth and differentiation. *EMBO J.* 2002; 15:3919-26.
88. Pytela R, Pierschbacher MD, Ruoslahti E. Identification and isolation of a 140 kd cell surface glycoprotein with properties expected of a fibronectin receptor. *Cell.* 1985 Jan; 1:191-8.
89. Desgrosellier JS, Cheresch DA. Integrins in cancer: biological implications and therapeutic opportunities. *Nat Rev Cancer.* 2010; 1:9-22. doi: 10.1038/nrc2748.
90. Burridge K, Fath K, Kelly T, Nuckolls G, Turner C. Focal adhesions: transmembrane junctions between the extracellular matrix and the cytoskeleton. *Annu Rev Cell Biol.* 1988;4:487-525.
91. Assoian RK, Klein EA. Growth control by intracellular tension and extracellular stiffness. *Trends Cell Biol.* 2008; 18:347–352.
92. Hehlhans S, Haase M, Cordes N. Signalling via integrins: implications for cell survival and anticancer strategies. *Biochim Biophys Acta.* 2007; 1:163-80.
93. Aoudjit F, Vuori K. Matrix attachment regulates Fas-induced apoptosis in endothelial cells: a role for c-flip and implications for anoikis. *J. Cell Biol.* 2001; 152:633–643.
94. Aoudjit F, Vuori K. Integrin signaling inhibits paclitaxel-induced apoptosis in breast cancer cells. *Oncogene.* 2001; 20:4995–5004.

95. Scatena M, Almeida M, Chaisson ML, Fausto N, Nicosia RF, Giachelli CM. NF- κ B mediates α v β 3 integrin-induced endothelial cell survival. *J. Cell Biol.* 1998; 141:1083–1093.
96. Stupack DG, Puente XS, Boutsaboualoy S, Storgard CM, Cheresch DA. Apoptosis of adherent cells by recruitment of caspase-8 to unligated integrins. *J. Cell Biol.* 2001; 155:459–470.
97. Guo W, Pylayeva Y, Pepe A, Yoshioka T, Muller WJ, Inghirami G, et al. Beta 4 integrin amplifies ErbB2 signaling to promote mammary tumorigenesis. *Cell.* 2006; 3:489-502.
98. Bakewell SJ, Nestor P, Prasad S, Tomasson MH, Dowland N, Mehrotra M, et al. Platelet and osteoclast beta3 integrins are critical for bone metastasis. *Proc Natl Acad Sci U S A.* 2003; 24:14205-10.
99. Felding-Habermann B, O'Toole TE, Smith JW, Fransvea E, Ruggeri ZM, Ginsberg MH, et al. Integrin activation controls metastasis in human breast cancer. *Proc Natl Acad Sci U S A.* 2001; 4:1853-8.
100. Rivera J, Lozano ML, Navarro-Núñez L, Vicente V. Platelet receptors and signaling in the dynamics of thrombus formation. *Haematologica.* 2009; 5:700-11. doi: 10.3324/haematol.2008.003178.
101. Kato A. The biologic and clinical spectrum of Glanzmann's thrombasthenia: implications of integrin alpha IIb beta 3 for its pathogenesis. *Crit. Rev. Oncol. Hematol* 1997;1:1–23.
102. Dumon S, Walton DS, Volpe G, Wilson N, Dassé E, Del Pozzo W, et al. Itga2b regulation at the onset of definitive hematopoiesis and commitment to differentiation. *PLoS One.* 2012; 8:e43300. doi: 10.1371/journal.pone.0043300.
103. Lu C, Takagi J, and Springer TA. Association of the membrane proximal regions of the alpha and beta subunit cytoplasmic domains constrains an integrin in the inactive state. *J. Biol. Chem* 2001b; 18: 14642–14648.
104. Hynes RO. Integrins: bidirectional, allosteric signaling machines. *Cell.* 2002; 6:673-87.
105. Jain S, Harris J, Ware J. Platelets: linking hemostasis and cancer. *Arterioscler Thromb Vasc Biol.* 2010; 12:2362-7. doi: 10.1161/ATVBAHA.110.207514.

106. Zhao F, Li L, Guan L, Yang H, Wu C, Liu Y. Roles for GP IIb/IIIa and $\alpha\beta 3$ integrins in MDA-MB-231 cell invasion and shear flow-induced cancer cell mechanotransduction. *Cancer Lett.* 2014; 1:62-73. doi: 10.1016/j.canlet.2013.10.019.
107. Lu X, Wan F, Zhang H, Shi G, Ye D. ITGA2B and ITGA8 are predictive of prognosis in clear cell renal cell carcinoma patients. *Tumor Biol.* 2016; 1:253-62. doi: 10.1007/s13277-015-3792-5.
108. Delwel GO, de Melker AA, Hogervorst F, Jaspars LH, Fles DL, Kuikman I, et al. Distinct and overlapping ligand specificities of the alpha 3A beta 1 and alpha 6A beta 1 integrins: recognition of laminin isoforms. *Mol Biol Cell.* 1994 ; 2:203-15.
109. Kikkawa Y, Sanzen N, Sekiguchi K. Isolation and characterization of laminin-10/11 secreted by human lung carcinoma cells. laminin-10/11 mediates cell adhesion through integrin alpha3 beta1. *J Biol Chem.* 1998; 25:15854-9.
110. Yauch RL, Kazarov AR, Desai B, Lee RT, Hemler ME. Direct extracellular contact between integrin alpha(3)beta(1) and TM4SF protein CD151. *J Biol Chem.* 2000;13):9230-8.
111. Hodivala-Dilke KM, DiPersio CM, Kreidberg JA, Hynes RO. Novel roles for alpha3beta1 integrin as a regulator of cytoskeletal assembly and as a trans-dominant inhibitor of integrin receptor function in mouse keratinocytes. *J Cell Biol.* 1998; 5:1357-69.
112. Sterk LM, Geuijen CA, Van den Berg JG, Claessen N, Weening JJ, Sonnenberg A. Association of the tetraspanin CD151 with the laminin-binding integrins alpha3beta1, alpha6beta1, alpha6beta4 and alpha7beta1 in cells in culture and in vivo. *J Cell Sci.* 2002; 6:1161-73.
113. Chattopadhyay N, Wang Z, Ashman LK, Brady-Kalnay SM, Kreidberg JA. alpha3beta1 integrin-CD151, a component of the cadherin-catenin complex, regulates PTPmu expression and cell-cell adhesion. *J Cell Biol.* 2003; 6:1351-62.
114. Goodman SL, Picard M. Integrins as therapeutic targets. *Trends Pharmacol Sci.* 2012; 7:405-12. doi: 10.1016/j.tips.2012.04.002.
115. Hideshima T, Richardson P, Chauhan D, Palombella VJ, Elliott PJ, Adams J, et al. The proteasome inhibitor PS-341 inhibits growth, induces apoptosis, and

overcomes drug resistance in human multiple myeloma cells. *Cancer Res.* 2001; 7:3071-6.

116. Erovic BM, Harris L, Jamali M, Goldstein DP, Irish JC, Asa SL, et al. Biomarkers of parathyroid carcinoma. *Endocr Pathol.* 2012; 4:221-31. doi: 10.1007/s12022-012-9222-y.

117. Bradley KJ, Bowl MR, Williams SE, Ahmad BN, Partridge CJ, Patmanidi AL, et al. Parafibromin is a nuclear protein with a functional monopartite nuclear localization signal. *Oncogene* 2007; 8: 1213–21.

118. Chen H, Shi N, Gao Y, Li X, Teng M, Niu L. Crystallographic analysis of the conserved C-terminal domain of transcription factor Cdc73 from *Saccharomyces cerevisiae* reveals a GTPase-like fold. *Acta Crystallogr. D Biol. Crystallogr* 2012;8: 953–9. doi: 10.1107/S0907444912017325.

119. Amrich CG, Davis CP, Rogal WP, Shirra MK, Heroux A, Gardner RG, et al. Cdc73 subunit of Paf1 complex contains C-terminal Ras-like domain that promotes association of Paf1 complex with chromatin. *J. Biol. Chem* 2012; 14:10863–75. doi: 10.1074/jbc.M111.325647.

120. Cantile M, Scognamiglio G, La Sala L, La Mantia E, Scaramuzza V, Valentino E, et al. Aberrant expression of posterior HOX genes in well differentiated histotypes of thyroid cancers. *Int. J. Mol. Sci* 2013; 11: 21727–40. doi: 10.3390/ijms141121727.

121. Paziienza V, la Torre A, Baorda F, Alfarano M, Chetta M, Muscarella LA, et al. Identification and functional characterization of three NoLS (Nucleolar Localisation Signals) mutations of the CDC73 gene. *PLoS One* 2013; 12: e82292. doi: 10.1371/journal.pone.0082292.

122. Bradley KJ, Hobbs MR, Buley ID, Carpten JD, Cavaco BM, Fares JE, et al. Uterine tumours are a phenotypic manifestation of the hyperparathyroidism-jaw tumour syndrome. *J Int Med.* 2005; 1:18–26.

123. Zhang JF, Chen Y, Qiu XX, Tang WL, Zhang JD, Huang JH, et al. The vascular delta-like ligand-4 (DLL4)-Notch4 signaling correlates with angiogenesis in primary glioblastoma: an immunohistochemical study. *Tumour Biol.* 2016; 3:3797-805. doi: 10.1007/s13277-015-4202-8.

124. Lin X, Sun B, Zhu D, Zhao X, Sun R, Zhang Y, et al. Notch4+ cancer stem-like cells promote the metastatic and invasive ability of melanoma. *Cancer Sci.* 2016; 8:1079-91. doi: 10.1111/cas.12978.
125. Xiong J, Zhang X, Chen X, Wei Y, Lu DG, Han YW, et al. Prognostic roles of mRNA expression of notch receptors in non-small cell lung cancer. *Oncotarget.* 2017; 8:13157-13165. doi: 10.18632/oncotarget.
126. Cheung CC, Lun SW, Chung GT, Chow C, Lo C, Choy KW, et al. MicroRNA-183 suppresses cancer stem-like cell properties in EBV-associated nasopharyngeal carcinoma. *BMC Cancer.* 2016;16:495. doi: 10.1186/s12885-016-2525-5.
127. Widowati T, Melhem S, Patria SY, de Graaf BM, Sinke RJ, Viel M, et al. RET and EDNRB mutation screening in patients with Hirschsprung disease: Functional studies and its implications for genetic counseling. *Eur J Hum Genet.* 2016; 6:823-9. doi:1038/ejhg.2015.214.
128. Niedzwiedz W, Mosedale G, Johnson M, Ong CY, Pace P, Patel KJ. The Fanconi anaemia gene FANCC promotes homologous recombination and error-prone DNA repair. *Mol Cell.* 2004; 4:607-20.
129. Levitus M, Waisfisz Q, Godthelp BC, de Vries Y, Hussain S, Wiegant WW, et al. The DNA helicase BRIP1 is defective in Fanconi anemia complementation group. *J Nat Genet.* 2005; 9:934-5.
130. Ford D, Easton D F, Stratton M, Narod S, Goldgar D, Devilee P, et al. Genetic heterogeneity and penetrance analysis of the BRCA1 and BRCA2 genes in breast cancer families. The Breast Cancer Linkage Consortium. *Am J Hum Genet.* 1998; 3: 676–689.
131. Petersen DL, Berthelsen J, Willerslev-Olsen A, Fredholm S, Dabelsteen S, Bonfeld CM, et al. A novel BLK-induced tumor model. *Tumour Biol.* 2017; 7:1010428317714196. doi: 10.1177/1010428317714196.
132. Williams SJ, McGuckin MA, Gotley DC, Eyre HJ, Sutherland GR, Antalis TM. Two novel mucin genes down-regulated in colorectal cancer identified by differential display. *Cancer Res.* 1999; 16:4083-9.
133. Li B, Liu HY, Guo SH, Sun P, Gong FM, Jia BQ. Association of MLL3 expression with prognosis in gastric cancer. *Genet Mol Res.* 2014; 3:7513-8. Doi:10.4238/2014. September.12.18.

134. Koshizuka K, Hanazawa T, Kikkawa N, Arai T, Okato A, Kurozumi A, et al. Regulation of ITGA3 by the anti-tumor miR-199 family inhibits cancer cell migration and invasion in head and neck cancer. *Cancer Sci.* 2017; 8:1681-1692. doi: 10.1111/cas.13298.
135. Tang XR, Wen X, He QM, Li YQ, Ren XY, Yang XJ, et al. MicroRNA-101 inhibits invasion and angiogenesis through targeting ITGA3 and its systemic delivery inhibits lung metastasis in nasopharyngeal carcinoma. *Cell Death Dis.* 2017; 1:e2566. doi: 10.1038/cddis.2016.486.
136. Sakaguchi T, Yoshino H, Yonemori M, Miyamoto K, Sugita S, Matsushita R, et al. Regulation of ITGA3 by the dual-stranded microRNA-199 family as a potential prognostic marker in bladder cancer. *Br J Cancer.* 2017; 8:1077-1087. doi: 10.1038/bjc.2017.43.
137. Kurozumi A, Goto Y, Matsushita R, Fukumoto I, Kato M, Nishikawa R, et al. Tumor-suppressive microRNA-223 inhibits cancer cell migration and invasion by targeting ITGA3/ITGB1 signaling in prostate cancer. *Cancer Sci.* 2016; 1:84-94. doi: 10.1111/cas.12842.
138. Canaff L, Vanbellinthen JF, Kanazawa I, Kwak H, Garfield N, Vautour L, et al. Menin missense mutants encoded by the MEN1 gene that are targeted to the proteasome: restoration of expression and activity by CHIP siRNA. *J Clin Endocrinol Metab.* 2012; 2:E282-91. doi: 10.1210/jc.2011-0241.
139. Guarnieri V, Battista C, Muscarella LA, Bisceglia M, de Martino D, Baorda F, et al. CDC73 mutations and parafibromin immunohistochemistry in parathyroid tumors: clinical correlations in a single-centre patient cohort. *Cell Oncol (Dordr).* 2012; 6:411-22. doi: 10.1007/s13402-012-0100-x.
140. Chiofalo MG, Sparaneo A, Chetta M, Franco R, Baorda F, Cinque L, et al. A novel CDC73 gene mutation in an Italian family with hyperparathyroidism-jaw tumour (HPT-JT) syndrome. *Cell Oncol (Dordr).* 2014; 37:281-8. doi: 10.1007/s13402-014-0187-3.
141. Teh BT, Kytölä S, Farnebo F, Bergman L, Wong FK, Weber G, et al. Mutation analysis of the MEN1 gene in multiple endocrine neoplasia type 1, familial acromegaly and familial isolated hyperparathyroidism. *J Clin Endocrinol Metab.* 1998; 8:2621-6.

142. Yaguchi H, Ohkura N, Takahashi M, Nagamura Y, Kitabayashi I, Tsukada T. Menin missense mutants associated with multiple endocrine neoplasia type 1 are rapidly degraded via the ubiquitin-proteasome pathway. *Mol Cell Biol.* 2004; 15:6569-80.
143. Yang YJ, Song TY, Park J, Lee J, Lim J, Jang H et al. Menin mediates epigenetic regulation via histone H3 lysine 9 methylation. *Cell Death Dis.* 2013;4:e583. doi: 10.1038/cddis.2013.98.
144. Yamaguchi S, Yachiku S, Morikawa M. Analysis of proliferative activity of the parathyroid glands using proliferating cell nuclear antigen in patients with hyperparathyroidism. *J Clin Endocrinol Metab.* 1997;8:2681-8.
145. Wei CH, Harari A. Parathyroid carcinoma: update and guidelines for management. *Curr Treat Options Oncol.* 2012 ;1:11-23. doi: 10.1007/s11864-011-0171-3.
146. Gogusev J, Murakami I, Telvi L, Goguin A, Sarfati E, Jaubert F. Establishment and characterization of a human parathyroid carcinoma derived cell line. *Pathol Res Pract.* 2015; 4:332-40. doi: 10.1016/j.prp.2014.12.008.
147. Starker LF, Svedlund J, Udelsman R, Dralle H, Akerström G, Westin G, et al. The DNA methylome of benign and malignant parathyroid tumors. *Genes Chromosomes Cancer.* 2011; 9:735-45. doi: 10.1002/gcc.20895.
148. Haven CJ, Howell VM, Eilers PH, Dunne R, Takahashi M, Van Puijenbroek M, et al. Gene expression of parathyroid tumors: molecular subclassification and identification of the potential malignant phenotype. *Cancer Res.* 2004; 20:7405-11.
149. Newey PJ, Nesbit MA, Rimmer AJ, Attar M, Head RT, Christie PT, et al. Whole-exome sequencing studies of nonhereditary (sporadic) parathyroid adenomas. *J Clin Endocrinol Metab.* 2012; 10:E1995-2005. doi: 10.1210/jc.2012-2303.
150. Cinque L, Sparaneo A, Salcuni AS, de Martino D, Logoluso F, Palumbo O, et al. MEN1 Gene Mutation with Parathyroid Carcinoma: First Report 1 of a Familial Case. *Endocrine Connections.* 2017. doi:10.1530/EC-17-0207 in press.
151. Kasaian K, Wiseman SM, Thiessen N, Mungall KL, Corbett RD, Qian JQ, et al. Complete genomic landscape of a recurring sporadic parathyroid carcinoma. *J Pathol.* 2013; 3:249-60. doi: 10.1002/path.4203.

152. Yu W, McPherson JR, Stevenson M, van Eijk R, Heng HL, Newey P, et al. Whole-exome sequencing studies of parathyroid carcinomas reveal novel PRUNE2 mutations, distinctive mutational spectra related to APOBEC-catalyzed DNA mutagenesis and mutational enrichment in kinases associated with cell migration and invasion. *J Clin Endocrinol Metab.* 2015; 2:E360-4. doi: 10.1210/jc.2014-3238.
153. Pandya C, Uzilov AV, Bellizzi J, Lau CY, Moe AS, Strahl M, et al. Genomic profiling reveals mutational landscape in parathyroid carcinomas. *JCI Insight.* 2017;(6):e92061. doi: 10.1172/jci.insight.92061.
154. Ford DJ, Dingwall AK. The cancer COMPASS: navigating the functions of MLL complexes in cancer. *Cancer Genet.* 2015; 5: 178-91. doi: 10.1016/j.cancergen.2015.01.005.
155. Roberts SA & Gordenin DA. Hypermutation in human cancer genomes: footprints and mechanisms. *Nature Reviews: Cancer.* 2014; 14: 786–800.
156. Völkel P, Angrand PO. The control of histone lysine methylation in epigenetic regulation. *Biochimie.* 2007; 1:1-20.
157. Müller J, Hart CM, Francis NJ, Vargas ML, Sengupta A, Wild B, et al. Histone methyltransferase activity of a Drosophila Polycomb group repressor complex. *Cell.* 2002; 2:197-208.
158. Sanpaolo E, Miroballo M, Corbetta S, Verdelli C, Baorda F, Balsamo T, et al. EZH2 and ZFX oncogenes in malignant behaviour of parathyroid neoplasms. *Endocrine.* 2016 ; 1:55-59.
159. Taube JM, Galon J, Sholl LM, Rodig SJ, Cottrell TR, Giraldo NA, et al. Implications of the tumor immune microenvironment for staging and therapeutics. *Mod Pathol.* 2017. doi: 10.1038/modpathol.
160. Wilson RAM, Evans TRJ, Fraser AR, Nibbs RJB. Immune Checkpoint Inhibitors: New strategies to checkmate cancer. *Clin Exp Immunol.* 2017. doi: 10.1111/cei.13081.
161. Coulie PG, Van den Eynde BJ, Van der Bruggen P, Boon T. Tumour antigens recognized by T lymphocytes: at the core of cancer immunotherapy. *Nat Rev Cancer.* 2014;2:135-46. doi: 10.1038/nrc3670.

162. Albariño CG, Romanowski V. Phenol extraction revisited: a rapid method for the isolation and preservation of human genomic DNA from whole blood. *Mol Cell Probes* 1994;8:423e7.
163. Chai V, Vassilakos A, Lee Y, Wright JA, Young AH. Optimization of the PAXgene blood RNA extraction system for gene expression analysis of clinical samples. *J Clin Lab Anal.* 2005;5:182-8.
164. Chen R, Im H, Snyder M. Whole-Exome Enrichment with the Agilent SureSelect Human All Exon Platform. *Cold Spring Harb Protoc.* 2015; 7:626-33. doi: 10.1101/pdb.prot083659.
165. Andrews S. FastQC: a Quality Control Tool for High Throughput Sequence Data, 2010 available online at: <http://www.bioinformatics.babraham.ac.uk/projects/fastqc>.
166. Li H, Durbin R. Fast and accurate short read alignment with Burrows-Wheeler transform. *Bioinformatics.* 2009; 14:1754-60. doi: 10.1093/bioinformatics/btp324.
167. McKenna A, Hanna M, Banks E, Sivachenko A, Cibulskis K, Kernytsky A, et al. The Genome Analysis Toolkit: a MapReduce framework for analyzing next-generation DNA sequencing data. *Genome Res.* 2010; 9:1297-303. doi: 10.1101/gr.107524.110.
168. Hummel M, Bonnin S, Lowy E, Roma G. TEQC: an R package for quality control in target capture experiments. *Bioinformatics.* 2011; 9:1316-7. doi: 10.1093/bioinformatics/btr122.
169. Wang K, Li M, Hakonarson H. ANNOVAR: functional annotation of genetic variants from high-throughput sequencing data. *Nucleic Acids Res.* 2010; 16:e164. doi: 10.1093/nar/gkq603.
170. Sherry ST, Ward MH, Kholodov M, Baker J, Phan L, Smigielski EM, et al. dbSNP: the NCBI database of genetic variation. *Nucleic Acids Res.* 2001; 1:308-11.
171. Exome Aggregation Consortium. Analysis of protein-coding genetic variation in 60,706 humans. *Nature.* 2016; 7616:285-91. doi: 10.1038/nature19057.
172. Liu X, Jian X, Boerwinkle E. dbNSFP: a lightweight database of human nonsynonymous SNPs and their functional predictions. *Hum Mutat.* 2011; 8:894-9. doi: 10.1002/humu.21517.

173. Haven CJ, Howell VM, Eilers PH, Dunne R, Takahashi M, van Puijenbroek M, et al. Gene expression of parathyroid tumors: molecular subclassification and identification of the potential malignant phenotype. *Cancer Res.* 2004; 20:7405-11.
174. Krämer A, Green J, Pollard J Jr, Tugendreich S. Causal analysis approaches in Ingenuity Pathway Analysis. *Bioinformatics.* 2014; 4:523-30. doi: 10.1093/bioinformatics/btt703.
175. Zhan S, Cahalan MD. Purifying Plasmid DNA from Bacterial Colonies Using the Qiagen Miniprep Kit. *J. Vis. Exp.* (6), e247, doi:10.3791/247.
176. Dalby B, Cates S, Harris A, Ohki EC, Tilkins ML, Price PJ, et al. Advanced transfection with Lipofectamine 2000 reagent: primary neurons, siRNA, and high-throughput applications. *Methods.* 2004; 2:95-103.
177. Li J, Zhang D, Ward KM, Prendergast GC, Ayene IS. Hydroxyethyl disulfide as an efficient metabolic assay for cell viability in vitro. *Toxicol In Vitro.* 2012; 4:603-12. doi: 10.1016/j.tiv.2012.01.007.

RINGRAZIAMENTI

Al termine di questi tre anni di dottorato è doveroso ringraziare le persone che hanno condiviso con me questo progetto di ricerca e senza le quali non sarebbe stato possibile realizzare il mio lavoro di tesi.

Desidero ringraziare il Prof. V. M. Fazio, relatore di questa tesi, per la grande disponibilità e per i preziosi consigli elargiti durante il dottorato di ricerca. A lui va la mia gratitudine per avermi dato l'opportunità di condurre il mio progetto, seguendomi passo dopo passo in questi proficui tre anni di dottorato.

Ringrazio il Dott. V. Guarnieri che, in qualità di supervisor, ha creduto in me sin dall'inizio, mi ha sostenuto e aiutato nel raggiungimento di questo importante traguardo per la mia formazione. Un ringraziamento sentito va a lui per gli insegnamenti teorici e di vita e per essersi sempre prodigato affinché facessi esperienze costruttive e utili alla mia crescita come dottore di ricerca.